Effect of Microcrystalline Cellulose from Bagasse on the Adhesion Properties of Tapioca Starch and/or Polyvinyl alcohol based Adhesives

Sunan Jonjankiat

A Thesis Submitted in Partial Fulfillment of the Requirements for the Degree of Master of Science in Packaging Technology

Prince of Songkla University

2010

Thesis Title	Effect of Microcrystalline Cellulose from Bagasse on the Adhesion Properties of Tapioca Starch and/or Polyvinyl alcohol based Adhesives
Author	Miss Sunan Jonjankiat
Major Program	Packaging Technology

Major Advisor :	**Examining Committee :**
…….....	……..Chairperson
(Dr.Waranyou Sridach)	(Asst. Prof. Dr.Saowakon Wattanachant)
	…….....
Co-Advisor :	(Dr.Waranyou Sridach)
…….....	…….....
(Asst. Prof. Dr.Thawien Wittaya)	(Asst. Prof. Dr.Thawien Wittaya)
	…….....
	(Dr.Rangrong Yoksan)

The Graduate School, Prince of Songkla University, has approved this thesis as partial fulfillment of the requirements for the Degree of Master of Science in Packaging Technology.

……..……

(Prof. Dr.Amornrat Phongdara)

Dean of Graduate School

ชื่อวิทยานิพนธ์ ผลของไมโครคริสตัลไลน์เซลลูโลสจากชานอ้อยต่อสมบัติการยึดติดของกาวจากสตาร์ชมันสำปะหลัง และ/หรือพอลิไวนิลแอลกอฮอล์

ผู้เขียน นางสาวสุนันท์ จรเจนเกียรติ

สาขาวิชา เทคโนโลยีบรรจุภัณฑ์

ปีการศึกษา 2553

บทคัดย่อ

ไมโครคริสตัลไลน์เซลลูโลส (MCC) สามารถเตรียมได้โดยการต้มเยื่อชานอ้อยด้วยกรดไนตริกความเข้มข้นร้อยละ 15 อัตราส่วนระหว่างเยื่อแห้งต่อกรดเท่ากับ 1 ต่อ 20 ต้มที่อุณหภูมิ 90 องศาเซลเซียส เป็นระยะเวลา 30 นาที หลังจากนั้นฟอกสีด้วยโซเดียมไฮโปคลอไรท์ที่มีความเข้มข้นของคลอรีนร้อยละ 10 จะให้ผลผลิต (yield) ของเยื่อเซลลูโลส เท่ากับร้อยละ 48.43 จากการวิเคราะห์ลักษณะของ MCC ที่เตรียมได้พบว่า อนุภาคของ MCC มีลักษณะเป็นแท่งขนาดเส้นผ่านศูนย์กลางประมาณ 5-10 ไมโครเมตร และยาวประมาณ100-300 ไมโครเมตร เซลลูโลสมีปริมาณเพิ่มเป็นมากกว่าร้อยละ 80 และค่าความเป็นผลึกของ MCC มีค่าเท่ากับร้อยละ 54.38

การศึกษาผลของ MCC ต่อสมบัติของกาวจากสตาร์ชมันสำปะหลัง กาวพอลิไวนิลแอลกอฮอล์ และกาวเชื่อมขวางระหว่างพอลิไวนิลแอลกอฮอล์กับสตาร์ชมันสำปะหลังพบว่าปัจจัยสำคัญที่มีผลต่อสมบัติของกาวคอมโพสิทได้แก่ ชนิดของกาวและปริมาณของ MCC จากการทดลองพบว่า กาวสตาร์ชมันสำปะหลังที่มีปริมาณของแข็งหรือน้ำหนักแห้งร้อยละ 26 จะมีค่าความแข็งแรงการยึดติดแบบเฉือนสูงที่สุด โดยมีค่าความเสียหายของชิ้นไม้ทดสอบประมาณร้อยละ 70 และให้ค่าความหนืดที่เหมาะสมต่อการนำไปใช้งาน ($p<0.05$) การเติม MCC ในปริมาณร้อยละ 0.5 ถึง 1.5 โดยน้ำหนักแห้งของกาวจะปรับปรุงสมบัติของกาวสตาร์ชมันสำปะหลังให้มีค่าความแข็งแรงการยึดติดแบบเฉือนเพิ่มขึ้นจาก 18.71×10^5 นิวตันต่อตารางเมตรเป็น 29.01×10^5 นิวตันต่อตารางเมตร และทำให้อุณหภูมิหลอมเหลว (T_m) ของกาวสตาร์ชมันสำปะหลังมีค่าเพิ่มขึ้น นอกจากนี้ MCC สามารถกระจายตัวและแทรกตัวลงในเนื้อกาวสตาร์ชมันสำปะหลังได้อย่างสม่ำเสมอ

กาวพอลิไวนิลแอลกอฮอล์ (PVOH) ที่มีน้ำหนักโมเลกุลปานกลาง (M PVOH) และน้ำหนักโมเลกุลสูง (H PVOH) ที่ความเข้มข้นร้อยละ 12 จะให้ค่าความหนืด, ปริมาณของแข็ง และสมบัติความแข็งแรงการยึดติดแบบเฉือนเหมาะสมต่อการนำไปศึกษาผลของ MCC และเมื่อเติม MCC ในปริมาณร้อยละ 0.5 ถึง 1.5 โดยน้ำหนักแห้งของกาวจะสามารถปรับปรุงสมบัติของกาวพอลิไวนิลแอลกอฮอล์ให้มีค่าความแข็งแรงการยึดติดแบบเฉือนเพิ่มขึ้นจากประมาณ

15.45 ถึง17.94×10^5 นิวตันต่อตารางเมตรเป็น 21.52×10^5 ถึง 24.14×10^5 นิวตันต่อตารางเมตร โดยมีค่าความเสียหายของชิ้นไม้ทดสอบเพิ่มขึ้นเป็นร้อยละ 70 และทำให้อุณหภูมิหลอมเหลว (T_m) และอุณหภูมิการเปลี่ยนสถานะคล้ายแก้ว (T_g) ของกาวพอลิไวนิลแอลกอฮอล์มีค่าเพิ่มขึ้น

สำหรับกาวเชื่อมขวางระหว่างพอลิไวนิลแอลกอฮอล์กับสตาร์ชมันสำปะหลัง (PVOH/St cross-linked adhesive) พบว่า สัดส่วนของสตาร์ชมันสำปะหลังและการเติมกรดซิตริกเป็นสารเร่งปฏิกิริยาจะมีผลต่อสมบัติของกาวเชื่อมขวางระหว่างพอลิไวนิลแอลกอฮอล์กับสตาร์ชมันสำปะหลัง โดยสัดส่วนของสตาร์ชที่สูงขึ้นและการเติมกรดซิตริกจะทำให้กาวสามารถเกิดการเชื่อมขวางโมเลกุลกันเป็นร่างแหได้อย่างสมบูรณ์ ส่งผลให้กาวเชื่อมขวางมีประสิทธิภาพในการใช้งานที่ดีกว่ากาวสตาร์ชมันสำปะหลังและกาวพอลิไวนิลแอลกอฮอล์ ดังนั้นการเติม MCC ในปริมาณร้อยละ 1.5 โดยน้ำหนักแห้งของกาวจะสามารถปรับปรุงสมบัติของกาวเชื่อมขวางให้มีความแข็งแรงการยึดติดแบบเฉือนเพิ่มขึ้นจาก 26.50×10^5 นิวตันต่อตารางเมตรเป็น 32.93×10^5 นิวตันต่อตารางเมตร โดยมีค่าความเสียหายของชิ้นไม้ทดสอบเป็นร้อยละ 100 และทำให้อุณหภูมิการเปลี่ยนสถานะคล้ายแก้ว (T_g) ของกาวเชื่อมขวางมีค่าสูงขึ้นและมีอุณหภูมิหลอมเหลว (T_m) เท่ากับ 175.60 องศาเซลเซียส นอกจากนี้ยังพบว่า MCC จะเกิดปฏิสัมพันธ์ทางเคมีระหว่างพันธะไฮโดรเจนกับกาวทั้งสามประเภทนี้ ทำให้สมบัติทางเคมีและสมบัติทางกลของกาวคอมโพสิทเปลี่ยนแปลงไป อย่างไรก็ตามเมื่อเพิ่มปริมาณ MCC เป็นร้อยละ 2.5 ถึง 3.5 พบว่า ค่าความแข็งแรงในการยึดติดจะมีค่าลดลงตามลำดับ ($p<0.05$).

Thesis Title	Effect of Microcrystalline Cellulose from Bagasse on the Adhesion Properties of Tapioca Starch and/or Polyvinyl alcohol based Adhesives
Author	Miss Sunan Jonjankiat
Major Program	Packaging Technology
Academic Year	2010

ABSTRACT

Microcrystalline cellulose (MCC) could be prepared by acid hydrolysis of sugarcane bagasse fiber (SBF) with nitric acid at the concentration of 15% (w/w). SBF was cooked in acid solution with the ratio of 1:20 of the dried SBF to acid liguor at 90°C for 30 min and then bleached with sodium hypochlorite at 10% active chlorine. The optimal cellulose fiber yield was 48.43%. The MCC was rod-shaped particle. The diameter and the lengths of MCC rod-shaped particle were 5-10 μm and 100-300 μm, respectively. The cellulose content increased to 80% up and the crystallinity of MCC was 54.38%.

Study the effect of MCC on the properties of tapioca starch adhesive, polyvinyl alcohol adhesive and polyvinyl alcohol/starch cross-linked adhesive showed type of adhesive and MCC content were important factors on the composited adhesives. The starch adhesive having dried weight of 26 wt% were the highest shear strength value which contribute 70% wood failure and optimal viscosity ($p<0.05$). Addition of MCC at 0.5-1.5 wt% of dried weight adhesive could improve the shear strength of starch adhesives from 18.71×10^5 N/m^2 to 29.01×10^5 N/m^2 and increased the melting temperature (T_m) of starch adhesive. Moreover, MCC was evenly dispersed and embedded in starch matrix.

PVOH adhesives having medium molecular weight (M PVOH) and high molecular weight (H PVOH) at the concentration of 12 wt% contributed the optimal viscosity, solid content and shear strength which were suitable to study the effect of MCC on the adhesive properties. Addition of MCC at 0.5-1.5 wt% of dried weight adhesive could improve the shear strength from 15.45×10^5-17.94×10^5 N/m^2 to 21.52×10^5-24.14×10^5 N/m^2, and increased the wood failure to 70%. T_m and glass

transition temperature (T_g) of PVOH adhesive were also increased with adding the MCC.

For PVOH/St cross-linked adhesives, it was found that starch ratio and catalyst, citric acid (CA), had effected to the properties of cross-linked adhesive between PVOH and starch (PVOH/St cross-linked adhesive). The results of high starch ratio and added CA are the completely cross-linked reaction and increased the efficiency of adhesive application which was better than starch and PVOH adhesive. Addition of MCC at 1.5 wt% of dried weight adhesive could improve the shear strength from 26.50×10^5 N/m^2 to 32.93×10^5 N/m^2 which had the 100% wood failure. T_g of cross-linked adhesive was increased and T_m value was 175.60°C. In addition, there occurred the chemical binding between hydrogen bond of 3 adhesive matrixes and MCC molecules. It had affected to the chemical and mechanical properties of composite adhesives. However, the increasing of MCC content to 2.5 and 3.5 wt% had reduce the strength of adhesion ($p>0.05$).

ACKNOWLEDGEMENT

I would like to express my deepest appreciation and sincere gratitude to my advisor, Dr.Waranyou Sridach from the Department of Material Product Technology, Faculty of Agro-Industry, Prince of Songkla University, for his kindness, guidance and supervision during my study.

I also express my profound gratitude to my co-advisor, Asst.Prof.Dr.Thawien Wittaya from the Department of Material Product Technology, Faculty of Agro-Industry, Prince of Songkla University, for his kindness, support and guidance.

I am also grateful to my examining committee, Asst.Prof.Dr.Saowakon Wattanachant from the Department of Food Technology, Faculty of Agro-Industry, Prince of Songkla University and Dr.Rangrong Yoksan from the Department of Packaging and Materials Technology, Faculty of Agro-Industry, Kasetsart University.

My deep gratitude is also due to all my friends and staffs who shared a hard time with me during my study and give me their help.

My deepest gratitude and sincere appreciation always go to my parents who always encourage and look after me.

This study could not be successful without the University–Industry Research Collaboration Program (U-IRC) Scholarship from National Science and Technology Development Agency (NSTDA) and the financial support from the Graduate School, Prince of Songkla University.

Sunan Jonjankiat

CONTENTS

Page

Chapter **Page**

Chapter **Page**

Chapter **Page**

LIST OF TABLS

Table **Page**

LIST OF TABLES (Continued)

Table **Page**

LIST OF FIGURES

Figure **Page**

LIST OF FIGURES (Continued)

Figure **Page**

LIST OF FIGURES (Continued)

Figure **Page**

LIST OF FIGURES (Continued)

Figure **Page**

CHAPTER 1

INTRODUCTION

High performance wood adhesives are required in many processing industries include packaging, particleboard, wood panels and wood component and etc. (Khan *et al*., 2004; Desai *et al*., 2003). Among the various adhesives used for the production of these articles, resole phenol formaldehyde, urea-formaldehyde and polyurethane are the most common type of wood adhesive. These adhesives are in adequate supply today, but scarcity of petroleum products could affect the future cost and environmental problems. Moreover, formaldehyde vapor is potentially carcinogenic and hazardous to human health, causing eye and throat irritations as well as respiratory discomfort (Peshkova and Li, 2003; Kim, 2009; Khan *et al*., 2004). So, there is an urgent need to develop renewable source-based environmental benign adhesives. Starch is one of the most promising materials for biodegradable adhesives because it is a versatile biopolymer with immense potential and low price. However, adhesives based solely on polysaccharides have adhesive strength lower than general commercial wood adhesives. These may be suitable for non-structural applications. In addition, the high molecular weight of polysaccharides imparts the substantial cohesive strength necessary in a useful adhesive (Hagg *et al*., 2006).

The properties of starch-based adhesives can be improved by chemical modifying, blending, cross-linking and physical modifying, e.g. adding reinforcement (Shi *et al*., 2008). The use of agricultural residue in biocomposite is a prospective commercial application. There are some useful studies in the literature on agricultural fibers in biocomposites (Wang *et al.*, 2006; Bondeson and Oksman, 2007; Alemdar and Sain, 2008a; Roohani *et al*., 2008). However, no research has been study in biocomposite adhesive. It is interesting to use cellulose from crop residue for composite adhesive. In addition, the applying of agricultural residue such as sugarcane bagasse is the value-added of useless materials and reduces the environmental problems from the disposal.

Review of Literature

1. Theories and mechanisms of adhesion

Wood adhesive is a substance that has the capability to hold wood panels together. The manner by which adhesives are able to serve this function is due to a surface attachment that is resistant to separation. Adhesives may come from either natural or synthetic sources. Petrochemical-based adhesive is a majority of synthetic sources. Since the Second World War, they replaced bio-based adhesives such as proteins, starch, lignin and cellulose in most applications based upon cost, production efficiencies, and better durability. However, several technologies and environmental factors have led to a resurgence of the bio-based adhesive, as an important adhesive for several applications such as interior plywood, paperboard, packaging and wood flooring.

The challenges and opportunities for wood bonding are derived by the nature of the interaction of substrate with adhesive. A bond occurs when the adhesive molecules adsorb onto a solid surface and chemically react with it.

Adhesion is involved whenever solids are brought into contact, as in coatings, paints, and varnishes; multilayered sandwiches; polymer blends; filled polymers; and composite materials. Since the final performance of these multicomponent materials depends significantly on the quality of the interface that is formed between the solids. This variety of approaches is emphasized by the fact that many theoretical models of adhesion have been proposed, which together are both complementary and contradictory:

1. Mechanical interlocking
2. Electronic theory
3. Theory of boundary layers and interphases
4. Adsorption (thermodynamic) theory
5. Diffusion theory
6. Chemical bonding theory

Among these models, one usually distinguishes rather arbitrarily between mechanical and specific adhesion, the latter being based on the various types of bonds (electrostatic, secondary, chemical) that can develop between two solids.

Actually, each of these theories is valid to some extent, depending on the nature of the solids in contact and the conditions of formation of the bonded system. Therefore, they do not negate each other and their respective importance depends largely on the system chosen (Schult and Nardin, 2003).

1.1 Mechanical interlocking

The mechanical interlocking model, proposed by MacBain and Hopkins in 1925, conceives of mechanical keying, or interlocking, of the adhesive into the cavities, pores, and asperities of the solid surface to be the major factor in determining adhesive strength. The effects of both mechanical interlocking and thermodynamic interfacial interactions could be taken into account as multiplying factors for estimating the joint strength G:

G = (constant) × (mechanical keying component) × (interfacial interactions component)

Therefore, according to the foregoing equation, a high level of adhesion should be achieved by improving both the surface morphology and physicochemical surface properties of substrate and adhesive. However, in most cases, the enhancement of adhesion by mechanical keying can be attributed simply to the increase in interfacial area due to surface roughness, insofar as the wetting conditions are fulfilled to permit penetration of the adhesive into pores and cavities.

1.2 Electronic theory

The electronic theory of adhesion was proposed primarily by Deryaguin and co-workers in 1948 (Deryaguin and Smilga, 1969; Deryaguin *et al*., 1978). These authors have suggested that an electron transfer mechanism between the substrate and the adhesive, having different electronic band structures. This phenomenon could induce the formation of a double electrical layer at the interface, and Deryaguin *et al*. (1978) have proposed that the resulting electrostatic forces can contribute significantly to the adhesive strength.

1.3 Theory of weak boundary layers: concept of interphase

It is now well known that alterations and modifications of the adhesive and/or adherend can be found in the vicinity of the interface leading to the formation of an interfacial zone exhibiting properties (or properties gradient) that differ from those of the bulk materials. Bikerman (1961), who stated that the cohesive strength of a weak boundary layer (WBL) can always be considered as the main factor in determining the level of adhesion, even when the failure appears to be interfacial. According to this assumption, the adhesion energy G is always equal to the cohesive energy G_c(WBL) of the weaker interfacial layer.

However, the creation of interfacial layers has received much attention in recent years and has led to the concept of ‘‘thick interface’’ or ‘‘interphase,’’ widely used in adhesion science. Such interphases are formed whatever the nature of both adhesive and substrate, their thickness being between the molecular level (a few angstroms or nanometers) and the microscopic scale (a few micrometers or more). Many physical, physicochemical, and chemical phenomena are responsible for the formation of such interphases: the orientation of chemical groups or the overconcentration of chain ends to minimize the free energy of the interface, migration toward the interface of additives, the growth of a transcrystalline structure, for example, when the substrate acts as a nucleating agent, formation of a pseudoglassy zone resulting from a reduction in chain mobility through strong interactions with the substrate, and modification of the thermodynamics and/or kinetics of the polymerization or cross-linking reaction at the interface through preferential adsorption of reaction species or catalytic effects.

1.4 Adsorption (or thermodynamic) theory

The thermodynamic model of adhesion, generally attributed to Sharpe and Schonhorn (Schult and Nardin, 2003), is certainly the most widely used approach in adhesion science at present. This theory is based on the belief that the adhesive will adhere to the substrate because of interatomic and intermolecular forces established at the interface, provided that an intimate contact is achieved. The most common interfacial forces result from Vander Waals and Lewis acid–base interactions. The magnitude of these forces can generally be related to fundamental thermodynamic

quantities, such as surface free energies of both adhesive and adherent. Generally, the formation of an assembly goes through a liquid–solid contact step, and therefore criteria of good adhesion become essentially criteria of good wetting, although this is a necessary but not sufficient condition.

1.5 Diffusion theory

The diffusion theory of adhesion is based on the assumption that the adhesion strength of polymers to themselves (autohesion) or to each other is due to mutual diffusion (interdiffusion) of macromolecules across the interface, thus creating an interphase. The macromolecular chains or chain segments are sufficiently mobile and mutually soluble. This is of great importance for many adhesion problems, such as healing and welding processes. Therefore, if interdiffusion phenomena are involved, the joint strength should depend on different factors, such as contact time, temperature, nature and molecular weight of polymers, and so on.

The diffusion phenomena do actually contribute greatly to the adhesive strength in many cases involving polymer–polymer junctions. Nevertheless, the interdiffusion of macromolecular chains requires both polymers to be sufficiently soluble and the chains to possess a sufficient mobility. These conditions are obviously fulfilled for autohesion, healing, or welding of identical polymers processes. However, diffusion can become a most unlikely mechanism if the polymers are not or only slightly soluble, if they are highly cross-linked or crystalline, or put in contact at temperatures far below their glass transition temperature. Nevertheless, in the case of junctions between two immiscible polymers, the interface could be strengthened by the presence of a diblock copolymer, in which each molecule consists of a block of the first polymer bonded to a block of the second polymer, or each of the two blocks is miscible with one of the polymers. The copolymer molecules concentrate generally at the interface and each block diffuses or ‘‘dissolves’’ into the corresponding polymer. Therefore, the improvement in joint strength can also be related to an interdiffusion process.

1.6 Chemical bonding theory

The chemical bonds formed across the adhesive–substrate interface can greatly participate to the level of adhesion between both materials. These bonds are generally considered as primary bonds in comparison with physical interactions, such as Vander Waals, which are called *secondary force interactions*. The terms primary and secondary stem from the relative strength or bond energy of each type of interaction. The typical strength of a covalent bond, for example, is on the order of 100 to 1000 kJ/mol, whereas those of Vander Waals interactions and hydrogen bonds do not exceed 50 kJ/mol. It is clear that the formation of chemical bonds depends on the reactivity of both adhesive and substrate. Different types of primary bonds, such as ionic and covalent bonds, at various interfaces. One of the most important adhesion fields involving interfacial chemical bonds is the use of adhesion promoter molecules, generally called coupling agents, to improve the joint strength between adhesive and substrate. They are widely employed in systems involving glass or silica substrates, and more particularly in the case of polymer-based composites reinforced by glass fibers (Schult and Nardin, 2003).

Therefore, adhesion is a very complex field beyond the reach of any single model or theory. The bonding mechanism of adhesives is also due to complex chemistry of the cellulosic substrate, i.e. hydrogen bonding with some adhesive and attractive weak Vander Walls forces with others (Charles, 1973; Somani *et al*., 2003). The main application of adhesion is bonding by adhesives, this technique replacing, at least partially, more classical mechanical attachment techniques such as bolting or riveting (Schult and Nardin, 2003). The quality of bonding and hence the properties and performance of the wood-based panels and beams are determined by three main parameters:

- the wood, especially the wood surface which result in the interaction between interface of wood surface and the bondline.
- the applied adhesive, amount of adhesive.
- the working conditions and process parameters which depending on type of adhesive.

Good quality bonding and adequate properties of the wood-based panels can be attained only if each of these three parameters contributes to the necessary extent to the bonding and production process (Dunky, 2003).

The bonding of the adhesive to wood fibers is a balance of several common thermodynamic and kinetic parameters and their interaction. For a bond to form, the adhesive needs to wet and flow over a surface, and in some cases penetrate into the substrate. Wetting is the ability of an adhesive drop to form a low contact angle with the surface. In contrast, flow involves the adhesive spreading over that surface under reasonable time. Flow is important because covering more of the surface allows for a stronger bond. Thus, a very viscous adhesive may wet a surface, but it might not flow to cover the surface in a reasonable time frame. Penetration is the ability of the adhesive to move into the voids on the substrate surface or into the substrate itself (Frihart, 2005). The difference between flow, penetration, and transfer are illustrated in Figure 1. However, good wetting does not assure good bonding. Adhesive distribution and adhesive properties strongly influence the final bonded product. Wood bulk properties and surface properties also influence the interaction of adhesive and substrate (Gollob and Wellons, 1990).

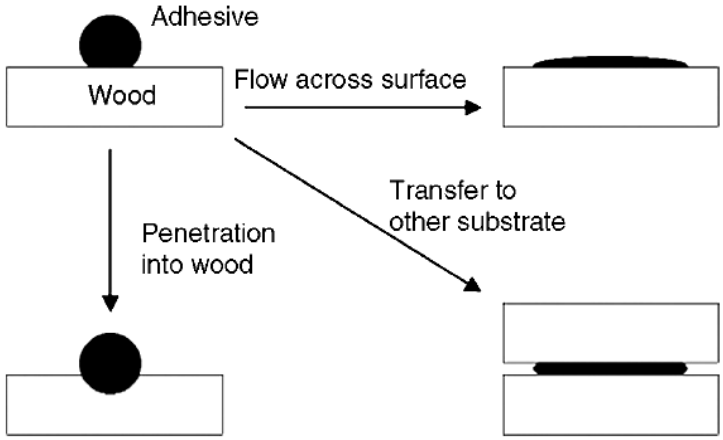

Figure 1. Adhesive wetting of wood surfaces, showing the difference between flow, penetration, and transfer.

Source: Frihart (2005)

2. Environmental friendly wood adhesives

With the rising economic and industrial standards in several country concerns about human health and the environment have been raised due to the increasing demand for a wide range of wood adhesive products. Among commercial wood adhesives, consumption of urea-formaldehyde resins (UF) holds first, followed by phenol formaldehyde (PF) resins, and then by melamine formaldehyde resins. The formaldehyde-based resins, however, have a tendency to release residual formaldehyde during the manufacturing and use of wood panels. The world Health Organization recently concluded that formaldehyde is a human carcinogen. At present, the occupational safety limit for released formaldehyde is about 1 ppm (Peshkova and Li, 2003). In addition, with dwindling petroleum resources and unstable fossil fuel prices, there exists a great deal of uncertainty about the future cost and availability of synthetic adhesives (Imam *et al*., 2001; Liu and Li, 2007; Kim, 2009; Kim and Kim, 2005; Desai *et al*., 2003; Hagg *et al*., 2006). Therefore, environmental friendly wood adhesives have been a subject of interest for many years because of their potential to protect the human health and environment (Imam *et al*., 2001).

Plant polysaccharide (starch) is one class of biomaterials that has been used as an adhesive in a wide range of products, including binders, sizing material, glues, and pastes (Jarowenko, 1977). It is also used for a wide range of adherent such as paper, carton, wood, plastics, leather, and so on (Emengo *et al*., 2002). Characteristic functional groups of starch are ethers and hydroxyls which, due to their polar nature and hydrogen-bonding ability, impart strong adhesion to high energy surfaces like wood. In addition, the high molecular weight of polysaccharides imparts substantial cohesive strength necessary in a useful adhesive. However, the adhesives based solely on polysaccharides have adhesive strengths lower than commercial wood adhesives. Modified starch structure or blended with other materials is making starch-based products commercially acceptable (Das *et al*., 2010; Follain *et al*., 2005). An effective method for overcoming this issue is to blend them with synthesized polymer gel networks in order to form natural and synthesized polymer blend hydrogels (Shi *et al*., 2008). Among the existing synthesized polymers, PVOH possesses many useful properties, such as excellent chemical resistance, water

solubility, optical properties, physical properties, and excellent biocompatibility. Moreover, PVOH/starch blends have demonstrated excellent compatibility, strong interaction of starch, and PVOH through X-ray diffraction (XRD) analysis and produced a strong moisture resistance wood adhesive (Follain *et al*., 2005; Han *et al*., 2009; Imam *et al*., 2001).

2.1 Starch-based adhesives

Starch is one class of biomaterials that has been used as an adhesive for several of products (Jarowenko, 1977) but has not found much utility in wood bonding (Baumann and Conner, 2003). Starch is widely used in paper bonding, especially in the construction of corrugated board used in many packaging applications, but generally lacks the strength and water resistance needed for use in wood bonding (Frihart, 2005). However, their polar nature and hydrogen-bonding ability impart strong adhesion to high energy surfaces like wood and the high molecular weight of polysaccharides imparts substantial cohesive strength necessary in a useful adhesive. There may be suitable for non-structural applications (Hagg *et al*., 2006). In order that the adhesive properties depending on the functionality and sources of starch.

2.1.1 Structure and functionality of starch

Starch is produced by higher plants for energy storage and is the second largest biomass produced on earth, next to cellulose. Starch is also the major energy source in human and animal diets. Starch consists of two major types of molecules, primarily linear amylose and highly branched amylopectin. Normal starch consists of about 75% amylopectin and 25% amylose. In addition to amylose and amylopectin, most cereal normal starches also contain lipids and phospholipids which have profound impacts on the pasting property of the starch. Most tuber and root starches and some cereal starches consist of phosphate monoester derivatives that are found exclusively on amylopectin molecules (Jane, 2004). Starches from various sources are chemically similar, yet their granules are heterogeneous with respect to their size, shape, and molecular constituents (Chiou *et al*., 2005).

Most amylose molecules (molecular weight ~10^5−10^6 Da) are linear and consist of (1→4) linked α-D-glucopyranosyl units. A few molecules are branched

to some extent by (1→6) α-linkages (Figure 2). Amylose molecules can vary in their molecular weight distribution and in their degree of polymerization (DP). These fundamental molecular characteristics affect their solution viscosity, which is essential for processing, and their retrogradation/recrystallization behavior, which is critical for product performance.

Amylopectin is the highly branched polysaccharide component of starch that consists of hundreds of short chains formed of α-D-glucopyranosyl residues with (1→4) linkages. These are interlinked by (1→6)-α-linkages, from 5 to 6% of which occur at the branch points. Despite the amylopectin's high molecular weight (107−109 Da), its intrinsic viscosity is very low (120−190 ml/g) because of its extensively branched molecular structure (Chiou *et al*., 2005).

Starch granules are usually processed by heating in aqueous media, which results in their gelatinization. When starch is heated in water, it absorbs water and swells. This is the process of gelatinization, a process that causes a tremendous change in the rheological properties of the starch suspension (Eliasson and Gudmundsson, 2006). Gelatinization occurs from irreversible swelling of the granules, leading to starch solubilization as amylose leaches from the granules and amylopectin becomes fully hydrated. This process results in the loss of molecular order and the melting of native starch crystals (Chiou *et al*., 2005). The properties of starch gels are very sensitive to factors such as shearing, temperature, heating or cooling rate, and, of course, the source of the starch and the presence of other components. The gelatinization process depends on the presence of both crystalline and amorphous domains in the starch granule (Eliasson and Gudmundsson, 2006).

2.1.2 Tapioca starch

The tropical belt, which covers around 40% of the total land area encompassing five continents and many countries, harbours a number of starch bearing crops that include cereals, tree, fruit and vegetable crops and most important the root crops (Moorthy, 2004). The most important one is root starches, such as taro, some sweet potatoes, tapioca and iris (Hizukuri *et al*., 2006). Minor quantities of starch are extracted from other crops such as screw pine fruits, and the tuber crops

like colocasia, amorphophallus, yams, arrowroot, canna and curcuma but they have no commercial importance.

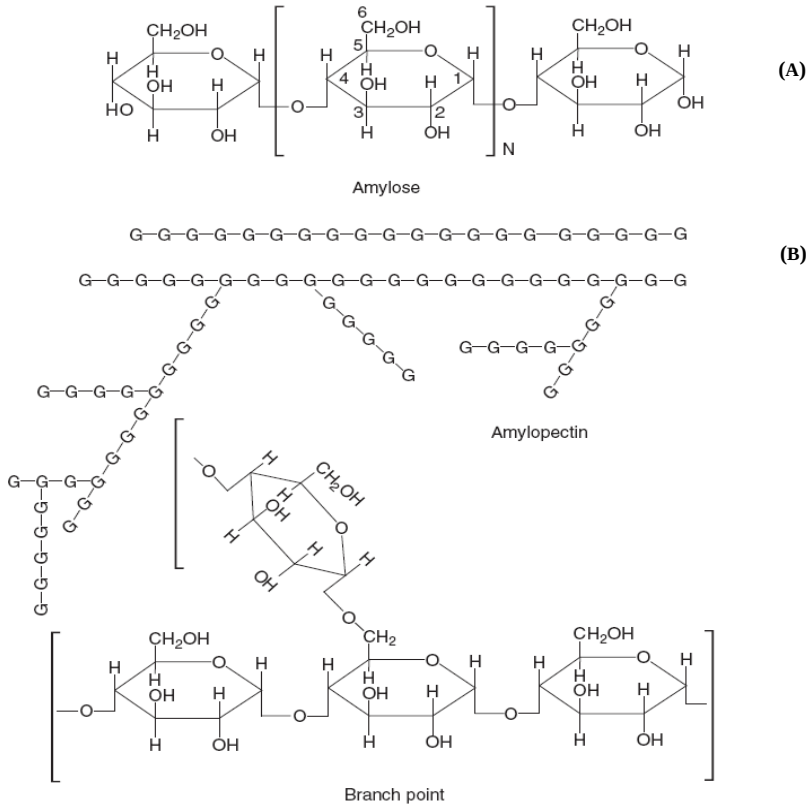

Figure 2. Chemical structures of amylose (A) and amylopectin (B). G is an anhydroglucose unit.

Source: Chiou *et al*. (2005)

Tropical root crops

The major tropical root crops of the world are cassava or tapioca (*Manihot esculenta*), sweet potato (*Ipomoea batatas*), yarns (Dioscorea spp.) and taro (*Colocasia esculenta and Xanthosoma sagittifolium*). The tropical root and tuber crops are important food crops serving either as subsidiary or subsistence food in different parts of the tropical belt. They are rich sources of starch. Cassava and to a small extent, sweet potato (*Ipomoea batatas Lam*) are used for starch extraction in countries like India, Brazil, Thailand, Indonesia, Philippines and China (Moorthy, 2004). They are grown over a range of climates and altitudes and on a variety of soils. Taro is best adapted to wet and flooded areas and is also tolerant to shade. Cassava and sweet potato are grown from high rainfall to semi-arid regions because they

tolerate drought and will grow in a wide range of soils. However, a disadvantage of root crops is that, except for yams, they cannot be stored for long after harvest, and because they perish rapidly. Therefore, they are difficult to transport to markets (Bradbury and Holloway, 1988).

Tapioca starch or cassava starch

The cassava plant has been classified as *Manihot utilissima* Pohl of the family Euphorbiaceae. The name *Manihot esculenta* is being increasingly adopted.

Cassava is the term usually applied in Europe and in the United States to the roots of the plant, whereas, *tapioca is* the name given the processed products of cassava. The word tapioca is derived from tapioca, the Tupi Indian name for the meal which settles out of the liquid expressed from rasped tubes and made into pellets and then called triiocet.

Cassava (*Manihot esculenta Crantz*) is a major crop in the tropics and over half a billion of the world's population depends on it (Aryee *et al*., 2006; Matsui *et al*., 2004). Moreover, it is one of the economically important crops in Thailand and the cheapest raw material of starch production (Bangyekan *et al*., 2006).

Tapioca starch is easily extractable since the tubers contain a very low quantity of proteins, fats, etc. Hence the extraction process is simple and the starch obtained is pure white in color if the process is carried out properly. Since the lipid content in the starch is very little (<0.1%) (Table 1).

Table 1. The minor componential characteristics of starch granules.

Starch	Granule size μm	Amylose %	Lipid %	Proteins %	Ash %	Phosphorus %	Source
Wheat	2-35	25	0.80	0.40	0.20	0.06	Cereal
Potato	15-100	22	0.05	0.06	0.40	0.08	Tuber
Maize	5-25	26	0.70	0.35	0.10	0.02	Cereal
Yam	22.8	26	neg.*	0.10	-	0.01	Root
Tapioca	5-35	20	0.10	0.10	0.20	0.01	Root

*neg., negligible.

Source: Adapted from Collado and Corke (2003); Zaidul *et al*. (2007)

The presence of high amounts of lipid in maize and wheat starch has unfavorable effects. The lipids repress the swelling and solubilization of maize and wheat starch granules. The lipids also increase the pasting temperatures and reduce the water-binding ability of these starches. The presence or formation of insoluble amylose–lipid complexes causes turbidity and precipitation in starch pastes and starch solutions Collado and Corke (2003).

The tapioca starch granules are mostly round with a flat surface on one side containing a conical pit, which extends to a well-defined eccentric hilum. The granules exhibit wide variation in size range (5±40 μm) and variation in granular size distribution among varieties and during growth period during different seasons.

Table 1 shows the tapioca starch has very little lipid and phosphorus content. The amylose content in the starch is in the range similar to most other starches. For The gelatinization temperatures of tapioca starch determined microscopically by various workers ranged from 49±64°C to 62±73°C and gelatinization enthalpy is in range from 4.823 to 16 J/g. Among different tuber starches, tapioca starch possesses the lowest gelatinisation temperatures. It depends on a number of factors like crystallinity, intermolecular bonding, rate of heating of the starch suspension, presence of other chemicals, etc (Moorthy, 2004).

Root and tuber starches, such as potato and tapioca, consist of little lipids and thus display lower pasting temperatures and greater peak viscosities (Jane, 2004). Viscosity is an important starch property on which many applications are based. Studies on viscosity of tapioca starch have been carried out extensively and almost all their studies indicate a high viscosity level for tapioca starch compared with most other tuber starches and the cereal starches. The viscosity characteristics are influenced by varietal differences, environmental factors, rate of heating, other ingredients present in the system etc. When the starch granules swell and they are subjected to heat and shear, the starch undergoes fragmentation and the resulting reduction in viscosity indicates the breakdown of the starch. Tapioca starch has a higher breakdown compared to most other starches, especially the cereal starches (Moorthy, 2004).

With a variety of useful properties of tapioca starch such as gelatinization, crystallinity, polar nature and hydrogen-bonding ability, allows the use

of tapioca starch in a wide range of products, either as a raw material like starch based adhesive or as a food additive. It can works as a thickener, as a gelling agent, as an absorber of water, as a source of energy in fermentation, as a bulking agent, or as an antisticky/sticky agent. As for the majority of starch-derived adhesives are used in the paper and textile industries as binders and sizing materials.

2.1.3 Applications of starch adhesives

The majority of starch adhesives are used in numerous adhesive applications, such as tube winding, paper, laminating, case, carton sealing, bottle labeling, flat gumming, envelope sealing, gummed tape manufacture and textile industries as binders and sizing materials (Baumann and Conner, 2003; Kennedy and Fischer, 1984). In addition, starch adhesive that is used as a binder and adhesive in building materials, paints and molded pulp products should have a thin consistency, good tackiness and stable viscosity (Chung and Manhattan, 1991).

Unmodified and modified starch extracted from root crops, cereals and a legume such as sweet potato, yam, tapioca, corn, rice and soybean starch have been assessed as bases for adhesives for paper-paper, paper-cardboard, paper-metal and paper-glass substrates by the study of Emengo *et al*. (2002). They found that adhesives based on unmodified starch from all the crops investigated produced low or high tack for paper-paper and paper-cardboard depending on the intensity of mechanical action or heat applied in the formulation process. However, none of the starches produced good tack for paper-metal and paper-glass. Whilst, adhesives based on starch from yam, tapioca, potatoes and corn modified by acid moisturing and roasting at temperature between 220°C and 250°C produced high tack and bonding strength for paper-paper and paper-glass (Table 2). Because of starch modifying reduced their number average molar masses thereby conferring adhesive action.

However, as known that starch adhesive also lacks the strength needed for use in wood bonding (Frihart, 2005). Therefore, starch must be modified before it can be used as an adhesive. Methods for opening the starch granules include heating, alkali treatment, acid treatment and oxidation (Baumann and Corner, 2003).

Table 2. Effects of roasting temperature on paper-paper and paper-glass bonding strength of various starch-based adhesives[a]

Roasting temperature	Paper-paper and paper-glass bonding strength			
°C	yam	tapioca	potato	corn
-	M	M	M	M
200	H	H	H	H
220	H	H	H	H
250	H	H	H	H
260	M	M	M	M
280	L	L	L	L

[a] L: low, M: medium, H: high

Source: Emengo *et al*. (2002)

1. Heat treatment : the simplest method of breaking up starch granules is well known to the cook. During the heating process, the starch granules first swell and then burst with a coincident thickening of the suspension. The temperature at which this thickening occurs is called the gelation temperature. Suspensions of amylose and high-amylose starches have a tendency to harden and become solid upon cooling. This process is called retrogradation or setback and is a result of the tendency of linear molecules to align with one another. This aligning effect also means that at the same solids content, suspensions with a higher ratio of amylose to amylopectin have a higher viscosity.

2. Alkali treatment : the gelation temperature can be lowered by the addition of sodium hydroxide to a starch suspension. If sufficient alkali is added, the starch can be induced to gel at room temperature.

3. Acid treatment (thin-boiling starches) : is achieved by heating the starch to 49–54°C with small amounts of aqueous mineral acid, followed by neutralization with base. The acid acts mainly on the amorphous regions of the starch granules. Dried acid-modified starch appears very similar to its unmodified counterpart. This makes the modified starch useful in applications that require higher solids content.

4. Oxidation is commonly obtained by aqueous alkaline hypochlorite treatment. A starch suspension at pH 8–10 is treated with hypochlorite (5–10% Cl

based on starch) for long enough to produce the desired viscosity. There appears to be little change in the crystalline region of the starch. Dried oxidized starch is generally whiter than unmodified starch, since the oxidation and subsequent rinsing tend to remove impurities that may be present in native starch. Oxidized starches behave similarly to the acid-modified starches upon gelling. However, the oxidized starches have greater tack and adhesive character, and thus they are used more frequently in adhesive preparations.

Chung and Seib (1991) prepared thin-boiling and non-gelling adhesive, granular wheat and corn starches were thinned by treatment with aqueous hydrochloric acid or sodium hypochlorite and then hydroxypropylated with propylene oxide. They found that chlorine oxidation gave more rapid chain cleavage and whiter products with better freeze-storage stability than acid-treatment. The best adhesive was judged by bonding strength, viscosity stability and freeze-thaw stability, resulted from wheat or corn starch oxidized with 0.82% Cl at pH 8.0 for 1 h followed by hydroxypropylation to molar substitution.

2.2 PVOH-based adhesives

Polyvinyl alcohol (PVOH) is the largest synthetic water polymer produced in the world (Ramaraj, 2007). It is highly regarded as a biodegradable polymer which has created great impact through its application in innovations in domestic and specialist industries. The chemical resistance and physical properties of PVOH have led to its broad industrial use (Krumova *et al*., 2000; Jaffe and Rosenblum, 1990). The end uses of PVOH include textile, paper treatment, paper sizing, wet-strength adhesives, polymerization aid, joint cements for building construction, water-soluble film for hospital laundry bags and emulsion polymerization. In addition, they are excellent adhesives and highly resistant to solvents, oil and grease (Ebewele, 2000; Jaffe and Rosenblum, 1990).

2.2.1 Structure and properties of PVOH

Herrmann and Haehnel were the first to prepare PVOH in 1924 by saponifying polyvinyl esters with stoichiometric amounts of caustic soda solution. PVOH is one of the few linear, non-halogenated, aliphatic polar polymers. The backbone of the PVOH macromolecular chain possesses mainly 1, 3-diol units. The

content of 1,2-diol units in PVOH obtained by hydrolysis of polyvinyl acetates is about less than 1–2% (Das *et al*., 2009a).

PVOH is known to have not only good chemical stability, good film-forming and mechanical properties, but also be an excellent alcohol barrier, water-soluble synthetic resin and a cheap polymer (Gu *et al*., 2008). However, the physical properties of PVOH depend to a greater extent on the method of preparation than it is the case with other polymers (Blomstrom, 1989; Krumova *et al*., 2000). They are produced by the hydrolysis of polyvinyl acetate; the theoretical monomer, CH_2=CHOH, does not exist. The final properties are affected by the polymerization conditions of the parent polyvinyl acetate as well as by the hydrolysis conditions, drying and grinding. It is difficult to assign specific physical properties to solid PVOH as this designation refers to an array of products, including copolymers of vinyl acetate-vinyl alcohol (Krumova *et al*., 2000).

Generally, PVOH is an odourless and tasteless, translucent, white or cream colored granular powder. They are soluble in water, slightly soluble in ethanol, but insoluble in most common organic solvents, e.g., gasoline, kerosene, benzene, xylene, trichloroethylene, carbon tetrachloride, methanol, ethylene glycol, acetone and methyl acetate. Typically a 5% solution of PVOH exhibits a pH in the range of 5.0 to 6.5. PVOH has a melting point of 180 to 190°C. It has a molecular weight of between 26,300 and 30,000 and a degree of hydrolysis of 86.5 to 89% (Saxena, 2004). A wide range of grades, depending on weight and degree of hydrolysis, is offered by PVOH manufacturers. Grade include both the fully hydrolyzed form on polyvinyl acetate and products containing residual, i.e., unhydrolyzed, acetate groups (Jaffe and Rosenblum, 1990). However, two main types of PVOH, partially hydrolyzed (Figure 3 (A)) and fully hydrolyzed (Figure 3 (B)), are of industrial importance (Skeist, 1990; DeMerlis and Schoneker, 2003).

The physical properties of PVOH are controlled by molecular weight and the degree of hydrolysis such as solubility and solution viscosity, as shown in Figure 4. The degree of hydrolysis of PVOH is controlled during the alcoholysis and is independent of molecular-weight control. However, the viscosity of PVOH solution is also controlled by concentration and temperature. Degree of hydrolysis does not strongly affect viscosity, although the viscosity is proportional to degree of

hydrolysis at constant molecular weight. The viscosities of partially hydrolyzed PVOH solution remain stable if the solutions are stored at high temperatures over a wide range of concentrations.

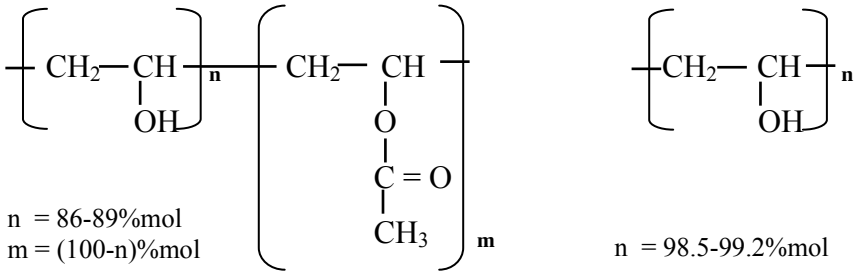

(A) (B)

Figure 3. Structural formula of polyvinyl alcohol: (A) partially hydrolyzed; (B): fully hydrolyzed.

Source: DeMerlis and Schoneker (2003)

However, viscosities of concentrated solutions of fully hydrolyzed PVOH gradually increase over a period of days when stored at room temperature and gelation occurs in products that contains <1 mol % acetate groups. This viscosity increase of gelation can be reversed by reheating. Lower solution concentrations and lower degrees of hydrolysis eliminate viscosity instability associated with long-term solution storage (Jaffe and Rosenblum, 1990). Furthermore, PVOH is a crystalline polymer. The degree of crystallinity depends strongly on the structure. The degree of crystallinity of fully saponified PVOH is increased by heat treatment, which also lowers the solubility in water. This effect is less marked for PVOH that possesses acetyl groups (Das *et al*., 2009).

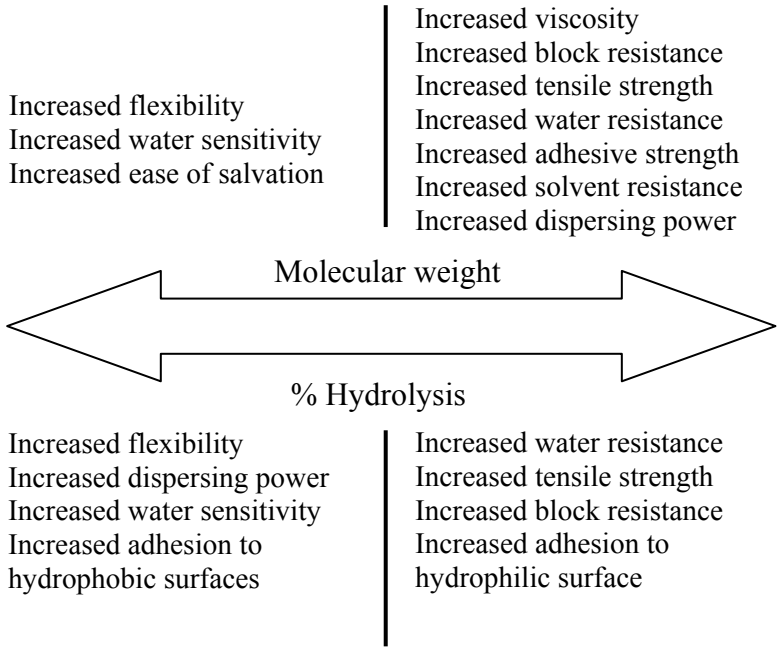

Figure 4. Properties of polyvinyl alcohol.
Source: Jaffe and Rosenblum (1990)

The end uses of PVOH include textile and paper treatment and wet-strength adhesives. It is also used as a polymerization aid such as a thickening and stabilizing agent in emulsion polymerization in cosmetics and as packaging film requiring water solubility. With their much higher water absorption capacity and cottonlike feel, formaldehyde-modified polyvinyl alcohol fibers, vinal or vinylon fibers, can replace cotton in applications requiring body contact. These PVOH fibers have good dimensional stability and abrasion resistance, wash easily, and dry quickly (Ebewele, 2000).

2.2.2 Applications of PVOH adhesives

PVOH is a first-class adhesive in its own right. It also serves as an excellent additive for modifying the properties of polyvinyl acetate emulsion adhesives. Furthermore, PVOH adheres particularly well to cellulosic substrates such as wood or paper (Ebewele, 2000; Jaffe and Rosenblum, 1990). Both fully hydrolyzed grade and tackfied grade have been extensively used as adhesive for paper and paper board. For example, they can be used in formulating quick-setting water resistant adhesives for bag seam and bag bottom pastes. They are also used as paper

laminating adhesive for the manufacture of solid fiberboard, liner board, spiral wound tubes and drums. In many of these applications, PVOH are used in combination with extender such as clay, starch and dextrin. They set rapidly to form water resistant bonds and also give excellent mileage. On the other hand, chemical cross-linking of PVOH can provide feasible routes for the improvement of the mechanical properties, water resistance and thermal stability which due to reaction of hydroxyl groups can be used to obtain tridimensional networks in PVOH (Krumova *et al*., 2000). Moreover, the need to meet exacting end-use requirements and at the same time reduce costs is stimulating a broad spectrum of polymer development involving the use of fillers and reinforcements to upgrade product performance rather than the development of new and usually more expensive resins (Ebewele, 2000).

2.3 Development of starch/PVOH based wood adhesive

Due to the fact that the adhesives based solely on polysaccharides have an adhesive strength lower than commercial wood adhesives. These may be suitable for non-structural applications (Hagg *et al*., 2006). Starch is also brittle, poor mechanical properties and high moisture sensitivity. To overcome these drawbacks and to make starch-based products commercially acceptable, it is suitably modified or blended with other materials (Das *et al*., 2010). PVOH/starch blends have demonstrated excellent compatibility, strong interaction of starch, PVOH through X-ray diffraction (XRD) analysis, and produced a strong moisture resistant wood adhesive (Follain *et al*., 2005; Han *et al*., 2009; Imam *et al*., 2001). Some researchers studied the performance PVOH/starch blends treated with a cross-linking agent were higher than the pure blends (Das *et al*., 2010; Imam *et al*., 2001; Imam *et al*., 1999).

2.3.1 Polyblending

Polyblending has become one of the most commercially important and inexpensive ways to produce high performance materials (Cazacu and Popa, 2005). Polymer blend is one of the effective methods for providing new desirable polymeric materials for a variety of applications. Polymer blend technique is a mixing of two or more polymers together to produce blend, for achieving a specified portfolio of physical properties without the need to synthesize specialized polymer system (Hope and Folkes, 1993). Polymer blend can be subdivided into two main categories:

incompatible and compatible blends. Incompatible or immiscible blends are blends in which the two components consist of separate well-defined phases or domains and are characterized by poor mechanical properties, representing the large majority of polymer blends. Compatible or miscible blends present a single phase and their mechanical properties may be superior to those of the component polymers (Cazacu and Popa, 2005).

Many researchers studied preparation and characterization of starch and PVOH blending (Tudorachi *et al*., 2000; Hyder and Chen, 2010; Han *et al*., 2009). Because of starch and PVOH molecules have a large number of hydroxyl groups and have demonstrated excellent compatibility (Follain *et al*., 2005). However, the blended polymers display a hydrophilic nature. Thus the water resistance of blended polymer needs to be improved for it to be used in environmental and adhesive applications. Moreover, Siddaramaiah and Somashekar (2004) found that the addition of starch to PVOH does not improve its physical properties. The mechanical properties and water resistance of this blended polymer need to be improved for adhesive to be used in the environment (Shi *et al*., 2008).

2.3.2 Cross-linking

Cross-linking reaction is chemically modifying the blended polymer during or after the blending process (Shi *et al*., 2008). Where the functionality of one of the monomers is greater than 2, then a cross-linked polymer is formed (Figure 5). Thermosets like phenol–formaldehyde, urea–formaldehyde, and epoxy resins develop their characteristic properties through cross-linking (Ebewele, 2000). PVOH can be readily cross-linked for improved water resistance (Jaffe and Rosenblum, 1990). Examples of cross-linking reagents include glutaraldehyde (Ramaraj, 2007), borax acid (Das *et al*., 2010), hexamethoxymethylmelamine (HMMM) (Imam *et al*., 2001), melamine-formaldehyde and epichlorohydrin. An acid catalyst, e.g., citric acid, ammonim sulfate or ammonium chloride are necessary with the HMMM and formaldehyde cross-linkers, respectively (Jaffe and Rosenblum, 1990; Imam *et al*., 2001).

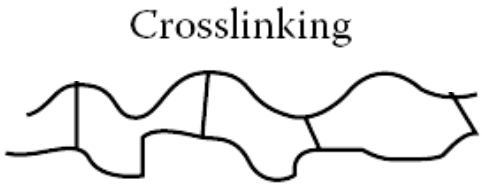

Figure 5. Schematic of cross-linked polymer.
Source: Das *et al.* (2009)

- Borax or sodium tetraborate decahydrate in the presence of small amounts of sodium hydroxide is the most widely used additive to starch-based adhesives. It increases the viscosity and acts as a tackifier and viscosity stabilizer. These effects are particularly important in machine application of adhesive to substrate. Enough sodium hydroxide is added to convert the borax to sodium metaborate, which is the active boron species in thickening. The metaborate is able to hook two starch molecules together, forming a complex (Figure 6) (Baumann and Corner, 2003). Then, the gelation is usually accomplished using boric acid or borax (Frihart, 2005). Moreover, borax reacts strongly with PVOH and is widely used industrially as gelling agents. PVOH is extremely sensitive to borax, which causes gelation by forming a bisdiol complex (Jaffe and Rosenblum, 1990). Some researchers also use borax as a cross-linker and studied thermal, mechanical and surface properties of borax cross-linked starch/PVOH. They reported that the mechanical properties and thermal stability of starch/PVOH blends treated with borax were higher than the pure blends (Das *et al*., 2010).

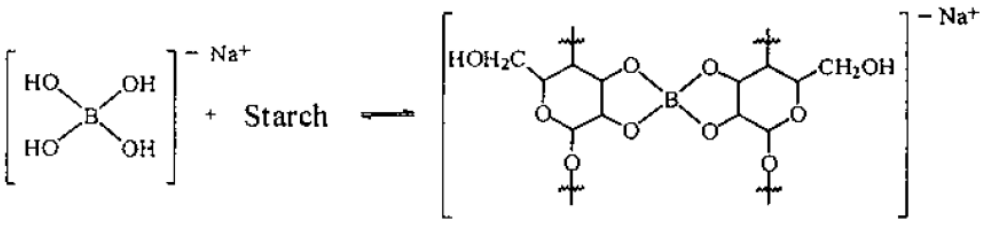

Figure 6. Complexation of starch molecules by the borax in basic solution.
Source: Baumann and Corner (2003)

- Hexamethoxymethylmelamine (HMMM) is a crosslinker that can be cross-linked with a molecule having OH and carboxyl groups such as starch,

PVOH and waterborne polyurethane (Rahman *et al*., 2009). HMMM has a low methylol and a high imino content and can be described as oligomeric in nature with main functionalities, methoxymethyl and imino. They react according to general acid catalysis with a high tendency towards self-condensation reactions that improve the reaction speed but limit the flexibility of the cured films. These methylated high imino melamine resins have a low tendency towards demethylolation reactions and consequently they release very low amounts of formaldehyde upon curing. HMMM can use in various coating application such as metal, automotive, coil, paper and general industrial coating (Cytec, 2009). Figure 7 shows chemical cross-linking reaction between starch, PVOH and cellulose molecule with the HMMM cross-linker.

- Citric acid (CA) with one hydroxyl and three carboxyl groups exists widely in citrus fruits and pineapples, where it is the main organic acid (Shi *et al*., 2008). CA was chosen as the additive for the following reasons. First of all, as a result of its multi-carboxyl structure, esterification could take place between the carboxyl groups on CA and the hydroxyl groups on the PVOH or starch. Such an esterification would improve the water resistibility (Borredon *et al*., 1997). Furthermore, because of the multi-carboxyl structure, CA may serve as a cross-linking agent to improve the mechanical properties and water resistibility. Second, the residual-free CA in the blends may act as a plasticizer. As compared to the hydroxyl groups on glycerol, the carboxyl groups on CA can thus form stronger hydrogen bonds with the hydroxyl groups on PVOH/starch blends, thus improving the interactions between the molecules (Yu *et al*., 2005; Shi *et al*., 2008). The third point, CA is rated as nutritionally harmless since it is a nontoxic metabolic product of the body. Consequently, it has already been approved by FDA for use in humans. These nontoxic properties will benefit the incorporation of CA in food packaging industry.

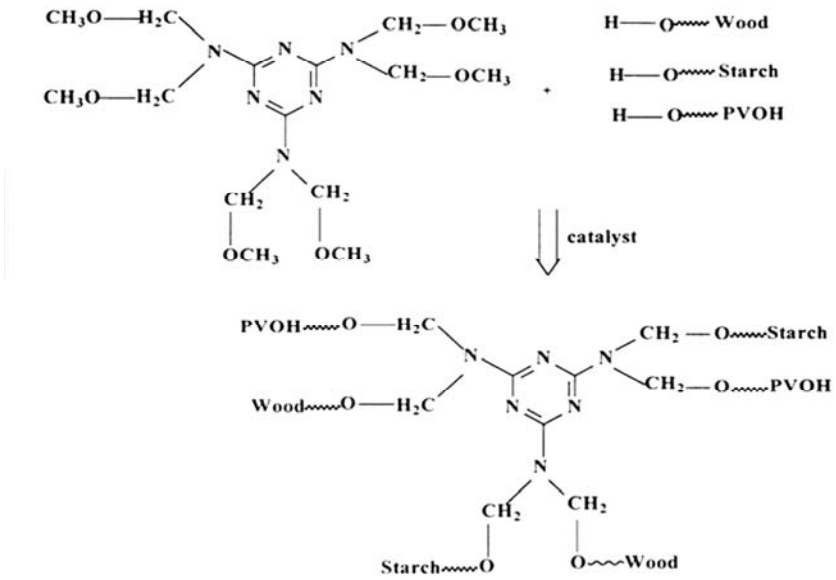

Figure 7. Schematic representation of chemical cross-linking reaction.
Source: Imam *et al*. (2001).

Imam *et al*. (2001) and US Department of Agriculture (USDA) scientists used HMMM as the cross-linking agent in the presence of a catalytic amount of citric acid for preparation of wood adhesive. They succeed to development a starch-based adhesive in which starch was chemically cross-linked with PVOH. The cross-linker can improve the physical properties of PVOH/starch blend (Hyder and Chen, 2009). Many researchers have used HMMM as a cross-linker for adhesives such as waterborne polyurethane (WBPU) adhesive (Mequanint and Sanderson, 2003; Rahman *et al*., 2007). The results showed the methoxy groups in HMMM can participate in a cross-linking reaction with WBPU, via the carboxyl groups or hydroxyl groups. They found that two methoxy groups per HMMM molecule, containing six methoxy groups, participated in the cross-linking reaction upon to optimum HMMM content and optimum pressing conditions for joint values (175°C and 500 psi). The adhesive strength was significantly increased by cross-linking, up to the optimum content of HMMM and gave the highest failure temperature and thermal stability of adhesives. However, some researcher also found that the cross-linked films showed little or no disintegration when exposed to aqueous environment and cross-linking did not affect the biodegradability of the films (Das *et al*., 2010).

2.3.3 Reinforcing filler

Fillers and reinforcements have used to upgrade product performance rather than the development of new and usually more expensive resins. Because of their advantageous light weight, high strength, fatigue life, and corrosion resistance, structural composites have been used successfully and admirably in aircraft and in numerous industrial and consumer applications in place of conventional materials like metals in term of composite materials (Ebewele, 2000).

A composite is a multi-phase material consisting of two or more physically distinct components, a continuous (matrix) phase and a dispersed (filler or reinforcement) phase (Figure 8). Filler size has an impact on composite properties, with high aspect ratio and nano-sized particles displaying significant improvements in composite properties, including strength, thermal stability and gas barrier, with considerably lower volume fraction compared with their counterpart macro-sized particles (Spoljaric *et al*., 2009).

Different types of fillers are employed in resin formulations; the most common are calcium carbonate, talc, silica, clay, calcium sulfate, mica, glass structures, alumina trihydrate and crops fiber (Ebewele, 2000). Fiber-reinforced materials have moved within a short time from being a curiosity to having a central role in engineering materials development. Polymers, thermoplastics, and thermosets can be reinforced to produce quite frequently a completely new kind of structural materials. Furthermore, fiber-reinforced plastic (FRP) composites are increasingly being used as reinforcement for wood (Davalos and Qiao, 2003). New FRP–wood hybrid materials for high volume construction applications are being developed from low-cost constituents. Two types of FRP–wood reinforcements are being employed: FRP strips (plates) bonded to wood and wood cores wrapped with FRP by filament winding. There are some useful studies in the literature on agricultural fibers in biocomposite films (Wang *et al.*, 2006; Bondeson and Oksman, 2007; Alemdar and Sain, 2008a; Roohani *et al*., 2008). There has been a growing interest for cellulose whisker, microfibrillated cellulose, microcrystalline cellulose and cellulose nanofibers (Bondeson and Oksman, 2007).

PVOH and starch are well suited for blends with cellulose since they are highly polar and can be dispersed in water solutions (Roohani *et al*., 2008). In

numerous researchers prepared and characterized cellulose reinforced PVOH and starch composite films. The results indicated that the strong interactions between fillers and between the filler and matrix play a key role in reinforcing the resulting composites. Incorporating cellulose fiber into PVOH and starch matrix lead to an improvement in tensile strength, young's modulus, water resistance thermal property, lower density, manufacturing process and crystallization (Lu *et al*., 2005; Lu *et al*., 2006; Lu *et al*., 2008; Alemdar and Sain, 2008b; Bhatnagar and Sain, 2005; Wang and Sain, 2006; Roohani *et al*., 2008).

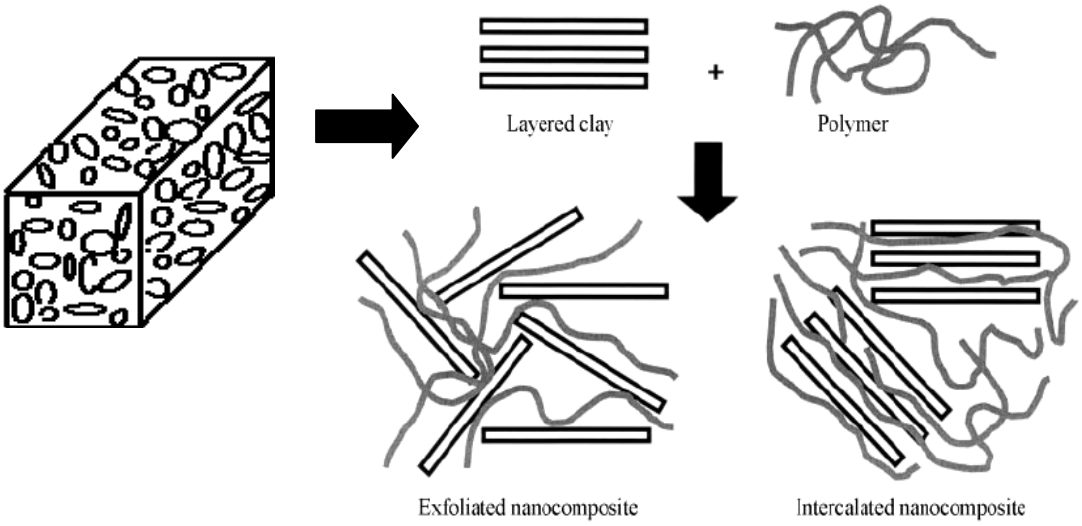

Figure 8. Schematic of exfoliated and intercalated nanocomposite formation.
Source: Dean and Yu (2005)

3. Cellulose biomass sources

3.1 Introduction

Cellulose is the world's most abundant naturally occurring organic substance, rivaled only by chitin. It has been estimated that nature synthesizes from 100 to 1000 billion (10^{11} to 10^{12}) metric tons of cellulose every year (Coffey *et al.*, 2006). It is therefore not surprising that humans have made use of cellulose on a vast scale in the paper, building and allied industries, and as a source of bioenergy. Cellulose is the major structural polysaccharide in the cell walls of higher plants and can be obtained from many agricultural by-products such as rye, barley, wheat, oat straw, corn stalks, and sugarcane. Moreover, there also found in the cell walls of

green algae and membranes of fungi (Izydorczyk *et al.*, 2005). This applies to cellulose in its natural state, isolated, or as a source of raw material for modification into products having different properties from those of pure cellulose. Wood pulp is the main source of processed cellulose, the bulk of which is converted to paper and cardboard, and about 2%, amounting to just over 3 million tons, into regenerated fiber and films or chemical derivatives (Coffey *et al.*, 2006).

Cellulosic biomass includes agricultural (e.g., corn stover and sugarcane bagasse) and forestry (e.g., sawdust, thinnings, and mill wastes) residues, portions of municipal solid waste (e.g., waste paper), and herbaceous (e.g., switchgrass) and woody (e.g., poplar trees) crops. Such materials are abundant and competitive in price with petroleum, and cellulosic biomass can provide a sustainable resource that is truly unique for making organic products (Wyman *et al.*, 2005). An addition, natural fibers from crop residues are a low-priced, sustainable natural resource and have a much lower density than most reinforcement fillers that are in use today (Bhattacharya *et al*., 2008). With increasing environmental protection consciousness, natural fibers as a relatively new group of environmental friendly materials are in considerable demand in recent years, by unifying technological, economical and ecological aspects (Bledzki *et al*., 2001).

3.2 Sugarcane bagasse fibers

The agricultural sector of Thailand annually produces large amounts of biomass in crops such as corn straw, rice straw, soy hulls and sugarcane bagasse. The sugarcane bagasse (Figure 9) is a by-product obtained after sucrose extraction from the sugarcane plant. Addition, sugarcane bagasse have been the subject of papermaking developments on numerous occasions and for the future, with advances in pulping technology, it is conceivable that bagasse pulping operations can be made feasible where the economics of competitive materials will allow it (Ott *et al.*, 1954). However, the fibers has a high proportion of cellulose, which can be readily isolated from the other components namely lignin and hemicellulose, by pulping. The sugarcane bagasse provides an ideal opportunity for producing value-added products from such an inexpensive source of biomass. The sugarcane bagasse is also a by-product of the Thailand sugar cane to bioethanol program where it is burned in

cogeneration facilities (Zanin *et al*., 2000). It could equally well be used, in part, as a source of cellulose nanoparticles (Bhattacharya *et al*., 2007). Basic composition of different natural fibers source indicated in Table 3.

Figure 9. Sugarcane bagasse fibers.

Table 3. Chemical composition of different cellulose based natural fibers.

Composition	**Cotton**[1]	**Jute**[1]	**Flax**[1]	**Soy hulls**[2]	**Wheat straw**[2]	**Sugarcane bagasse**[3]
Cellulose	82.7	64.4	64.1	56.4	43.2	50.0
Hemi-cellulose	5.7	12.0	16.7	12.5	34.1	25.0
Lignin	-	11.8	2.0	18.0	22.0	20.0
Others	11.6	11.8	17.2	13.1	0.7	5.0

Source: [1] Adapted from Bledzki and Gassan (1999)

[2] Adapted from Alemdar and Sain (2008b)

[3] Adapted from Arib *et al*. (2006)

Moreover, for an application, the nonfibrous cellulose material produced is used as a stiffening agent in paperboard manufacture, and bleached cellulose fiber is used for light-weight and high-grade papers for numerous uses. Four tons of the bagasse has been found to yield one ton of high-grade bleached cellulose fiber (Ott *et al.*, 1954).

3.3 The nature and structure of cellulose

3.3.1 Cellulose and its cell wall

As the known that cellulose is the essential component of all plant-fibres. In 1838, Anselme Payen suggested that the cell walls of large numbers of

plants consist of the same substance, to which he gave the name cellulose (Bledzki and Gassan, 1999). Thus, cellulose is the major structural polysaccharide in the cell walls of plants. In fact, the primary cell wall is a glycoproteinaceous layer composed of pectin, cellulose, hemicellulose, and proteins. The Figure 10 indicated a schematic of the plant cell walls. Cellulose chains are formed into microfibrils, which constitute the basic framework of the cell conveying a great resistance to tensile forces (Perez and Mazeau, 2005). Cellulose microfibrils associated with smaller molecules, hemicelluloses, and lignins, can provide a type of liquid crystalline matrix in which microfibrils can slide past one another, or else cause a disordered arrangement that resists further cell wall extension.

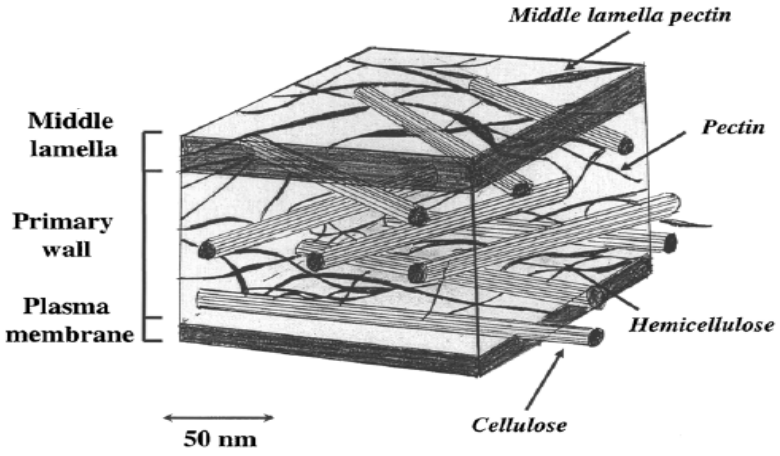

Figure 10. Schematic representation of the plant cell walls along with the location of the main polysaccharides components.

Source: McCann *et al*. (1990); Perez and Mazeau (2005)

3.3.2 Chemical composition and cellulose structure

Cellulose is a high molecular weight polymer of (1→4)-linked β-D-glucopyranose residues that average of 3000 units per chain, corresponding to an average molecular weight of about 500000 (Chebli and Cartilier, 1998). The pyranose rings are in the $^4C_1$ conformation, which means that the $–CH_2OH$ and –OH groups, as well as the glycosidic bonds, are equatorial with respect to the mean planes of the rings (Bledzki and Gassan, 1999). The Haworth projection formula of cellulose is given by Figure 10. The β-(1→4) linkages give this polymer an extended ribbon-like

conformation. Every second residue is rotated 180°, which enables formation of intermolecular H-bonds between parallel chains. The tertiary structure of cellulose, stabilized by numerous intermolecular H-bonds and Vander Waals forces, produces three-dimensional fibrous crystalline bundles (Izydorczyk *et al*., 2005). The β-1,4 diequatorial configuration results in a rigid and linear structure for cellulose. The abundance of hydroxyl groups and concomitant tendency to form intra- and intermolecular hydrogen bonds results in the formation of linear aggregates. This contributes to the strength shown by cellulose-containing structures in plants and also to the virtual insolubility of cellulose in common solvents, particularly water (Coffey, *et al.*, 2006).

Figure 11 shows the different reactivities of hydroxyl groups of each glucose. The C-6 OH group (OH^1) is the most reactive (primary carbon), the C-2 OH group is less reactive (OH^2) and the C-3 OH group (OH^3) is the weakest for the 'bent' conformation with reasonable distance which allows the formation of a hydrogen bond between C-3 OH and the neighboring oxygen molecule (Chebli and Cartilier, 1998). The molecular size of polymer molecules can be conveniently described in terms of degree of polymerization (DP), which is an average value of the number of monomer units by various physical techniques (intrinsic viscosity measurement, light scattering, etc.) (Coffey *et al.*, 2006). In general, the DP of cellulose from primary walls of vascular plants is about 4000 (Franz and Blaschek, 1990; Laosinchai, 2002). The degree of polymerization (DP) of native celluloses depends on the source and it is not well established. In fact, the combination of procedures required to isolate, purify, and solubilize cellulose generally causes scission of the chains. Values of DP ranging from hundreds and several tens of thousands have been reported (Mark, 1981). For the mechanical properties of natural fibers depended on its cellulose type, because each type of cellulose has its own cell geometry and the geometrical conditions determine the mechanical properties (Pérez and Mazeau, 2005).

From these reasons of cellulose composition and their structure had result in that cellulose is distinguished analytically from the extractives by its insolubility in water and organic solvents. Cellulose was different from the hemicelluloses by its insolubility in aqueous alkaline solutions, and from lignin by its relative resistance to oxidizing agents and susceptibility to hydrolysis by acids.

However, cellulose dissolves in strong mineral acids with hydrolysis to dextrins and oligosaccharides, and ultimately to D-glucose. Cellulose is soluble in a few solvents such as cuprammonium and cupriethylenediamine hydroxides (Browning, 1967).

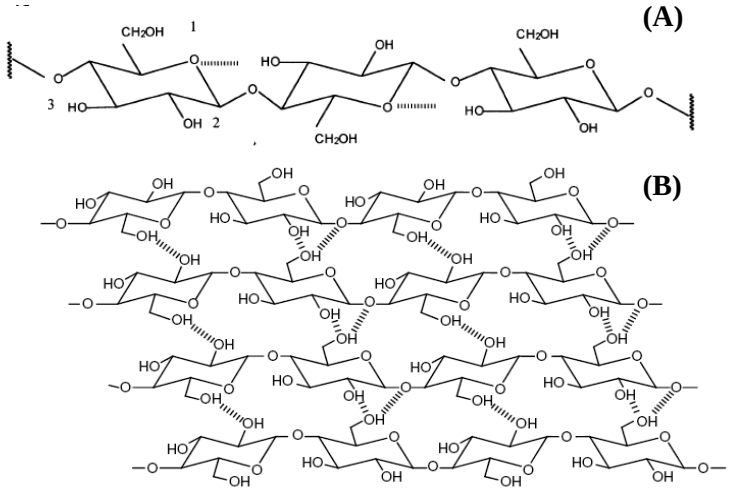

Figure 11. Basic structure of cellulose: repeating units (A), illustration of intermolecular hydrogen bonds (B).

Source: Izydorczyk *et al.* (2005).

3.4 Crystallinity and polymorphism of cellulose

It has been known that the cellulose chains are biosynthesized and self-assembled into microfibrils. These microfibrils are constituted by amorphous and crystalline domains. The degree of crystallinity (ratio between the mass of crystalline domains and the total mass of the cellulose) and typical dimensions are dependent on their origin, although the biosynthetic mechanism is the same in all organisms (Lima and Borsali, 2004).

The great interest in cellulose macromolecules is because of their crystalline orientation. Their physical properties are strongly influenced by their crystallinity. The structure of the microcrystalline cellulose surfaces and their interactions with other macromolecules is also dependent on the crystalline structure and on the packing of the cellulose sheets (Lima and Borsali, 2004). However, crystalline cellulose has a very limited accessibility to water and chemicals. Chemical attack can therefore be expected to occur primarily on amorphous cellulose and crystalline surface (Bledzki and Gassan, 1999).

Crystalline Structure

The free hydroxyl groups present in the cellulose macromolecules are likely to be involved in a number of intramolecular and intermolecular hydrogen bonds, which may give rise to various ordered crystalline arrangements (Pérez and Mazeau, 2005). The X-ray diffraction had use to experiment of different native cellulose sources led to the models of native cellulose differing in the number and orientation of glucose units in the unit cell. Seven crystal polymorphs have been identified for cellulose, which are designated as I_{α}, I_{β}, II, III_{I}, III_{II}, IV_{I}, and IV_{II}. In nature, cellulose I_{α} and I_{β} are the most abundant crystal forms and hence are referred to as native cellulose (Wyman *et al*., 2005).

3.4.1 Cellulose I

Cellulose I or native cellulose, apparently is the most abundant form. Its three-dimensional structure is highly complex and not yet completely resolved as a result of the coexistence of two distinct crystalline forms, cellulose I_{α} and I_{β}. This was a major discovery and led to a revival of interest in the study of cellulose structure. Cellulose I consists of chains arranged in a parallel fashion such that the $(1\rightarrow4)$ glycosidic bonds point in the same direction along the microfibril (Wyman *et al*., 2005). Addition, cellulose I can be made to undergo an irreversible transition to a stable crystalline form, cellulose II (Perez and Mazeau, 2005). .

The ultrastructure of native cellulose (cellulose I) has been discovered unexpected complexity in the form of two crystal phases: I_{α} and I_{β} (Bledzki and Gassan, 1999). The I_{α}-rich specimens have been found in the cell wall of some algae and in bacterial cellulose, whereas I_{β}-rich specimens have been found in cotton, wood, and ramie fibers (Bledzki and Gassan, 1999). Figure 12 shows two lattices, I_{α} and I_{β}, the conformation of the polysaccharide chains is the same although the hydrogen bonding pattern is different. The I_{α} may be converted into the I_{β} form by annealing the cellulose chains in the solid state. This process is irreversible because the I_{β} form is more stable (Lima and Borsali, 2004).

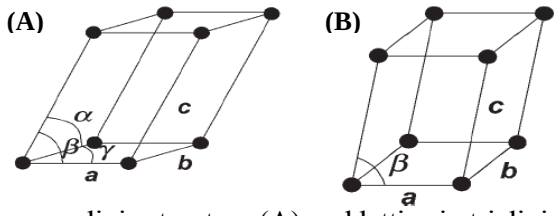

Figure 12. Lattice in monoclinic structure (A) and lattice in triclinic structure (B).
Source: Lima and Borsali, (2004)

3.4.2 Cellulose II

Cellulose II is the major polymorph in industrially processed cellulose. Cellulose II can be formed upon regeneration or mercerization of cellulose I and is also the most thermodynamically stable allomorph (Wyman *et al*., 2005). However, Fink *et al*. (1994) related measurements according to different authors and test methods in order to compare the Young's modulus for cellulose of type I and II. Most of the authors determined higher characteristic values for type I than for type II (Bledzki and Gassan, 1999).

3.5 Microcrystalline cellulose

Usually, cellulose still has a high amount of amorphous regions and size too large for use as filler and binder in other applications. The most common method of converting cellulose to useful products is a straightforward hydrolysis to cellulose derivatives (Fechner *et al*., 2003; Knill and Kennedy, 2005).

Microcrystalline cellulose is typically derived from the acid hydrolysis of cellulose (Bai and Li, 2009; Ashori and Nourbakhsh, 2010). Due to a high aspect ratio and a high Young's modulus of approximately 100 GPa of cellulose crystal (Lu *et al*., 2005). It has a higher degree of crystallinity because it is usually obtained by partially hydrolyzing cellulose with mineral acid (Fechner *et al*., 2003). The acid hydrolysis preferentially removes the amorphous regions of cellulose (Lin *et al*., 2008; Bai and Li, 2009). This is a low cost process for production of microcrystalline cellulose (Bai and Li, 2009; Ashori and Nourbakhsh, 2010).

A new class of cellulosic reinforcing agent is cellulose microfiber and microcrystalline cellulose. They have been widely used especially in food, cosmetic and medical industries as a water-retainer, a suspension stabilizer, a flow

characteristics controller in the systems used for final products. Cellulose microfiber and microcrystalline cellulose are mainly used as dry binder in manufacturing of tablets as well as in wet granulation, and it is the most important excipient in the extrusion process (Wang *et al*., 2006). In addition, microcrystalline cellulose is used in polymer composites as a reinforcing agent. When compared with glass fibers, silica and carbon black, microcrystalline cellulose in composites has many advantages: low cost, low density, little abrasion to equipment, renewability, and biodegradability process. Enhancement of material properties achieved with microcrystalline cellulose has stimulated active research in polymer composites, rubber composites (Bai and Li, 2009) and wood plastic composites (Ashori and Nourbakhsh, 2010).

3.5.1 Isolation of the microcrystalline cellulose

The isolation of cellulose from plant materials requires separation from extractives, lignin, and other noncellulose compounds. In the methods commonly used for the isolation and determination of cellulose, the other constituents are removed as completely as possible by procedures of extraction or solubilization, leaving a residue which is largely cellulose (Browning, 1967). Individual crystallites can prepare through acid hydrolysis of cellulose-containing materials under strictly controlled conditions of time and temperature (Matthews *et al*., 2001).

One method of isolation of the microcrystalline cellulose is hydrolyzed by acid such as hydrochloric and sulfuric acid. Hydrolysis of cellulose leads to a decrease in chain length of the polymer, then to formation of oligosaccharides and ultimately to D-glucose. In initial stages of hydrolysis the cellulose maintains its original fibrous form and the progress of the hydrolysis is evidenced by a decrease in physical strength of the fibers, a decrease in viscosity (or DP), an increase in the content of reducing groups, and increased solubility in aqueous alkaline solutions. With continued attack the fiber becomes progressively more brittle, and finally it may be reduced to a powder. Products prepared by partial hydrolysis of cellulose have been called *hydrocellulose*. The acid hydrolysis of polysaccharides occurs by attack of the hydronium ion (H_3O^+) at the hemiacetal linkage. The rate of hydrolysis in aqueous solution depends on the concentration of acid, the temperature, the nature of

the sugar unit, and the mode of linkage (α or β). The hydrolysis usually follows the kinetics of first-order reactions. The monosacchrides formed by hydrolysis are not immune to further attack by acids and are partially converted to furan-type compounds and other degradation products (Browning, 1967).

Delignification is an one process for purification of the cellulose (Bhattacharya, 2008). The procedures move a portion of the hemicelluloses along with the lignin, leaving with the cellulose variable amounts of the hemicelluloses depending on the nature of the delignification process. The precise physical dimensions of the crystallites depend on several factors, including the source of the cellulose, the extract hydrolysis conditions, and ionic strength. Additionally, complications in size heterogeneity are inevitable owing to the diffusion-controlled nature of the acid hydrolysis (Matthews *et al*., 2001).

The study of microcrystalline cellulose preparation of fiber crop such as rice hulls, bean hull, kenaf and soybean husk can be success by acid hydrolysis method. The particle size distribution patterns indicated that all kinds of microcrystalline cellulose samples fitted log-normal distribution and particle size mostly located in the range of 2–500 mm (Wang *et al*., 2010). Soybean husk cellulose was prepared as microcrystalline cellulose following by method of Uesu *et al*. (2000). The cellulose isolated from soybean husk was hydrolyzed with hydrochloric acid for microcrystalline cellulose preparation. The aim of work of Adel *et al*. (2010) was to prepare microcrystalline cellulose from rice hulls (RH) and bean hull (BH) with mixed acid. The hydrolysis experiments were carried out using a 2.5-L high pressure/high temperature reaction. Each dry sample (100 g) was mixed with 0.5–5% (w/w) sulfuric or hydrochloric acid and heated to the desired temperature (80–120°C) inside the closed reactor. The reactor was commenced for different lengths of time (30 to 120 min). By the end of pretreatments, solid residues were recovered by filtration, washed, oven dried, weighed to measure the solid yield, and stored in polyethylene bags for subsequent tests. Addition, Wang *et al*. (2010) have been made to produce microcrystalline cellulose from kenaf bast. Kenaf stalks are composed of long bast fibers (2–2.5 mm) as well as short core fibers (0.5–0.8 mm). Bleached kenaf bast was hydrolyzed with 5% (w/w) hydrochloric acid under reflux at 105±2°C for 60 min. The liquor ratio was 1:20. The hydrolyzed pulps were thoroughly washed with

distilled water and then vacuum-dried at 55 8C. The microcrystalline cellulose was obtained as dried cake, which was powdered and stored in a desiccator until further evaluation. Bhattacharya *et al*. (2008) used sugarcane bagsees as a source of producing highly crystalline microfibrils for future use as a nanoscale reinforcing filler. Initially, the dried bagasse was subjected to a conventional pulping process to eliminate lignin and hemicelluloses. Whole cellulose fibers thus obtained were then mechanically separated into their constituent microfibrils by a two-stage homogenization process and finally acid hydrolyzed by refluxing with 60% (w/v) sulfuric acid for 2.5 h at 60°C.

The advanced microcrystalline cellulose prepared requiring was an emphasis on the production of nano-size fibers from agricultural. The main gold of Alemdar and Sain (2008 a; b) works are to produce and characterize the bio-nanocomposites from wheat staw nanofibers. The cellulose nanofibers were extracted from wheat straw by soak in a concentrated sodium hydroxide solution, followed by hydrolyzed with 1 M of hydrochloric acid at 80±5°C for 2 h and treated once more with the 2% w/w of sodium hydroxide solution at 80±5°C for 2 h. The mechanical treatment procedure includes cryocrushing, disintegration and defibrillation was final process.

3.5.2 Microcrystalline cellulose reinforcement filler

It is known that microcrystalline cellulose had a high value of Young's modulus approximately 100 GPa of cellulose crystal (Lu *et al*., 2005). Therefore, the use of microcrystalline cellulose or cellulose crystal for preparation of high-performance composite material has been explored extensively in matrix of starch, soy protein, synthetic polymer, rubber, wood plastic and others matrix (Lu *et al*., 2005; Wang *et al*., 2006; Spoljaric *et al*., 2009; Bai and Li, 2010; Ashori and Nourbakhsh, 2010). Moreover, microcrystalline cellulose can improved thermal property (Alemdar and Sain, 2008a) and water absorption of composite application (Lu *et al*., 2005).

In rubber industry especially in the rubber tire application, the currently used reinforcing fillers mainly include carbon black and silica. In research of Bai and Li (2010) used microcrystalline cellulose as a third reinforcing filler to

partially replace silica in styrene butadiene rubber (SBR) and poly-butadiene rubber (BR) composites. The partial replacement of silica with microcrystalline cellulose significantly reduced the energy required for dispersion of fillers in rubber matrix and lowered the internal temperature during the compounding. Moreover, the partial replacement of silica with microcrystalline cellulose reduced Mooney viscosity, apparent shear stress, and apparent shear viscosity of the rubber composites, which facilitated the manufacturing process of the rubber composites.

In wood plastic composite, Ashori and Nourbakhsh (2010) studied the effects of using microcrystalline cellulose (Pulver-40 micron) as a reinforcing filler in wood plastic composites, through characterized microcrystalline cellulose/wood flour/polypropylene (PP) composites that were prepared containing polypropylene-graft-maleic anhydride (PP-g-MA) as compatibilizer. This work showed that microcrystalline cellulose along with wood flour could be effectively used as reinforcing agent in thermoplastic matrix. The weight ratio of the cellulosic materials to polymer matrix was 40:60 (w:w). The obtained results showed that tensile, flexural and impact strengths of the composites were significantly enhanced with addition of microcrystalline cellulose, as compared with pure PP and composites without microcrystalline cellulose. Scanning electron microscopy has shown that the composite, with compatibilizer, promotes better fiber–matrix interaction. However, it is to be noted that microcrystalline cellulose could not improve the thermal stability. Agreeing with Spoljaric *et al*. (2009) prepared and characterized PP–cellulose microfiber (average diameter ~40 μm) composites, with various cellulose microfiber concentrations (1%, 2%, 5% and 10% w/w), through modification of fiber surface and the addition of PP-g-MA as a compatibilising agent. Surface treatment of the cellulose microfiber involved the use of a fatty acid, a silane coupling agent and an alkyltitanate. Infrared spectroscopy confirmed surface treatment. Cellulose microfiber content and PP-g-MA can increased PP thermal stability. Tensile stress–strain analysis revealed increased modulus with cellulose microfiber content, PP-g-MA, alkyltitanate and stearic acid. Moreover, cellulose microfiber and PP-g-MA reduced creep deformation and increased permanent strain. Storage modulus, loss modulus and glass transition temperature increased with cellulose microfiber concentration due to effective interaction between PP and cellulose microfiber.

Many studies are on going to find ways to use cellulose microfiber and microcrystalline cellulose-based fibers in place of synthetic fibers as reinforcements (Ashori and Nourbakhsh, 2010), especially, in application of biocomposite films (Müller *et al*., 2009; Kumar and Singh, 2008; Lu *et al*., 2005). For water-soluble polymers like starch, PVOH and latex, the aqueous suspension of cellulose is reported to be better choice of reinforcement for achieving higher level of dispersion (Kumar and Singh, 2008; Dufresne and Vignon, 1998; Mathew and Dufresne, 2002; Angles and Dufresne, 2000; Averous and Boquillon, 2004). In the study of Kumar and Singh (2008), the composite films have been prepared from the aqueous dispersions of starch with microcrystalline cellulose using glycerol as plasticizer and irradiated under ultraviolet light using sodium benzoate as photo-sensitizer. Keeping the starch/microcrystalline cellulose ratios as 100/0, 95/05, 90/10, and 85/15 (relative to dry starch, with a total mass of 2 g) the weighed amount of starch and microcrystalline cellulose were separately dispersed in 20 ml and 10 ml of deionized water, respectively. Both, the incorporation of cellulose and photo-irradiation were found to decrease the water absorption, swelling in DMSO and increase the gel fraction. Thermal transitions indicated the anti-plasticization of amylopectin chains at the microcrystalline cellulose/matrix interface. The tensile modulus and strength were found to improve. It is summarized that the combination of microcrystalline cellulose reinforcement and photo-cross-linking of matrix has improved the physical and mechanical properties. Addition, film samples were prepared from solutions with 3% of tapioca starch, with the addition of 0, 0.10, 0.30 and 0.50 g of fibers/g of starch (Muller *et al*., 2009). SEM micrographs of the films showed a homogeneous and random distribution of the cellulose fibers, without pores or cracks. Films with fibers were more crystalline and had higher tensile strength and rigidity, but lower elongation capacity. On the other hand, addition of cellulose fibers increased the stability of starch-based films subjected to RH variations, solving a classical problem encountered with this kind of film. Thus, the addition of cellulose fibers to starch-based films is an effective way to prepare stronger and more stable films. Roohani *et al*. (2008) prepared composite materials from copolymers of polyvinyl alcohol (PVOH) and polyvinyl acetate (PVAc) and colloidal aqueous suspension of cellulose whiskers that prepared from cotton linter. PVOH is well suited for blends with

cellulose since it is highly polar and can be dispersed in water solutions. The cellulose content in the final composites was 0, 3, 6, 9, and 12 wt% for PVOH copolymer. The films were prepared by a casting/evaporation technique. All results show that strong filler/matrix interactions result in an increase of the glass temperature, and a decrease of both the melting point and degree of crystallinity of the polymeric matrix in dry atmosphere.

Objectives

1. To prepare the microcrystalline cellulose (MCC) from sugarcane bagasse fiber (SBF) and investigate the composition, morphological and chemical properties of prepared MCC.

2. To prepare and investigate the properties of starch, polyvinyl alcohol (PVOH) and PVOH/Starch cross-linked adhesives.

3. To study the effects of catalyst (citric acid), molecular weight of PVOH and PVOH/Starch ratio on the physical, chemical and mechanical properties of PVOH and PVOH/Starch cross-linked adhesives.

4. To study the effects of MCC addition on the physical, morphological, chemical and mechanical properties of starch, PVOH and PVOH/Starch cross-linked adhesives.

CHAPTER 2

MATERIALS AND METHODS

1. Materials

1.1 Raw materials

Tapioca starch was supplied by Universal Starch Public Ltd. (Thailand), which was composed of minimum 85% starch and 13% moisture content. Sugarcane bagasse fiber (SBF) was obtained from the local community in Songkhla province, Thailand.

1.2 Chemicals

N-Cetyl-N, N, N-trimethylammonium bromide (CTAB) was purchased from Merck (Germany). Sodium tetraborate decahydrate (Borax) and citric acid (CA) were supplied by RFCL Ltd. (India). Hexamethoxymethylmelamine (HMMM; Cymel 323) cross-linker was obtained from Cytec Industries BV (Thailand). Nitric acid, sodium hypochlorite, sulfuric acid, sodium hydroxide, acetone and acetic acid were purchased from High Science Co. Ltd. (Thailand). Polyvinyl alcohol (PVOH) was purchased from Chang Chun Petrochemical Ltd. (Taiwan), which was 98.5 to 99.2 % hydrolyzed with molecular weight of 22,000 (L PVOH), 75,000 to 80,000 (M PVOH), and 112,000 to 120,000 (H PVOH) dalton. Figure 13 and 14 show chemical structures of sodium tetraborate decahydrate (Borax) and hexamethoxymethylmelamine (HMMM) used in this study.

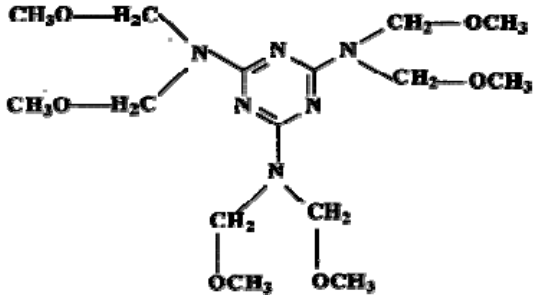

Figure 13. Chemical structure of hexamethoxymethylmelamine.

Source: Imam *et al.* (2001)

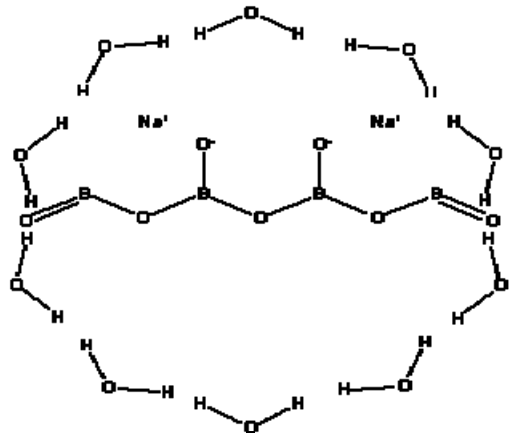

Figure 14. Chemical structure of sodium tetraborate decahydrate.

Source: Pollution control department (2001)

2. Instruments

The Instruments used in this experiment are shown in Table 4.

Table 4. List of instruments used in this work.

Instruments	Model	Company/Country
Hot air oven	UM-500	MEMMERT, Schwabach, Germany
Laboratory furnace	ELF11/14B	Carbolite, England
Hot Plate	EV-14	Gerhardt, Germany
Brabender viscoamylograph	Viscograph	BRABENDER, Germany
Water bath	W 350	MEMMERT, Schwabach, Germany
pH meter	pH/Ion 510	Eutech Instruments Pte Ltd., Singapore
Magnetic stirrer	Ro 15 power	IKA labortechnik, Stanfen, Germany
Stirrer	RW 20n	IKA labortechnik, Stanfen, Germany
Vortex mixer	G-560E	Scientific Industries Inc., NY, USA
Blender	HR 2021	Philips, China
Brookfield viscometer	DV-II	Brookfield Engineering Laboratories Inc., MA, USA
Universal testing machine	LR 30 K	LLOYD Instruments Ltd., Hampshire, UK
Fourier transform infrared spectrometer	Bruker Model Equinox 55	Bruker Co., Ettlingen, Germany
X-ray diffractometer	X'Pert MPD	Philips, Netherland
Scanning electron microscope	Quanta 400	FEI, Tokyo, Japan
Differential scanning calorimeter	DSC 7	Perkin Elmer, Norwalk, CT, USA

3. Methods

3.1 Preparation of microcrystalline cellulose and characterizations

3.1.1 Preparation of microcrystalline cellulose (MCC)

Microcrystalline cellulose was isolated from hot air dried sugarcane bagasse fiber (SBF), with a moisture content of about 11g/100g of the sample. Initially, the dried SBF was cut into 4-5 cm lengths and then hydrolyzed with 10 and 15% (w/w) of nitric acid under pressure control. The ratio of the dried SBF to acid liguor was 1:20 in a heat of 90°C for 30 and 60 min, respectively (Sridach, 2010). The pulp was bleached by sodium hypochlorite, 10% active chlorine. The ratio of the dried bagasse pulp to the bleaching agent was 5:1 and heat to the temperature of 90°C for 3 h (Kürschner and Hoffer, 1967). Bleached fiber was then reduced in size by a blender and screened by a sieve with mesh size no 200 (diameter size 0.074 μm). The sample designation and chemical treatment condition of the fibers are shown in Table 5.

Table 5. Sample designation and chemical treatment condition of the fibers.

Sample designation	Nitric acid %, w/w	Reaction time min
SBF	-	-
MCC-a	10	30
MCC-b	10	60
MCC-c	15	30
MCC-d	15	60

3.1.2 Characterizations of microcrystalline cellulose (MCC)

3.1.2.1 Chemical analysis

The SBF and MCC were chemically analyzed for moisture and ash content by using the A.O.A.C standard (1999). The cellulose and lignin content of the fibers was determined by acid-detergent fiber (ADF) according to Van Soest and Wine method (1968). The ADF analysis was used to measure the cellulose and lignin content by removal. The Kurschner-Hoffer cellulose method was used to measure the pure cellulose content. Before testing, the fibers were prepared by grinding and

screening with a sieve, mesh no 40. Screened fibers (1 g) were added in 100 ml of acid detergent (20 g CTAB in 1000 ml of 1 N sulfuric acid). The mixture was heated until boiled for 1 h. It was filtered through the quartz crucible and washed with hot water and acetone. Then, it was dried at 105°C for 3 h. The sample was soaked in 72% sulfuric acid for 3 h and washed with hot water again. After that it was dried at 105°C for 12 h and burned for 2 h. Cellulose content analysis was confirmed according to the method of Kürschner and Hoffer method (1967) using alcoholic nitric acid solution (65% nitric acid in 96% ethanol). Screened fibers (5 g) were added in 125 ml of alcoholic nitric acid solution at the reflux condition (70-80°C) for 4 h and dried the fibers at 105°C for 12 h.

3.1.2.2 Fiber morphology

Scanning Electron Microscopy (SEM) was used to study the morphology of the SBF and MCC. The samples were mounted on bronze stubs and sputtered with gold (Sputter coater SPI-Module, PA, USA) in order to make the samples conductive. The photographs were taken at selected magnifications. The images of SEM were taken at 10.0 kV with FEI model Quanta 400.

3.1.2.3 FT-IR spectroscopy

FT-IR spectroscopy was used to examine any changes in the structure of the SBF and MCC. The FT-IR spectra were measured with a Bruker Model Equinox 55 (Bruker Co., Ettlingen, Germany). The samples were prepared by mixing the fine powder with KBr and pressing. The spectra were obtained at a resolution of 4 cm^{-1} in the range of 4000 to 400 cm^{-1}.

3.1.2.4 X-ray diffractometry (XRD)

The crystallinity of the MCC was examined by using a Philips X'Pert MPD system (Philips Inc., Netherland). The diffracted intensity of Cu Kα radiation was assessed at a voltage of 40 kV and 30 mA. The samples were dried and measured in a 2θ range between 10 and 50 degrees. Crystallinity was commonly measured as ratio between the diffraction portion from the crystalline part of the sample, A_c, and the total diffraction from the same sample, A_{total}. The values of A_c could be obtained after an appropriate subtraction of the scattering portion from the background, A_b. The crystallinity was calculated following equation of Alemdar and Sain (2008b).

$$\text{Crystallinity, \%} = \frac{A_c * 100}{A_{total}}, \quad \text{where : } A_{total} = A_c + A_b.$$

3.2 Study the effect of amount of starch on some properties of starch adhesive

3.2.1 Preparation of starch adhesive

Three starch adhesives at various concentrations were prepared for a given intake of starch solid content of 22, 26 and 30 wt%. The mixture was stirred constantly until the solid was completely dispersed (10 min). In portion I, borax was then added at 0.22 wt% of starch and stirred. Whilst portion II, sodium hydroxide solution (19.35%, w/v) was added slowly at 2.24 wt% of starch with stirred constantly until obtained clear-brown solution. Starch adhesive was prepared by mixing slowly from the solution of portion II into portion I. Then, the starch adhesive was stirred gently at room temperature for 15 min. Finally, the total solid content of starch adhesives was adjusted to 22, 26 and 30 wt% of solid content, respectively.

3.2.2 Testing of starch adhesive

3.2.2.1 Solid content and viscosity

The adhesive was subjected to determine their physical properties. The adhesive viscosity and solid content were analyzed according to TIS.181-2530 and A.O.A.C standard, respectively.

3.2.2.2 Preparation of wood specimens

Wood specimen of mechanical testing was 0.5 cm thick veneer which was cut to a dimension of 2.5 × 10 cm^2. The face to which the adhesive was to be applied was freshly surfaced with polish using sandpaper grit no. 100 (140 μm).

3.2.2.3 Adhesive shear strength testing method

The testing method was modified from the standard of TIS.360 (2523) and ASTM D1002-72 (1982). The adhesive was applied by brushing about 0.030 to 0.040 g dry weight per glued area (6.25 cm^2, approximately) on one side of the wood specimen. Then the glued specimen was put over with another piece (Figure 15). The specimens were press under the pressure of 3.45 MPa (500 psi) at curing temperature of 175°C for 15 min (Imam *et al.*, 1999). After that, the test specimens were maintained at the temperature of 23°C and controlled relative humidity of 50% RH for 2 days before testing. Each wood joint specimen was tested for shear strength

using Universal Tester (LLOYD Instrument; model LR30K, England). Initial grip separation and crosshead speed were set at 80 mm and 1.3 mm/min, respectively. Shear strength was defined as the load required breaking the specimen divided by the area of the bond. The shear strength values were averages of ten measurements. It was calculated by using equation (1).

$$\text{Shear strength value} = \frac{\text{maximum force (N)}}{\text{glued area (mm}^2\text{)}} \quad (1)$$

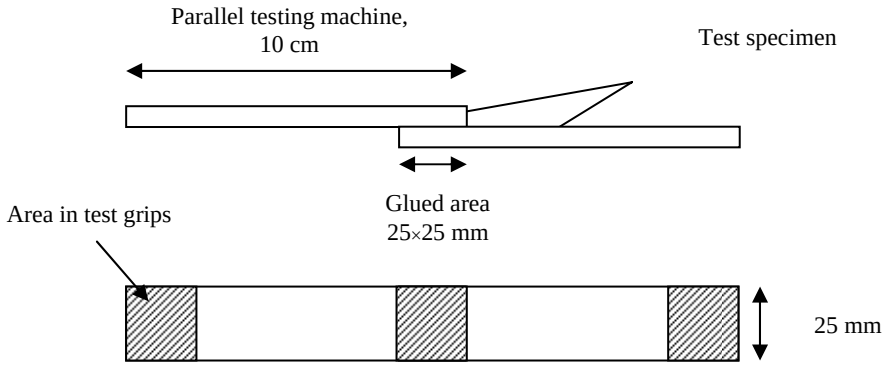

Figure 15. Form and dimensions of test specimen for shear strength.

3.3 Study the effect of microcrystalline cellulose (MCC) addition on some properties of starch composite adhesive

3.3.1 Preparation of starch composite adhesive

The microcrystalline cellulose (MCC) powder was added to 10 ml of adhesive. The amounts of MCC used varied from 0.5, 1.5, 2.5 and 3.5 wt% of total solid content of adhesive which had the highest mechanical properties as determined in section 3.2.2. The mixtures were stirred for 3 h to let the MCC filler dispersed in the starch adhesive (Lu *et al.*, 2008). The starch composite adhesives were analyzed the properties in section 3.3.2.

3.3.2 Testing of starch composite adhesive

3.3.2.1 Solid content and viscosity (as described in section 3.2.2.1)

3.3.2.2 Preparation of wood specimens (as described in section 3.2.2.2)

3.3.2.3 Adhesive shear strength testing method (as described in section 3.2.2.3)

3.3.2.4 Composite adhesive morphology

Morphology of surface and fracture surface of the dried starch adhesive and starch composite adhesive with MCC addition samples were visualized by using a scanning electron microscope (SEM) (Quanta 400, Tokyo, Japan) at an acceleration voltage of 10 kV. For cross section, samples were fractured prior to morphology visualization. Then, the samples were mounted on bronze stub and sputtered with gold (Sputter coater SPI-Module, PA, USA) in order to make the sample conductive, and photographs were taken at selected magnification.

The adhesive sample which contributed the highest mechanical properties was chosen to further study.

3.3.2.5 FT-IR spectroscopy

FT-IR spectroscopy was used to examine any changes in the structure of the starch adhesive and starch composite adhesive which had the highest mechanical properties. The FT-IR spectra were measured with a Bruker Model Equinox 55 (Bruker Co., Ettlingen, Germany). The samples were prepared by mixing the fine powder with KBr and pressing. The spectra were obtained at a resolution of 4 cm^{-1} in the range of 4000 to 400 cm^{-1}.

3.3.2.6 Differential scanning calorimetry (DSC)

Differential scanning calorimeter (DSC) thermograms were recorded by DSC 7 (Perkin Elmer, Norwalk, CT, USA) instrument for the starch adhesive and starch composite adhesive which had the highest mechanical properties. The sample (7 to 10 mg) was placed in an aluminium pan. The first heating scan was run with the temperature range between 25 and 260°C at the heating rate of 10°C/min. The second heating run was performed with samples which were suddenly cooled to 6°C and heated to 350°C.

3.4 Study the effect of polyvinyl alcohol (PVOH) molecular weight and concentration on some properties of PVOH adhesive

3.4.1 Preparation of PVOH adhesive

PVOH powder was added to de-ionized water. The mixture was heated to about 90-95°C with constant stirring until the solid was completely dissolved. The final concentration of low molecular weight of PVOH adhesives (L PVOH) were 8, 12, 16, 20, 24 and 28 wt%. The concentration of medium (M PVOH) and high molecular weight PVOH adhesives (H PVOH) were 8, 12 and 16 wt%. Volumes were adjusted by the addition of water at this time to yield final concentrations. The adhesive samples were stored in closed containers and used for analysis.

3.4.2 Testing of PVOH adhesive

3.4.2.1 Solid content and viscosity (as described in section 3.2.2.1)

3.4.2.2 Preparation of wood specimens (as described in section 3.2.2.2)

3.4.2.3 Adhesive shear strength testing method (as described in section 3.2.2.3 at ambient temperature)

3.5 Study the effect of microcrystalline cellulose (MCC) addition on some properties of polyvinyl alcohol (PVOH) composite adhesive

3.5.1 Preparation of PVOH composite adhesive

The microcrystalline cellulose (MCC) powder was added to 10 ml of adhesive. The amounts of MCC used varied from 0.5, 1.5, 2.5 and 3.5 wt% of total solid content of adhesive which had the highest mechanical properties as determined in section 3.4.2. The mixtures were stirred for 3 h to let the MCC filler dispersed in the PVOH adhesive (Lu *et al.*, 2008). The PVOH composite adhesives were analyzed the properties in section 3.5.2.

3.5.2 Testing of PVOH composite adhesive

3.5.2.1 Solid content and viscosity (as described in section 3.2.2.1)

3.5.2.2 Preparation of wood specimens (as described in section 3.2.2.2)

3.5.2.3 Adhesive shear strength testing method (as described in section 3.2.2.3 at ambient temperature)

3.5.2.4 Composite adhesive morphology

The PVOH adhesive samples with MCC addition were investigated the surface and fracture surface compared to the PVOH adhesive without MCC with an optical microscope at a magnification ×4 and a scanning electron microscope (SEM) (Quanta 400, Tokyo, Japan) at an acceleration voltage of 10 kV. The fluid adhesives were painted on slide plate before analysis with the optical microscope. For SEM testing, the dried adhesives were mounted on bronze stub and sputtered with gold (Sputter coater SPI-Module, PA, USA) in order to make the sample conductive. The photographs were taken at selected magnification.

The PVOH adhesive sample which contributed the highest mechanical properties was chosen to further study.

3.5.2.5 FT-IR spectroscopy

FT-IR spectroscopy was used to examine any changes in the structure of the PVOH adhesive and composite PVOH adhesive with MCC which had the highest mechanical properties. The FT-IR spectra were measured by a Bruker Model Equinox 55 (Bruker Co., Ettlingen, Germany). The samples were prepared by mixing the fine powder with KBr and pressing. The spectra were obtained at a resolution of 4 cm^{-1} in the range of 4000 to 400 cm^{-1}.

3.5.2.6 Differential scanning calorimetry (DSC)

Thermograms of differential scanning calorimeter (DSC) were recorded by DSC 7 (Perkin Elmer, Norwalk, CT, USA) instrument for the PVOH adhesive and PVOH composite adhesive which had the highest mechanical properties. The sample (7 to 10 mg) was placed in an aluminium pan. The first heating scan was run on the temperature range between 25 and 260°C at the heating rate of 10°C/min. The second heating run was performed with samples which were suddenly cooled to 6°C and heated to 300°C.

3.6 Study the effect of citric acid (CA), starch ratio and type of polyvinyl alcohol (PVOH) on properties of cross-linked PVOH/Starch adhesive

3.6.1 Preparation of cross-linked PVOH/Starch adhesive

Cross-linked PVOH/Starch adhesives were prepared by using a modified method of Imam *et al*. (2001). Typically, PVOH powder was dissolved in de-ionized water at the temperature of 90-95°C with constant stirring until complete

dissolution. The final concentration of PVOH was 12 wt%. Then the solution was cooled to 50°C and added the tapioca starch. The slurry was stirred at the temperature of 50°C for 5 min and slowly increased the temperature to 62-65°C during stir. The solution was cooled down to 25°C and added HMMM cross-linker with constant stirring for 10 min. The volumes were adjusted by addition of de-ionized water at this time to make the final concentrations.

For study the effect of CA on cross-linked structure, the CA was added immediately prior to adhesive application. The compositions of cross-linked PVOH/Starch adhesives in this study are shown in Table 6. The samples were applied to wood specimens at curing temperature, optimal time and under the optimal pressure as description in item 3.2.2.3.

Table 6. Sample designation and composition of cross-linked PVOH/Starch adhesives.

Sample designation	Composition (dry weight ratio)			HMMM	Citric acid
	PVOH; Medium (75,000-80,000 dalton)	PVOH; High (112,000-120,000 dalton)	Starch	wt %	wt %
M PVOH/ST = 1:0.5	1	-	0.5	6.38	0 and 0.24
M PVOH/ST = 1 : 1	1	-	1.0	6.38	0 and 0.24
M PVOH/ST = 1:1.5	1	-	1.5	6.38	0 and 0.24
M PVOH/ST = 1:1.8	1	-	1.8	6.38	0 and 0.24
M PVOH/ST = 1:2.1	1	-	2.1	6.38	0 and 0.24
M PVOH/ST = 1:2.4	1	-	2.4	6.38	0 and 0.24
H PVOH/ST = 1:0.5	-	1	0.5	6.38	0 and 0.24
H PVOH/ST = 1 : 1	-	1	1.0	6.38	0 and 0.24
H PVOH/ST = 1 : 1.5	-	1	1.5	6.38	0 and 0.24
H PVOH/ST = 1:1.8	-	1	1.8	6.38	0 and 0.24
H PVOH/ST = 1:2.1	-	1	2.1	6.38	0 and 0.24
H PVOH/ST = 1:2.4	-	1	2.4	6.38	0 and 0.24

3.6.2 Testing of cross-linked PVOH/Starch adhesive

3.6.2.1 Solid content and viscosity (as described in section 3.2.2.1)

3.6.2.2 Preparation of wood specimens (as described in section 3.2.2.2)

3.6.2.3 Adhesive strength testing method (as described in section 3.2.2.3)

3.6.2.4 FT-IR spectroscopy

FT-IR spectroscopy was used to examine any changes in the structure of the cross-linked adhesive that resulting from the effect of citric acid (CA), starch ratio and type of PVOH. The FT-IR spectra were measured with a Bruker Model Equinox 55 (Bruker Co., Ettlingen, Germany). The samples were prepared at curing temperature, optimal time and crushing prior mixing the fine powder with KBr and pressing. The spectra were obtained at a resolution of 4 cm^{-1} in the range of 4000 to 400 cm^{-1}.

3.6.2.5 Differential scanning calorimetry (DSC)

Thermograms of differential scanning calorimeter (DSC) were recorded by DSC 7 (Perkin Elmer, Norwalk, CT, USA) instrument for the cross-linked adhesive. The sample (7 to 10 mg) was placed in an aluminium pan. The first heating scan was run with the temperature range between 25 and 260°C at the heating rate of 10°C/min. The second heating run was performed with samples which were suddenly cooled to 6°C and heated to 300°C.

3.7 Study the effect of microcrystalline cellulose (MCC) addition on properties of cross-linked PVOH/Starch adhesive

3.7.1 Preparation of PVOH/Starch composite adhesive

The microcrystalline cellulose (MCC) powder was added to 10 ml of adhesive. The amounts of MCC used varied from 0.5, 1.5, 2.5 and 3.5 wt% of total solid content of adhesive which had the highest mechanical properties as determined in section 3.2.2. The mixtures were stirred for 3 h to let the MCC filler dispersed in the PVOH/Starch adhesive (Lu *et al*., 2008). The starch composite adhesives were analyzed the properties in section 3.7.2.

3.7.2 Testing of PVOH/Starch composite adhesive

3.7.2.1 Solid content and viscosity (as described in section 3.2.2.1)

3.7.2.2 Preparation of wood specimens (as described in section 3.2.2.2)

3.7.2.3 Adhesive strength testing method (as described in section 3.2.2.3)

3.7.2.4 Composite adhesive morphology

The cross-linked composite adhesive were investigated the surface and fracture surface compared to the cross-linked adhesive with a scanning electron microscope (SEM) (Quanta 400, Tokyo, Japan) at an acceleration voltage of 10 kV. The dried adhesives were mounted on bronze stub and sputtered with gold (Sputter coater SPI-Module, PA, USA) in order to make the sample conductive, and photographs were taken at the selected magnification.

The optimal condition of adhesive sample which had the highest mechanical properties was chosen for further study.

3.7.2.5 FT-IR spectroscopy

FT-IR spectroscopy was used to examine any changes in the structure of the cross-linked adhesive and cross-linked composite adhesive which had the highest mechanical properties. The FT-IR spectra were measured with a Bruker Model Equinox 55 (Bruker Co., Ettlingen, Germany). The samples were prepared by mixing the fine powder with KBr and pressing. The spectra were obtained at a resolution of 4 cm^{-1} in the range of 4000 to 400 cm^{-1}.

3.7.2.6 Differential scanning calorimetry (DSC)

Thermograms of differential scanning calorimeter (DSC) were recorded by DSC 7 (Perkin Elmer, Norwalk, CT, USA) instrument for the cross-linked adhesive and cross-linked composite adhesive which had the highest mechanical properties. The sample (7 to 10 mg) was placed in an aluminium pan. The first heating scan was run with the temperature range between 25 and 260°C at the heating rate of 10°C/min. The second heating run was performed with samples which were suddenly cooled to 6°C and heated to 300°C.

4. Statistical analysis

Experiments were run in duplicate. Data were subjected to analyze the variance (ANOVA) and the differences between means were evaluated by Duncan's Multiple Range Test (Steel and Torrie, 1980). SPSS statistic program (SPSS 15.0 for window, SPSS Inc., Chicago, IL, USA.) was used for data analysis.

CHAPTER 3

RESULTS AND DISCUSSION

1. Compositional profile of materials

Compositional and some properties of tapioca starch

The proximate composition of tapioca starch (*Manihot utilissima*) is shown in Table 7. Starch content was found as a major constituent at 85.00% (wet weight) while negligible pulp and ash contents were 0.15 and 0.08%, respectively. The peak viscosity of tapioca starch was 600 BU at the temperature of 74-83°C and the pasting temperature was 68°C. They were determined by Brabender basing on 6% starch, dry basis, with 450 ml of distilled water. The low peak viscosity indicated low water-holding capacity of starch (Sekine, 1996; Yuan *et al*., 2007) and low crystallinity of the starch was probably responsible for the low pasting temperature (68°C). They were measured according to the method of Yuan *et al*. (2007). Normally, the composition and properties of the starch are depended on species, production, planting area, etc.

Table 7. Compositions and some properties of tapioca starch.

Compositions/properties	Amount (%)
Moisture	11.13±0.22*
Ash	0.08±0.04*
Pulp	0.15±0.01**
Starch	85.00±0.50**
pH	6.5-7.0
Peak viscosity, BU	600.00
Color	White

*Mean ± SD from triplicate determinations.

**Specification of tapioca starch from Universal Starch Ltd.

2. Effect of chemical treatment on fiber characterizations

2.1 Composition of the sugarcane bagasse fiber (SBF) and microcrystalline cellulose (MCC)

The composition of sugarcane bagasse fiber and microcrystalline cellulose was determined by method of Van Soest and Wine (1968) and Kürschner and Hoffer (1967) e.g. lignin, acid detergent fiber (ADF) and cellulose content. Table 8 shows some of chemical compositions of the fibers. The contents of moisture, ash, lignin, ADF and cellulose (1) and (2) of SBF were 11.05, 1.82, 4.35, 32.72, 28.69 and 29.10%, respectively. Whilst the chemical composition of MCC after each stage of chemical treatment was found that the moisture, ash and lignin contents were decreased but the contents of ADF, cellulose (1) and cellulose (2) were increased (Table 8). It indicated that the chemical treatment with 15% (w/w) of nitric acid and 10% active chlorine of sodium hypochlorite could remove the most of hemicellulose, lignin, pectin and other non-cellulose from the SBF (Alemdar and Sain, 2008b).

Normally, hydrogen bonds between cellulose molecules were arranged in a regular system resulting in an ordered system with crystal-like properties (Alemdar and Sain, 2008b). The fine structure of cellulose materials was composed of crystalline and non-crystalline regions (Wang and Sain, 2006). Crystalline cellulose consisted of long chains whilst non-crystalline cellulose had shorter chains. Furthermore, non-crystalline cellulose was branched, whereas crystalline cellulose was unbranched. Non-crystalline cellulose had hemicellulose, lignin and other extractions. The chemical treatments had affected to the crystallinity of the cellulosic fibers. It was desirable to retain pure cellulose, whose crystalline form and high packing density resulted in a stronger composite. As a result, MCC-c which was treated with 15% (w/w) of nitric acid at the reaction time of 30 min indicated the optimal condition for all treatments (Table 8). It showed the maximum content of cellulose (1) and cellulose (2) that increased to 82.01 and 88.99%, respectively. Lignin content was the minimum decreased to 0.71%. Thus it meant that the crystalline region of the cellulose in fibers was increased after the acid-treatment. However, the result of Kurschner-Hoffer cellulose method (1) showed higher cellulose content than ADF analysis (2). It might cause by the rapid reaction of nitric

acid in alcoholic solutions and dissolves lignin to yield cellulose preparations containing cellulose and a portion of the hemicelluloses (Browning, 1967). In addition, yield of the fiber in c-condition showed the highest value of 48.43%.

Table 8. Principal chemical composition of the fibers.

Composition (%)*	SBF	MCC-a	MCC-b	MCC-c	MCC-d
Moisture	11.05±0.42	5.98±0.14	5.00±0.18	5.68±0.08	5.60±0.23
Ash	1.82±0.08	1.46±0.26	1.56±0.26	1.61±0.03	1.58±0.03
Lignin	4.35±0.84	1.23±0.06	1.12±0.12	0.71±0.09	0.82±0.13
Cellulose[1]	28.69±3.28	80.15±1.45	80.65±0.98	82.01±0.07	81.76±0.11
Cellulose[2]	29.10±3.68	82.13±2.19	85.13±3.10	88.99±2.54	86.87±2.58
Acid detergent fiber	32.72±0.91	81.04±0.24	81.52±0.28	82.92±0.29	82.56±0.33
Yield[3]	-	44.36±0.36	44.14±0.67	48.43±1.06	35.89±0.86

*Mean ± SD from triplicate determinations

[1] Cellulose content was analyzed by method of Van Soest and Wine method (1968)

[2] Cellulose content was analyzed by method of Kürschner and Hoffer method (1967)

[3]Yield of cellulose fiber after chemical treatment

2.2 Morphology of the fibers

A definite change in the morphological structure and size of the cellulose fibers occurred upon acid-hydrolysis and chemical treatment. The morphological structure and size of SBF and MCC were observed by using SEM. They are shown in Figure 16. The shapes of all fibers seemed to be a long rod. Figure 16 (A) shows SEM image of the untreated fibers (SBF). The surface of SBF tended to be smooth. Some small fractures on the fiber surface were result of a grinding process. The morphology of MCC surface was shown in Figure 16 (B) and (C). The outer layer and the surface cover on MCC were obviously destroyed and some chemical compositions were removed. A larger magnification showed that many terraces, steps and kinks form on the fiber surface after acid hydrolysis (Figure 16 (C)). These results had similar to the experiment of Bhatnagar and Sain (2005), Zhao *et al*. (2007), Bhattachaya *et al.* (2008) and Alemdar and Sain (2008b).

In addition, the chemical treatment had effected to size of the cellulose

fibers. MCC had the lengths of 100-300 μm and diameters of 5-10 μm, which were lower than the sizes of the macrofibrils of SBF. The SBF had the length higher than 1000 μm and diameters of 100-150 μm (Figure 15 (A)). The morphological structure and size of the fibers changed due to the removal of the amorphous regions of the cellulose by the treatment (Zhao *et al*., 2007). The macrofibrils had been hydrolyzed and the degree of polymer chains of the cellulose was reduced.

2.3 Fourier-transform infrared (FT-IR) spectroscopy

The chemical structures of SBF and MCC components were analyzed by using FT-IR spectroscopy. The FT-IR spectra in Figure 17 shows the spectra of SBF structure with removal of pectins, lignin and hemicelluloses due to the vanishing of characteristic band at 1733.44 cm^{-1} (carboxylate groups), 1605.51 cm^{-1} (acetyl groups) and 1252.30 cm^{-1} (methyl ester groups), 1513.89 and 1426.65 cm^{-1} (aromatic C=C stretch) in the spectra of MCC. SBF showed a characteristic strong carbonyl absorption peak at 1733.44 cm^{-1} due to the acetyl and uronic ester groups of the hemicelluloses or the carboxylate groups of the ferulic and *p*-coumeric acids of lignin and hemicelluloses. (Bhatnagar and Sain, 2005; Ma *et al.*, 2005; Alemdar and Sain, 2008b). The peaks at 1513.89 and 1426.65 cm^{-1} in the SBF representing the aromatic C=C stretch of aromatic rings of lignin were observed (Xiao *et al.*, 2001; Alemdar and Sain, 2008b). It indicated that the acid treatment could removed a large amount of pectins, lignin and hemicelluloses according to the chemical changes in the fiber surfaces results (item 2.1) and crystallinity by XRD analysis. For the peaks in the region 1200-950 cm^{-1} indicated the C-O stretching vibration of β-(1→4)-glycosidic linkage of cellulose (Proniewicz *et al.*, 2001; Colom and Carrillo, 2002; Ma *et al*., 2005; Oh *et al*., 2005; Alemdar and Sain, 2008b). The peak at 897.96 cm^{-1} assigned as C–H rocking vibration of glucose rings which indicated typical structure of cellulose (Rosa *et al.*, 2010; Socrates, 2010). The FT-IR results of SBF and MCC revealed the compositional changes in the fiber structures according to the chemical composition results.

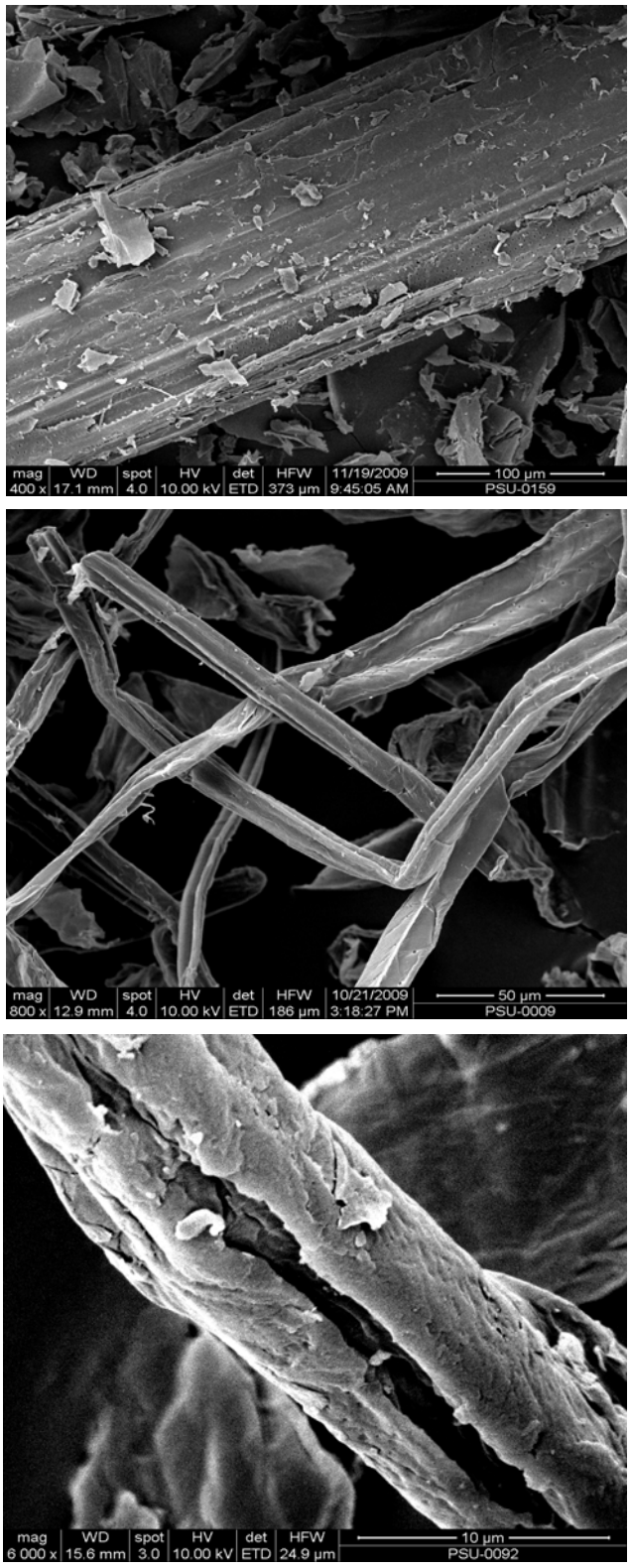

Figure 16. Scanning electron micrographs of SBF at magnification ×400 (A), MCC-c at magnification ×800 (B) and MCC-c at magnification ×6,000 (C).

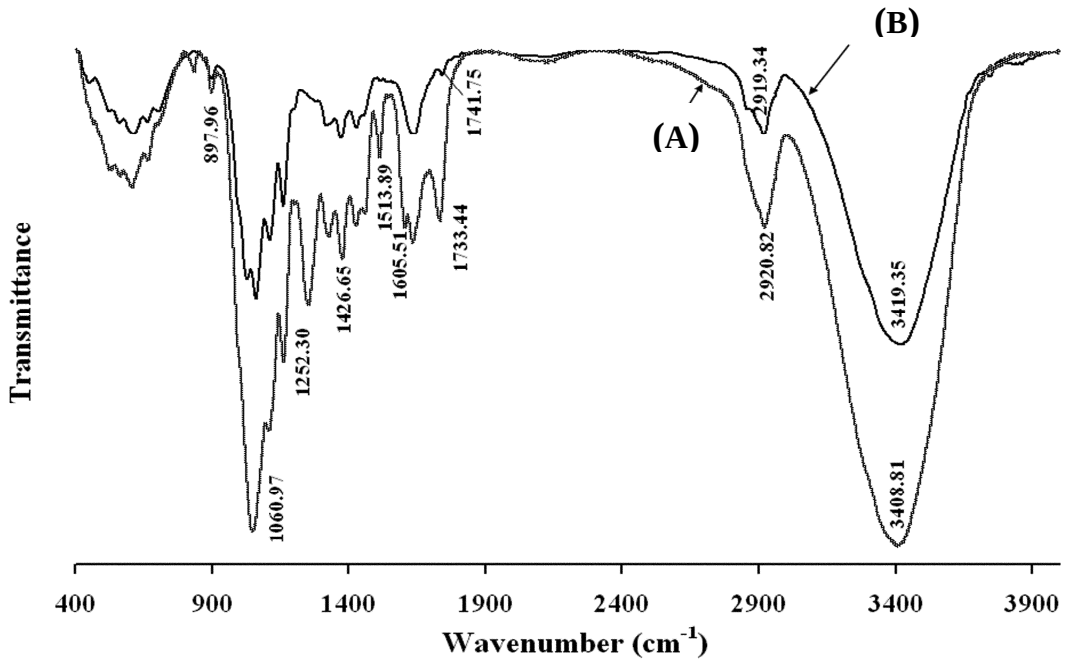

Figure 17. FT-IR spectra of SBF (A) and MCC-c (B).

2.4 X-ray diffractometry (XRD)

X-ray crystallography was used to investigate the crystallinity of SBF and MCC at different stages. X-ray diffraction patterns of SBF and MCC are shown in Figure 18. There were 3 peaks for each treatment (2θ = 15.5, 22 and 34.5 degrees). The peak at 2θ = 22 degree of MCC was sharper than that of SBF. The sharper diffraction peak indicated the higher degree of crystallinity in the structure of the treated fibers (Alemdar and Sain, 2008b).

The crystallinity values were estimated as 30% and 54.38%, for SBF and MCC, respectively. The crystallinity of the fiber increased after each stage of the chemical treatments. The increase in the crystallinity of MCC was due to the partial removal of the hemicelluloses and lignin (Alemdar and Sain, 2008b) according to the results in item 2.1, the composition of SBF and MCC. During the chemical treatments, cellulose chain breakage would occur at the amorphous regions first. The amorphous regions in the cellulose chains were susceptible to water or chemical penetration and degrade before the crystalline region (Wang and Sain, 2006). The increas in the number of crystallinity regions had increase the rigidity of cellulose. The higher crystallinity in MCC was associated with the higher tensile strength of the fibers (Alemdar and Sain, 2008a; b).

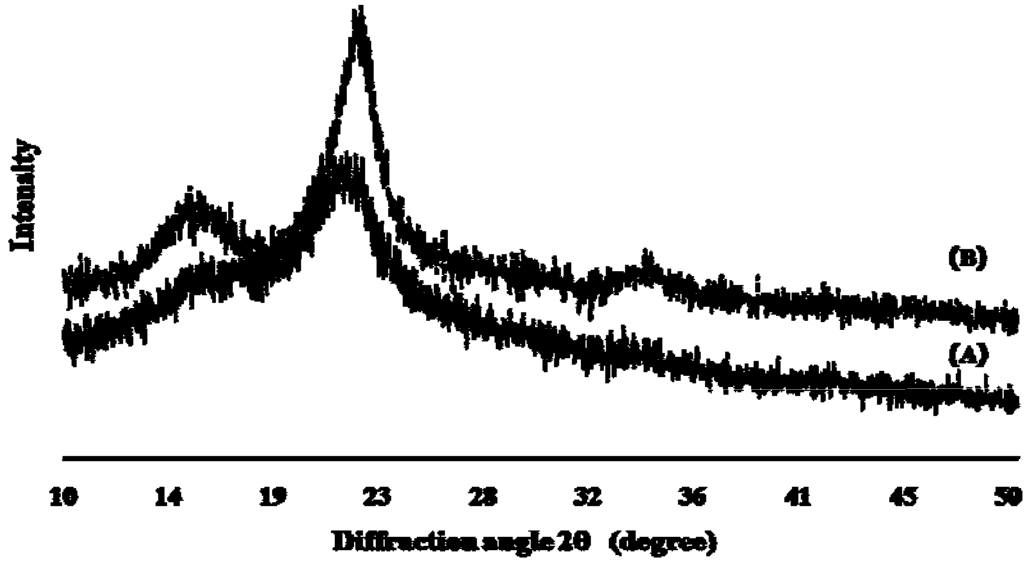

Figure 18. X-ray diffraction patterns of SBF (A) and microcrystalline cellulose (MCC-c) (B).

3. Effect of amount of starch on some properties of starch adhesive

3.1 Solid content and viscosity

Another important property of adhesive was adhesive viscosity which related to bonding property of adhesives (Lin and Gunasekaran, 2010). The viscosity of the adhesive was studied as a function of starch content and solid content. Three starch adhesives at various solid contents were prepared for a given intake of starch concentration such as 22, 26 and 30 wt%. The viscosity of adhesives was measured at lower solids contents (Table 9) as expected due to more diluted nature of the system that agreeing with the previous study of Hamarneh *et al*. (2010). They studied the development of soy proteins in polydetone-based wood adhesives. However, the viscosity of the commercial adhesive had the highest viscosity value, 3000 cps that was impacted from the highest of solid content, 63.00 % and their composition. The viscosity of starch adhesive at the concentration of 30 wt% (ST30), 2357.30 cps, was close to the highest viscosity of commercial adhesive. Therefore, the viscosity of starch adhesive depended on the solid content which was a clear function of the amount of starch in the formulation ($p<0.05$).

Table 9. Viscosity and solid content of commercial adhesive and starch adhesives at different concentration.

Type of adhesives	Concentration†	Viscosity at 26°C*	Solid content*
	%	cps	%
Commercial adhesive	-	3000.00±5.51^{d**}	63.00±1.41^{d**}
ST 22	22	1542.70±2.52^{a}	22.88±0.36^{a}
ST 26	26	1831.70±2.89^{b}	25.68±0.43^{b}
ST 30	30	2357.30±4.16^{c}	28.05±0.05^{c}

* Mean ± SD from triplicate determinations.

† Based on dry basis weight.

¥ Phenol-formaldehyde (PF).

** The different superscripts in the same column indicate the significant differences ($p<0.05$).

3.2 Mechanical properties: shear strength and mode of failure

The wood panels were prepared by applying the emulsions at solid content of 4.8–6.4 g/m^2 single adhesive line onto one side of (2.5×10) cm^2 veneer pieces. Then the wood panels were hot pressed at 175°C for 15 min under constant pressure of 3.45 MPa.

According to the European Standard, the shear strength should be higher than 1 MPa (>10^6 N/m^2) (Hamarneh *et al*., 2010). All the starch adhesives passed the EN-314 norm with higher shear strength than required. Bonding shear strengths of the starch adhesives of different total starch tested at dry conditions is shown in Table 10. It showed that the shear strength, mode of failure and average wood failure of starch adhesive at different concentration and solid content had significant effect on the shear strength. The average bonding strengths of commercial adhesive, ST-22, ST-26 and ST-30 adhesives were 17.48×10^5, 15.24×10^5, 18.71×10^5 and 15.71×10^5 N/m^2, respectively. The results of statistical analysis ($p>0.05$) indicated that the bonding strength was dependent on starch concentration and shear strength. The shear strength of ST-26 adhesive (18.71×10^5 N/m^2) was higher than the commercial adhesive (17.48×10^5 N/m^2). Thus, ST-26 adhesive was the optimal starch content and shear strength to use for wood adhesions which showed the highest

mechanical property due to its ability to disperse in water and on the interaction between starch adhesive and those of the substrate (Lin and Gunasekaran, 2010). These interactions could lead to increase adhesive strength of ST-26 adhesive with wood which agreed with the results of average wood failure (Table 10 and Figure 19). Table 10 shows percentage of adherent failure, which increased from 30% and 50% of commercial adhesive and low starch concentration of ST-22 adhesive to 70% of ST-26 adhesive. Although, ST-30 adhesive showed the low shear strength (15.71×10^5 N/m^2) and substrate failure (40%) but they indicated an extremely fracture (Figure 19 (D)).

Table 10. Shear strength, mode of failure and average wood failure of starch adhesives at different concentration.

Type of adhesive	Concentration[†]	Shear strength[*]	Mode of failure[**]	Average wood failure
	wt%	$N/m^2 \times 10^5$		%
Commercial adhesive[¥]	-	$17.48\pm1.03^{b***}$	C + S	30
ST 22	22	15.24 ± 1.15^{a}	C + S	50
ST 26	26	18.71 ± 1.24^{c}	C + S	70
ST 30	30	15.71 ± 1.08^{a}	C + S	40

[*] All values are reported as mean ($N \geq 10$)

[†] Based on dry basis weight.

[¥] Phenol-formaldehyde (PF)

[**] C-Cohesive failure of adhesive.

S-Failure of wood substrate.

[***] The different superscripts in the same column indicate the significant differences ($p<0.05$).

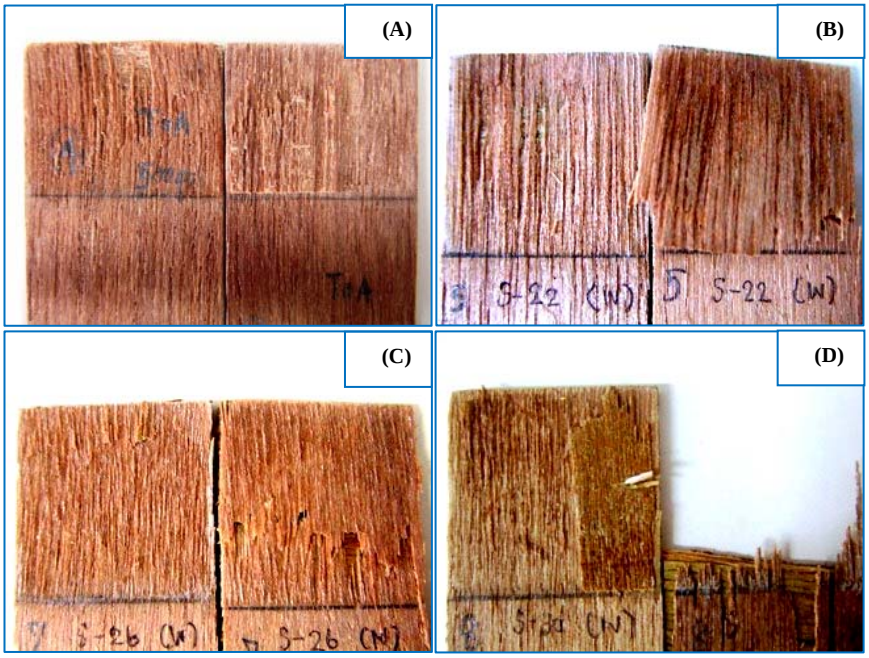

Figure 19. Photographs of the failure of starch adhesive joints at various amount of starch. Commercial adhesive (A), 22 wt% starch (B), 26 wt% starch (C) and 30 wt% starch (D), respectively.

4. Effect of microcrystalline cellulose (MCC) addition on the properties of starch composite adhesive

4.1 Solid content and viscosity

Viscosity was an important property governing the bonding property of adhesives. Different viscosity values had been suggested for different applications (Lin and Gunasekaran, 2010; Kumar *et al*., 2002). The viscosity value (at 26°C) of starch composite adhesives (at concentration of 26 wt%; ST-26) with various amount of MCC (0, 0.5, 1.5, 2.5 and 3.5 wt%, respectively) are presented in Table 11. The viscosity value was significantly increased with increasing amount of MCC ($p<0.05$). The relatively low viscosity made adhesives easy to mix and pour and high viscosity gives the good suspension properties of adhesives (Lin and Gunasekaran, 2010). Furthermore, the difference in viscosity also complicated the comparison of the adhesive properties, since the viscosity ought not to be too high or too low when the dispersion was applied on wood panel prior to pressing. If the viscosity was too high, it would be very difficult or even impossible to evenly spread the adhesive onto the

wood panel. On the other hand, if the viscosity was too low, the dispersion would either drain off or to a considerable extent penetrate the substrate, rendering the adhesive layer too thin (Nordqvist *et al*., 2010). However, the results showed that the viscosity of the starch adhesive with MCC addition could be use to adhere the wood panel. The viscosity and solid content of the starch composite adhesives were in range of 1841.00 to 2561.30 cps and 26.85 to 31.08 %, respectively.

Table 11. Effect of MCC addition on viscosity and solid content of starch adhesives at concentration of 26 wt%.

Type of adhesive	Amount of MCC[†] wt%	Viscosity at 26°C[*] cps	Solid content[*] %
ST26	-	1831.70±2.89[a**]	25.68±0.43[a**]
	0.5	1841.00±6.56[b]	26.85±0.15[b]
	1.5	1983.30±5.77[c]	28.48±0.38[c]
	2.5	2111.00±2.65[d]	30.28±0.23[d]
	3.5	2561.30±1.53[e]	31.08±0.07[e]

[*] Mean ± SD from triplicate determinations.

[†] Based on dry basis weight.

[**] The different superscripts in the same column indicate the significant differences ($p<0.05$).

4.2 Mechanical properties: shear strength and mode of failure

The objective of this section was to evaluate the mechanical properties of MCC-reinforced composites of starch adhesive. The shear strength measurements of dry wood substrates are presented in Figure 15 (Chapter 2). Table 12 shows the effect of MCC content (0, 0.5, 1.5, 2.5 and 3.5 wt%) on shear strength, mode of failure and average wood failure of starch composite adhesive. Most of shear strength values of starch composite adhesive were better than shear strength of starch adhesive without MCC addition, only if the shear strength of 3.5 wt% MCC in starch adhesive. According to the result of mode of adhesive failure (Table 12) and the photographs of the failure (Figure 20) of starch adhesive with 3.5 wt% MCC, they indicated that all joints failed cohesively at the interface between the adhesive and adhesive or cohesive near the interface fracture (Liu *et al*., 2005). There were no failure occurred at wood substrate region. Thus, the addition of MCC in starch adhesive was limited at 3.5

wt%. It might cause by starch adhesive with the higher MCC (>35 wt%) became high viscous (Table 11). The higher MCC amount decreased adhesive ability to properly wet, flow, and penetrate into the wood substrate. It was similarly to the research of Nordqvist *et al*. (2010). The adhesives need to fulfil for a proper bond to form. It must be able to wet the surface of the wood material, flow over it, and penetrate into the wood (Frihart, 2005). These three factors were partly dependent on the viscosity of the adhesive and thereby the dry content of the adhesive (Nordqvist *et al.,* 2010). However, the addition of MCC into starch adhesive phase could improve the adhesive mechanical properties when MCC was added at 0.5, 1.5 and 2.5 wt%, respectively. The extreme shear strength of starch composite adhesive with MCC increased from 18.71×10^5 N/m^2 for the starch adhesive without MCC to 29.01×10^5 N/m^2. Therefore, the MCC could be use as reinforcing filler in the starch matrix and for adhesive application that as other biopolymer matrix and biocomposites (Lu *et al.,* 2005; Wang *et al*., 2006; Builders *et al*., 2010 and Alemdar and Sain, 2008a)

Table 12. Effect of MCC addition on shear strength, mode of failure and average wood failure of starch adhesives.

Type of adhesive	Amount of MCC[†]	Shear strength[*]	Mode of failure[**]	Average wood failure[*]
	wt%	N/m^2 × 10^5		%
ST26	-	18.71±1.24^{b***}	C + S	70
	0.5	29.01±1.48^{d}	C + S	60
	1.5	28.41±2.88^{cd}	C + S	50
	2.5	25.07±1.55^{c}	C + S	20
	3.5	16.65±2.95^{a}	C	0

[*] All values are reported as mean (N ≥ 10)

[†] Based on dry basis weight.

[**] C-Cohesive failure of adhesive.

S-Failure of wood substrate.

[***] The different superscripts in the same column indicate the significant differences ($p<0.05$).

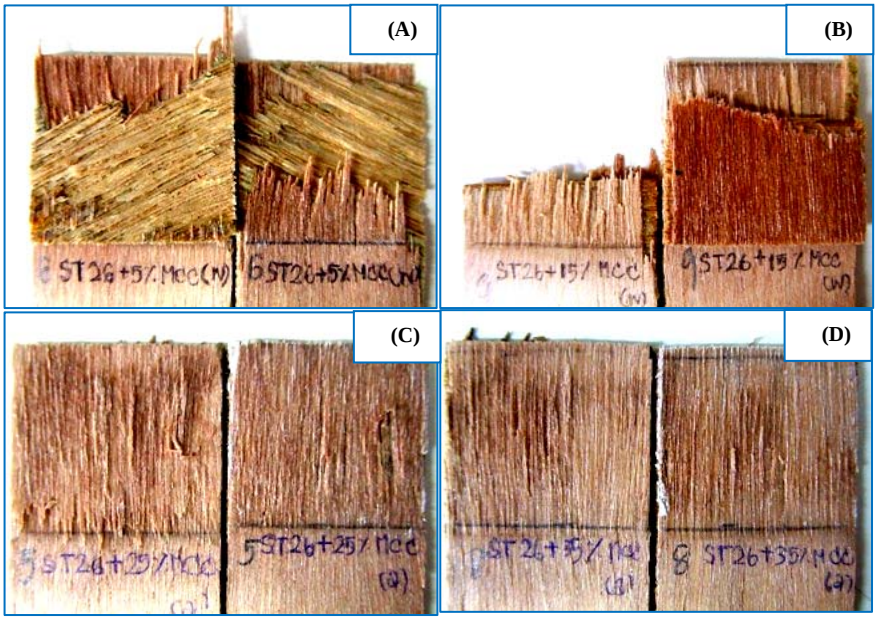

Figure 20. Photographs of the failure of starch composite adhesive joints at various amount of MCC. 0.5 wt% (A), 1.5 wt% (B), 2.5 wt% (C) and 3.5 wt% (D), respectively.

4.3 Morphology of the starch composite adhesive

The morphology of the starch adhesive and starch composite adhesive with MCC addition were examined under SEM. It was clearly observed from Figure 21 that the starch granules were collapsed partially gelatinization by NaOH agent. All of the starch adhesives were presented as partially destructured granules and indicated bonding through borax cross-linker (Das *et al*., 2010). Figure 21 (A) and (B) show morphology of the starch adhesive and starch composite adhesive with 0.5 wt% MCC. The MCC of starch composite adhesive was observed in starch matrix (Figure 21 (B)). The fibers were dispersed, covered and embedded in the starch matrix. The image showed that it had no aggregation of MCC in the matrix. Figure 21 (C) and (D) show the fracture surface of the starch composite adhesive at magnification of ×1000 and ×4000, respectively. The individual MCC filler dispersion distinguished in the starch adhesive. The SEM images displayed the fine adhesion between the MCC and the starch matrix which had uniform distribution of the MCC filler. Even after fracture, they seemed that MCC reinforcing fillers were recovered by the starch matrix,

implying good adhesion between MCC and starch matrix. Corresponding with the results of Lu *et al.* (2005) who studied morphology of cellulose crystallites dispersed in starch film. They implied the result was due to hydrogen bonding interactions between the hydroxyl groups of the components and, therefore, influence the physical properties of the resulting materials. In addition, the strength of these hydrogen bonds depended on the polarity of the fibers. Wang and Sain (2006) suggested that the polar cellulose fibers could be dispersed more easily with a polar polymer, because the polymer was able to wet the fibers very effectively and to prevent agglomerates of fibers. However, as the MCC content increased, the fracture surfaces display relatively rough structures by observation, similarly with Wang *et al*. (2006).

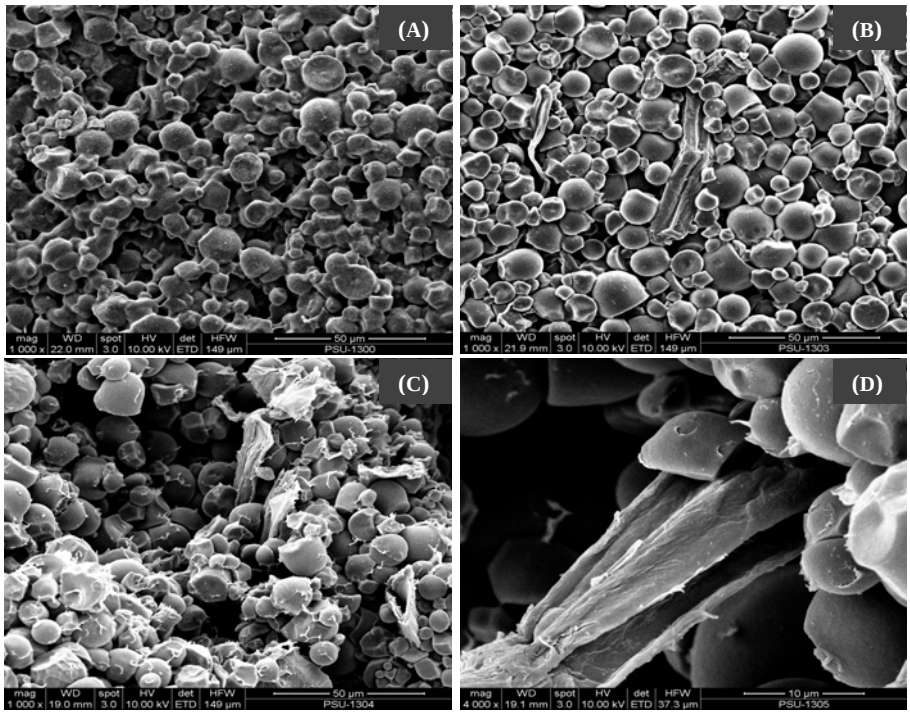

Figure 21. SEM micrographs of surface of the starch adhesive (ST26) (A), starch composite adhesive with 0.5 wt% MCC (B), cross-section at lower magnification (C) and at higher magnification (D) of the composite adhesive.

4.4 Fourier-transform infrared (FT-IR) spectroscopy

FT-IR spectroscopy was a quick and simple technique for identifying compound (Sherman, 1997). The FT-IR spectrum of a given compound was unique

and characteristic. This was because FT-IR spectrum distinguishes between the different kinds of bonds in a molecule (Builders *et al*., 2010). The FT-IR spectrum of starch adhesive at 26 wt% solid content or ST26, MCC and MCC/ST26 composite adhesive are presented in Figure 22. The FT-IR spectrum of ST26, MCC and composite adhesive were carried out as finger prints to identify composite adhesive relative to MCC and starch adhesive. The FT-IR spectrum of the composite polymers was different from those of starch adhesive and MCC (Figure 22 (A)). The spectra of MCC (Figure 22 (B)) and starch adhesive (Figure 22 (C)) were characterized by six and five strong peaks, which were identified at 3419.35, 2919.34, 1372.74, 1111.28, 1060.97 and 897.96 cm^{-1}, and 3431.72, 2923.15, 1636.52, 1021.63, 855.80 cm^{-1}, respectively. Whilst, the ST26+0.5% MCC composite adhesive (Figure 22 (A)) also showed six strong peaks and finger print region that was clearly observed. The peaks were identified at 3422.79, 2926.99, 1650.05, 1372.93, 1018.66 and 860.12 cm^{-1}. The peaks at 1018.66, 1060.97 and 1021.63 cm^{-1} of the starch composite adhesive, MCC and the starch adhesive, respectively, reflected comparable vibrational frequencies and correspond to absorption the finger prints region. The presence of similar absorbtion frequencies within finger prints region of absorption reflected the similarities of the polymers. According to the previous study, Buiders *et al.* (2010) confirmed that the three peaks of MCC/starch composite, MCC and starch are primary monomers of glucose. In addition, the peak of composite adhesive at 860.12 shifted from 855.81 cm^{-1} for starch adhesive which indicated C-O-C ring vibration in granular starch (Han *et al*., 2009; Das *et al*., 2010). The C-H asymmetric of MCC was found at 1372.93 cm^{-1} in the spectrum of starch composite adhesive. The presence of another prominent peak in the finger prints region of starch composite at 710.91 cm^{-1} could arise due to the exposure of a new functional group which were dislocation and reorientation of the monomers of the polymer chain (Builders *et al*., 2010). Apart from these prominent peaks identified, other peaks were present in the spectrum. The non-identification of these peaks could be due to either intra- or inter-molecular shielding of functional groups represented by these peaks that prevented the detection of their vibrations. FT-IR spectra suggested that some characteristic differences between the spectrum of composite adhesive and those of MCC and starch adhesive

in both of shifting, weakness, disappearance and occur of new peak indicated the result from various interactions between the different components and a new polymer type was formed (Han *et al*., 2009; Builders *et al*., 2010; Das *et al*., 2010).

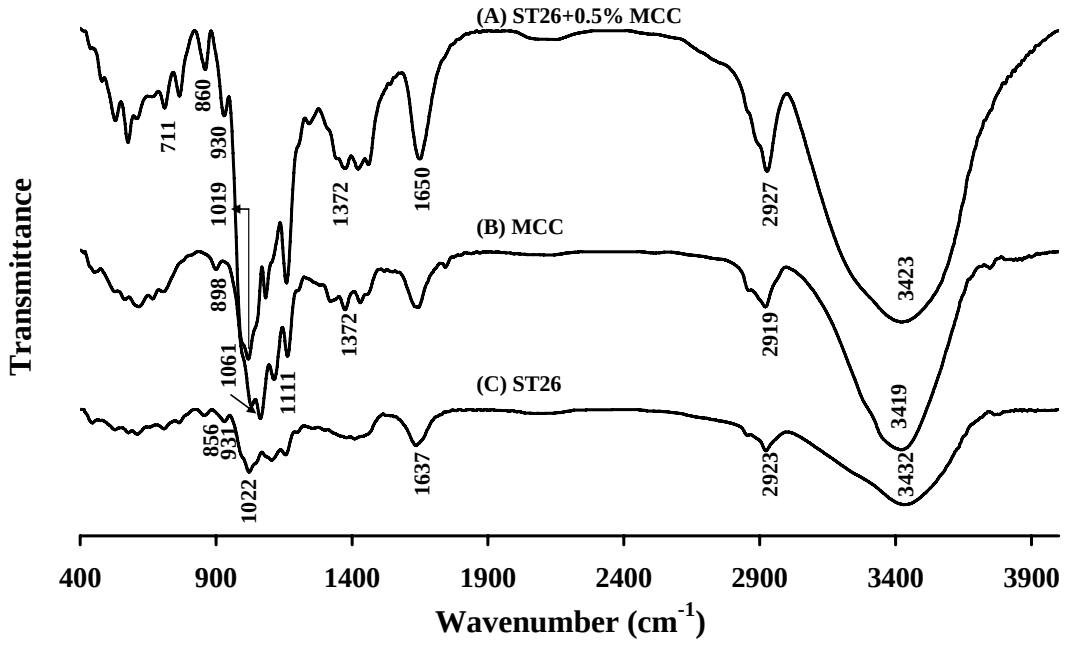

Figure 22. Effects of MCC addition on FT-IR spectra of starch adhesives. The ST26 adhesive+0.5% MCC (A), MCC (B) and ST26 adhesive without MCC (C).

4.5 Differential scanning calorimetry (DSC)

The thermal property of starch adhesive with and without MCC was investigated by DSC analysis. DSC was a useful method to characterize their exothermic and endothermic thermal transitions (Calandrelli *et al*., 2000; Builders *et al*., 2010). The DSC thermograms of composite adhesive (ST26+0.5%MCC) and starch adhesive (ST26) are shown in Figure 23. In general DSC thermograms of starch obtained from the first heating scan showed a broad endothermic peak at 105°C (Figure 23 (B)). At this peak, some researchers reported that it is the crystalline melting temperature in native starch molecules (Kaewtatip and Tanrattanakul, 2008). However, the peak was not appearing in the thermogram of composite adhesive. The starch adhesive could undergo two endothermal events which were melting of

amylopectin between 50 and 120°C and that of amylose between 120 and 170°C, in accordance with Silverio *et al.* (1996) and Kumar and Singh (2008). Whilst Ge *et al*. (2005) believed that the endothermic peak at 126.9°C was due to the crystalline melting which was formed between residue water and molecular chains of starch via hydrogen bonding. Mano *et al*. (2003) assumed that it might be due to water adsorption occurring above room temperature during heating scan. There was no conclusion for these explanations at this moment although all native starch showed this peak (Kaewtatip and Tanrattanakul, 2008). However, the starch composite adhesive (Figure 23 (A)) also appeared the small broad peak at 136°C. Generally, the plasticized starch film exhibits T_g transition at about 22°C (Lu *et al*., 2005). The starch composite adhesive showed high T_g value at 53.10°C, shown in Figure 23 (A). According to Lu *et al*., (2005) by incorporating MCC into starch matrix, the T_g transition of the starch-rich phase shifted to higher temperature from 23 to 48°C. The increase in T_g value dependence of the cellulose crystallites addition might be attribute to the interaction between starch and stiff crystallites, resulting in a decrease in the flexibility of macromolecular chain of starch.

A sharp endothermic peak at 157.33°C of starch adhesive was due to melting of amylose molecules, shown in Figure 23 (A). This peak was shift to the higher temperature at 188.33°C of starch composite adhesive. The effect of incorporation of MCC into the starch matrix (ST26) could be seen as shift in the higher melting endotherm. The result was according to addition of MCC into plasticized starch film. Kumar and Singh (2008) mentioned that the increased in peak temperature could be attributed to anti-plasticization of amylopectin-rich domains by incorporating the MCC. Agreeing with Angles and Dufresne (2000), the strong affinity of amylopectin molecules toward surface of cellulose fiber through high density of hydroxyl groups could reduce the global mobility of amylopectin domains. Therefore, the increase of T_g and T_m value resulted from decrease in the segment mobility and molecular interactions of the polymer (Shi *et al*., 2008).

Furthermore, Figure 23 (A) shows an extra peak in the exothermic peak of starch composite adhesive at 133°C. That not appeared in the peak of starch adhesive without MCC. Normally, the exothermic transition corresponds to the

polymer crystallization (Builders *et al*., 2010). Luz *et al*. (2008) revealed that the addition of fibers caused different crystallization in the matrix, because they were nucleating agents and changed the crystallization of the matrix around the fiber. The effects of chemical treated fiber addition act on fibers as nucleating agents of semi-crystalline thermoplastics, causing change in crystallization and melting heat of the final composite (Joseph *et al*., 2003). Evaluation of the thermograms of starch composite adhesive with MCC indicated that a new polymer type resulted from MCC addition might be attributed to the interaction between starch and MCC crystallites. The crystallinity of semicrystalline matrix polymers was an important factor that determines the stiffness, mechanical and fracture behavior of the crystallized matrix polymer.

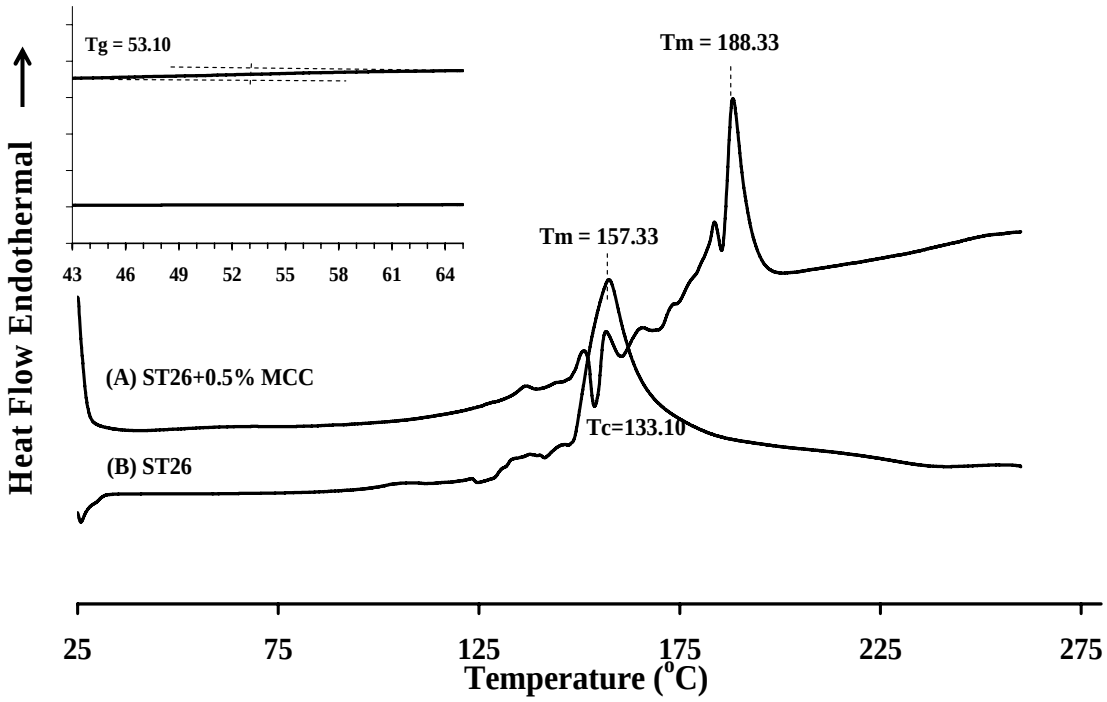

Figure 23. Effects of MCC addition on DSC curves of starch adhesives. Starch composite adhesive (ST26+0.5%MCC) (A) and starch adhesive (ST26) (B).

5. Effect of polyvinyl alcohol (PVOH) molecular weight and concentration on some properties of the adhesive

5.1 Solid content and viscosity

The viscosity of PVOH adhesives depended on the molecular weight (MW) and concentration. The relationship between solid content, viscosity and MW of PVOH is shown in Table 13. At the same concentration, the low molecular weight of the PVOH adhesive (L PVOH) gave the lowest viscosity ($p<0.05$). Similarly, the medium (M PVOH) and high (H PVOH) molecular weight of PVOH adhesives showed the medium and the highest viscosity, respectively ($p<0.05$). However, the molecular weight of PVOH did not relate to solid content of PVOH adhesives. The viscosity of the adhesive was associated with PVOH concentration.

Table 13. Viscosity and solid content of PVOH adhesives at different molecular weight and concentration.

Type of adhesives	Concentration[†] wt%	Viscosity at 26°C[*] cps	Solid content[*] %
Commercial adhesive[¥]	-	3000.00±5.51^{g**}	63.00±1.41^{g**}
L PVOH	8	69.00±1.58^{a}	7.64±0.02^{a}
	12	114.00±7.55^{b}	11.19±0.02^{b}
	16	150.00±2.08^{c}	14.95±0.02^{c}
	20	5550.00±7.21^{h}	19.04±0.10^{d}
	24	12447.00±5.86^{j}	22.71±0.10^{e}
	28	13330.00±5.00^{k}	25.78±0.01^{f}
M PVOH	8	263.00±2.63^{d}	8.22±0.07^{a}
	12	1468.00±1.15^{f}	11.05±0.03^{b}
	16	15631.00±7.55^{l}	14.81±0.07^{c}
H PVOH	8	750.00±1.10^{e}	7.94±0.02^{a}
	12	8570.00±6.66^{i}	11.36±0.16^{b}
	16	19666.00±2.08^{m}	14.62±0.07^{c}

[*] Mean ± SD from triplicate determinations.

[†] Based on dry basis weight.

[¥] Phenol-formaldehyde (PF).

[**] The different superscripts in the same column indicate the significant differences ($p<0.05$).

The concentrations of PVOH adhesive were increase from 8, 12, 16, 20, 24 and 28 wt% for the L PVOH adhesive and 8, 12 and 16 wt% for M PVOH and H PVOH adhesives. The viscosity of L, M and H PVOH adhesives from the lowest to highest concentration was raised from 69 to 13330, 263 to 15631 and 750 to 19666 cps, respectively ($p<0.05$). The adhesives with high viscosity (>10000 cps) spread with difficulty but contributed the better adhesion and bonding comparing to the low viscosity adhesives (< 10000 cps). Therefore the optimal viscosity values of the adhesives were 1000 to 10000 cps, depending on their ease of use.

5.2 Mechanical properties: shear strength and mode of failure

The adhesives were prepared from PVOH with various molecular weights and concentrations. The mechanical properties of PVOH adhesives depended on both molecular weight and concentration of PVOH used (Jaffe and Rosenblum, 1990). The molecular weights and concentration of PVOH had a dramatic effect on the adhesive properties as evidenced from the data presented in Table 14. The maximum concentrations of the prepared adhesive in each PVOH grades were different. It was due to the variation of the molecular weight and the chain length of PVOH. The maximum concentration of L, M and H PVOH adhesives were 28, 16 and 16 wt%, respectively. They showed the different shear strength, mode of failure and average wood failure of PVOH adhesives. The M PVOH and H PVOH adhesives contributed the higher shear strength and percentage of failure at wood compared to L PVOH adhesive at the same concentration ($p<0.05$). The failure of the adhesive joint is shown in Figure 24. These effects depended on molecular weights and concentration of PVOH adhesive.

The shear strength and percentage of wood failure of PVOH adhesives increased with increasing PVOH concentration. The lower concentration of each molecular weights of PVOH adhesive (low, medium and high) contributed the lower mechanical properties, whilst the higher concentration of the adhesives indicated higher mechanical properties. The concentration of PVOH had influence to the properties of PVOH adhesives. Higher concentrations gave the greater mechanical properties ($p<0.05$). Moreover, the PVOH adhesives at high concentration showed the higher shear strength and percentage of wood failure comparing to the commercial

adhesive, phenol-formaldehyde (PF). L PVOH adhesive at the highest concentration (28 wt%) showed the best mechanical properties of adhesion. However, the viscosity of this adhesive was too high. It was not suitable for application due to its spread.

Table 14. Shear strength, mode of failure and average wood failure of PVOH adhesive at different molecular weight and concentration.

Type of adhesive	Concentration[†]	Shear strength[*]	Mode of failure[**]	Average wood failure
	wt%	$N/m^2 \times 10^5$		%
Commercial adhesive[¥]	-	$17.48 \pm 1.03^{cd***}$	C + S	30
L PVOH	8	8.62 ± 1.55^{a}	C	0
	12	10.02 ± 0.53^{a}	C	0
	16	13.98 ± 0.36^{b}	C + S	30
	20	17.65 ± 1.14^{cd}	C + S	30
	24	21.25 ± 0.62^{e}	C + S	30
	28	25.62 ± 2.12^{f}	C + S	50
M PVOH	8	14.13 ± 0.75^{b}	C + S	20
	12	15.45 ± 0.67^{c}	C + S	50
	16	19.97 ± 2.53^{de}	C + S	80
H PVOH	8	12.94 ± 1.02^{b}	C + S	40
	12	17.92 ± 0.66^{cd}	C + S	60
	16	17.84 ± 0.46^{cd}	C + S	70

[*] All values are reported as mean ($N \geq 10$)

[†] Based on dry basis weight.

[¥] Phenol-formaldehyde (PF).

[**] C-Cohesive failure of adhesive.
S-Failure of wood substrate.

[***] The different superscripts in the same column indicate the significant differences ($p<0.05$).

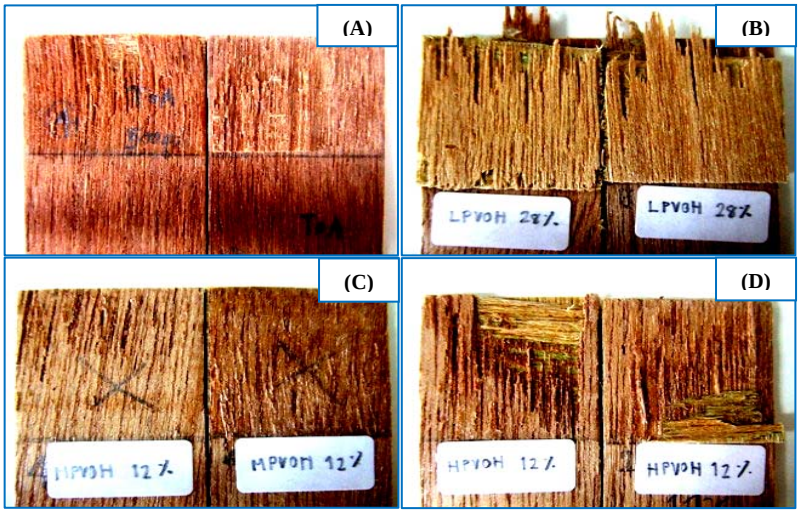

Figure 24. Photographs of the failure of commercial and PVOH adhesives joints at various types and concentrations. Commercial adhesive (A), L PVOH 28 wt% (B), M PVOH 12 wt% (C) and H PVOH 12 wt% (D), respectively.

6. Effect of microcrystalline cellulose (MCC) addition on properties of polyvinyl alcohol (PVOH) composite adhesive

6.1 Solid content and viscosity

As the previous results, M and H PVOH adhesives at the concentration of 12 wt% had the appropriated viscosity and shear strength properties for adhesive application. Then the adhesives were selected for this study. The amount of MCC had influence to the viscosity and solid content of PVOH adhesives, as shown in Table 15. The viscosity and solid contents of M PVOH adhesive containing MCC (0-3.5 wt% based on PVOH polymer) varied from 1468 to 2390 cps and 11.05 to 14.52 wt% when using MCC from 0 to 3.5 wt%, respectively ($p<0.05$). The PVOH adhesives with MCC filler contributed the higher viscosity compared to PVOH adhesive without MCC filler. However, this viscosity had no more effects on the efficiency of spreading on the surface of veneer specimens.

The viscosity and solid content of H PVOH adhesives also increased from 8570 to 10989 cps and 11.36 to 14.75 wt% after adding MCC from 0 to 3.5 wt%, respectively ($p<0.05$). In this case, the increase of the adhesive viscosity had affected on the efficiency of spreading on the test specimens, especially at MCC filler of 2.5 and 3.5 wt%. If the viscosity values of adhesives were over 10000 cps, the

adhesives were difficult to spread. Therefore, the addition of MCC filler into PVOH adhesives lead to raised viscosity and solid content in H PVOH adhesive. These effects might be caused by the swelling of the cellulose polymer in PVOH adhesives.

Table 15. Effect of MCC addition on viscosity and solid content of medium and high MW of PVOH adhesive at concentration of 12 wt%.

Type of adhesive	Amount of MCC† wt%	Viscosity at 26°C* cps	Solid content* %
M PVOH	-	1468.00±1.15[a**]	11.05±0.03[a**]
	0.5	1580.00±6.43[b]	11.98±0.02[c]
	1.5	1650.00±8.14[c]	12.50±0.13[d]
	2.5	1776.00±5.03[d]	13.36±0.03[f]
	3.5	2390.00±4.04[e]	14.52±0.01[h]
H PVOH	-	8570.00±6.66[f]	11.36±0.16[b]
	0.5	8909.00±3.51[g]	12.77±0.02[e]
	1.5	9001.00±1.53[h]	13.52±0.03[f]
	2.5	10432.00±4.16[i]	13.79±0.02[g]
	3.5	10989.00±2.65[j]	14.75±0.11[i]

* Mean ± SD from triplicate determinations.

† Based on dry basis weight.

** The different superscripts in the same column indicate the significant differences ($p<0.05$).

6.2 Mechanical properties: shear strength and mode of failure

Shear strength property was principal parameters that related to the mechanical property of adhesives. The shear strength of adhesives also affected the veneer failure, the higher shear strength, the higher veneer failure (Imam *et al*., 2001). The improvement of mechanical property of PVOH adhesives with MCC as an additive was investigated in this research. The criteria selected to judge PVOH adhesives for mechanical property improvement was shear strength, viscosity and compatibility with additives. Therefore, the optimal condition for a case study of MCC addition was M and H PVOH at the concentration of 12 wt%.

Table 16 shows the shear strength of PVOH adhesives containing various quantities of MCC additive (0-3.5 wt%). The shear strength of M PVOH adhesives increased from 15.45 to 24.14 MPa with increasing the MCC fillers content

from 0 to 1.5 wt%. The H PVOH adhesives increased shear strength from 17.94 to 21.52 MPa with increasing the MCC fillers content from 0 to 0.5 wt%. The results were the maximum shear force to separate or de-bond the glued veneers (Figure 25). This meant that incorporating MCC into PVOH adhesive resulted to increase the strong interactions between the adhesive and veneer. It was caused by the hydrogen bonds between cellulose and the PVOH matrix. Similar results were observed with MCC/PVOH composite films by Bhatnagar and Sain (2005). However, the addition of MCC at 2.5 and 3.5 wt% could induce the accumulation and gave too high viscosity value and solid content which actually decreased the effective reinforcing filler of MCC. Thus, PVOH adhesives reinforced with 2.5 and 3.5 wt% MCC content exhibited the lower shear strength than that with 0.5 and 1.5 wt%.

Table 16. Effect of MCC addition on shear strength, mode of failure and average wood failure of M and H PVOH adhesive at concentration of 12 wt%.

Type of adhesive	Amount of MCC† wt%	Shear strength* $N/m^2 \times 10^5$	Mode of failure**	Average wood failure* %
M PVOH	-	$15.45\pm0.68^{ab***}$	C + S	50
	0.5	22.13 ± 1.08^{e}	C + S	50
	1.5	24.14 ± 0.68^{f}	C + S	70
	2.5	16.72 ± 0.49^{bc}	C + S	40
	3.5	20.82 ± 1.34^{e}	C + S	30
H PVOH	-	17.94 ± 0.57^{cd}	C + S	60
	0.5	21.52 ± 1.64^{e}	C + S	70
	1.5	18.84 ± 1.12^{d}	C + S	60
	2.5	17.92 ± 0.41^{cd}	C + S	50
	3.5	14.83 ± 0.66^{a}	C + S	20

* All values are reported as mean ($N \geq 10$)

† Based on dry basis weight.

** C-Cohesive failure of adhesive.

S-Failure of wood substrate.

*** The different superscripts in the same column indicate the significant differences ($p<0.05$).

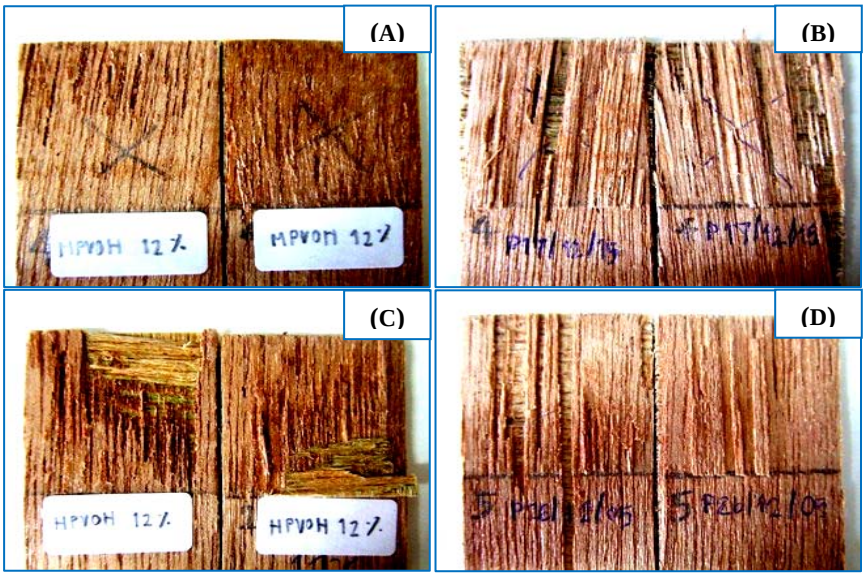

Figure 25. Photographs of the failure of PVOH and PVOH composite adhesives joints at PVOH concentration of 12 wt%. MPVOH (A), MPVOH+1.5 wt% MCC (B), HPVOH (C) and HPVOH+0.5 wt% (D), respectively.

6.3 Morphology of the polyvinyl alcohol (PVOH) composite adhesive

Figure 26 shows the appearance of PVOH composite adhesives at the concentration of 12 wt% with 1.5 wt% MCC. These images were investigated by optical microscope at a magnification ×4. The MCC phases seemed to consist of rod-like particles with the dimensions as previously presented. The results indicated that MCC fillers were evenly dispersed in the PVOH adhesive matrix.

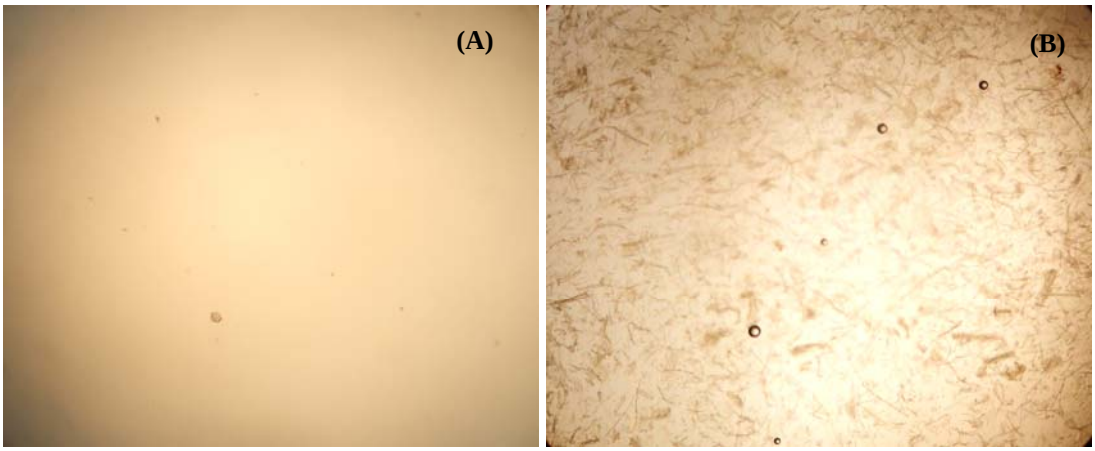

Figure 26. Optical microscope (×4) of surface morphology of the M PVOH adhesive at concentration of 12 wt%, pure PVOH adhesive (A) and PVOH composite adhesive with 1.5 wt% MCC (B).

The SEM images of the surface (at ×1000) and fracture (at ×4000) of M PVOH and MCC-filled PVOH composite adhesive are shown in Figure 27. The M PVOH adhesive, which was prepared from PVOH without MCC, was observed to have a relatively smooth and uniform surface as shown in Figure 27 (A).

The Figure 27 (B) shows cross-section of pure PVOH adhesive which were smooth. On the other hand, the surface and cross-section of M PVOH adhesive with 1.5 wt% MCC fillers (Figure 27 (C) and (D)) display reinforcing phase. It also indicated that no aggregates were present in PVOH composite adhesive and that the dispersion of the filler within the polymeric matrix was rather good. However, the aspect of the fractured surface was different and appeared to be more chaotic. The result was similar to cellulose whiskers reinforcing in PVOH matrix of Roohani *et al.* (2008). They ascribed to a higher degree of crystallinity of the material and/or strong interactions between the filler and the matrix leading to a fracture path through PVOH and nanoparticles. However, the MCC content increased the fracture surface of PVOH composite adhesives display relatively rough structure. Wang *et al*. (2006) suggested these effect that interfacial adhesion between polymer matrix (soy protein thermoplastic) and cellulose (whiskers) was relatively low. Moreover, more amount of MCC had effected during mixing difficulty between MCC and PVOH adhesive, especially at 3.5% MCC addition.

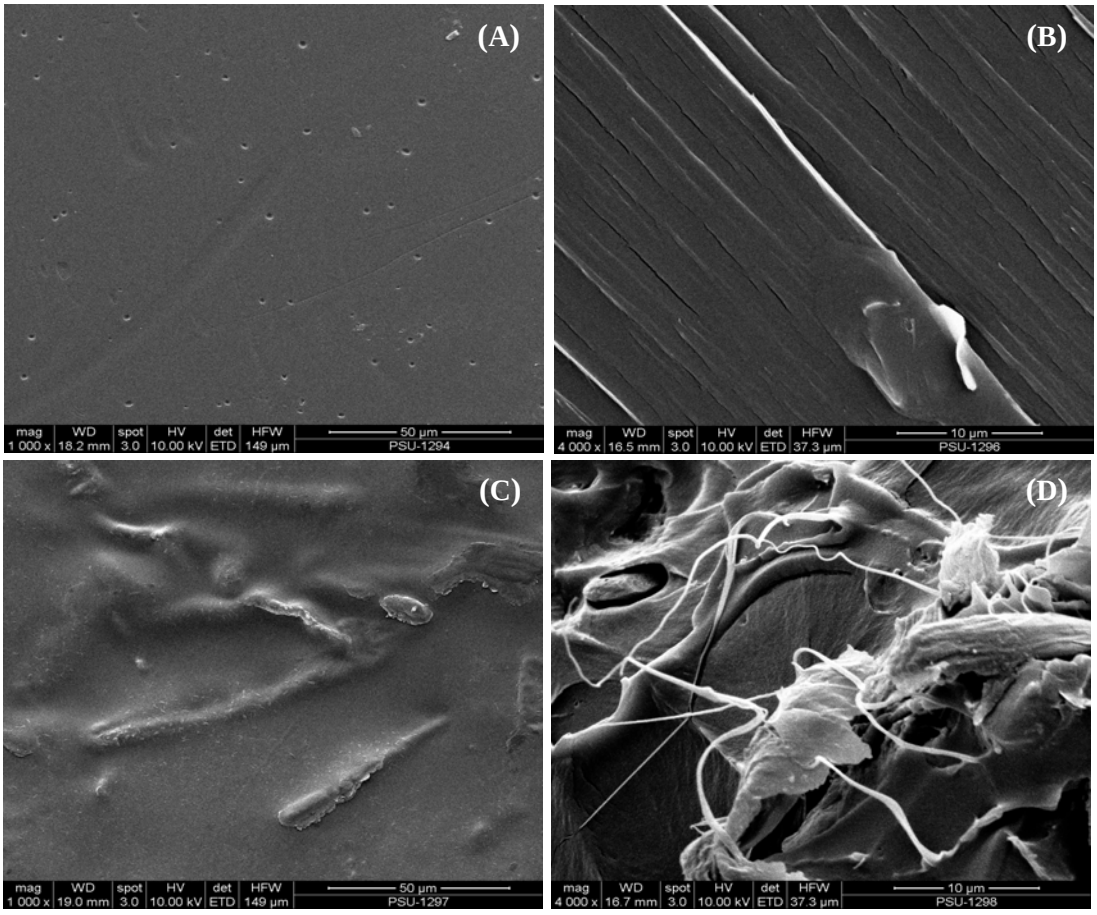

Figure 27. SEM micrographs of the surface (A), cross-section (B) of M PVOH adhesive and the surface (C) and cross-section (D) of PVOH composite adhesive with 1.5 wt% MCC, respectively.

6.4 Fourier-transform infrared (FT-IR) spectroscopy

FT-IR spectroscopy was used to investigate the change of chemical structure between PVOH adhesives and PVOH composite adhesives with MCC. The MCC made from sugarcane bagasse were used as the additive for the PVOH adhesives. Figure 28 shows the FT-IR spectra of M PVOH adhesive (Figure 28 (A)), H PVOH adhesive (Figure 28 (B)), M PVOH+1.5 wt% MCC adhesive (Figure 28 (C)), H PVOH+0.5 wt% MCC adhesive (Figure 28 (D)) and MCC (Figure 28 (E)). It was found that the transmittance variations and wavenumber of PVOH composite adhesives were shifted in both of M PVOH and H PVOH type with 1.5 and 0.5 wt% MCC, respectively. The bands of 3440.7 and 3434.8 cm^{-1} were the characteristic band of O-H groups while the bands of 859.8 and 855.5 cm^{-1} were the representative band

of C-H bending in M PVOH and H PVOH structure, respectively (Kürschner and Hoffer, 1967). They were become broader bands and shifted to lower wave numbers respectively in M and H PVOH composite adhesive structure, 3406.5, 3421 cm^{-1} and 851.2, 853.2 cm^{-1}, respectively. The FT-IR spectra suggested that the hydrogen-bonding interaction of hydroxyl groups in the PVOH and the cellulose in MCC formed the MCC/PVOH hybrid (Shao *et al*., 2003; Chen *et al*., 2010). The peaks at 2920.61, 2924.4 cm^{-1} (C-H stretching) and 906.5, 914.6 cm^{-1} (C-C stretching) were shifted to higher wavenumbers such as 2941.2, 2939.4 cm^{-1} and 919.2, 917.6 cm^{-1}, respectively. Furthermore, fingerprint region of 500-900 cm^{-1} indicated the PVOH structure (Focher *et al*., 2001). The composite adhesive spectrum showed the absorption peak at 705 cm^{-1} disappeared and the peak of 512 cm^{-1} and 628-648 cm^{-1} weakened. This region was similar to MCC spectra.

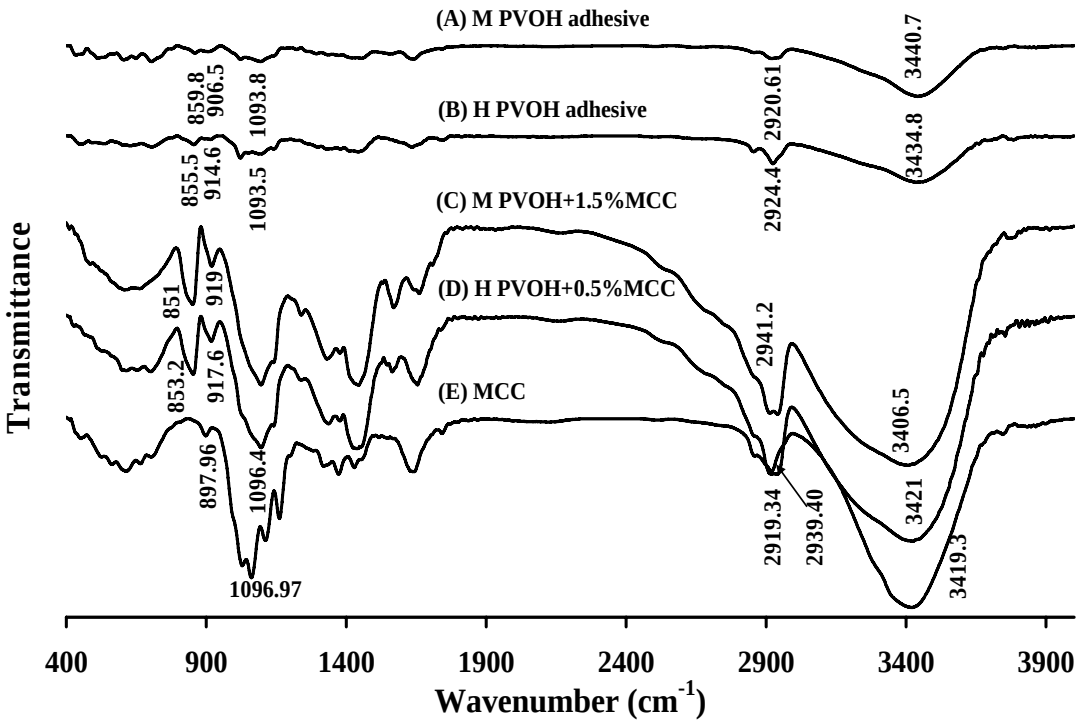

Figure 28. FT-IR spectra of the adhesives. M PVOH (A), H PVOH (B), M PVOH+1.5 wt% MCC (C), H PVOH+0.5 wt% MCC (D) and MCC (E).

The weakness, disappearance, and shift of the characteristic absorption band might result from the interaction of different OH groups in the PVOH and MCC molecular chains (Han *et al*., 2009). They indicated the development of new inter- and intramolecular hydrogen bonds and a change of the conformation between the PVOH and MCC (Oh *et al*., 2005). It could be concluded that there occur the chemical binding between PVOH and MCC molecules to effect on the improvement of compatibility and other properties of PVOH composite adhesives.

6.5 Differential scanning calorimetry (DSC)

The DSC was a useful method of characterizing polymers based on their exothermic and endothermic thermal transitions, such as glass transition temperature (T_g), melting temperature (T_m) and melting enthalpy (ΔH_m). The thermograms of PVOH and MCC/PVOH composite adhesives are shown in Figure 29. The values obtained for these parameters (Table 17) reflected the effect of MCC contents on the thermal properties of PVOH adhesives.

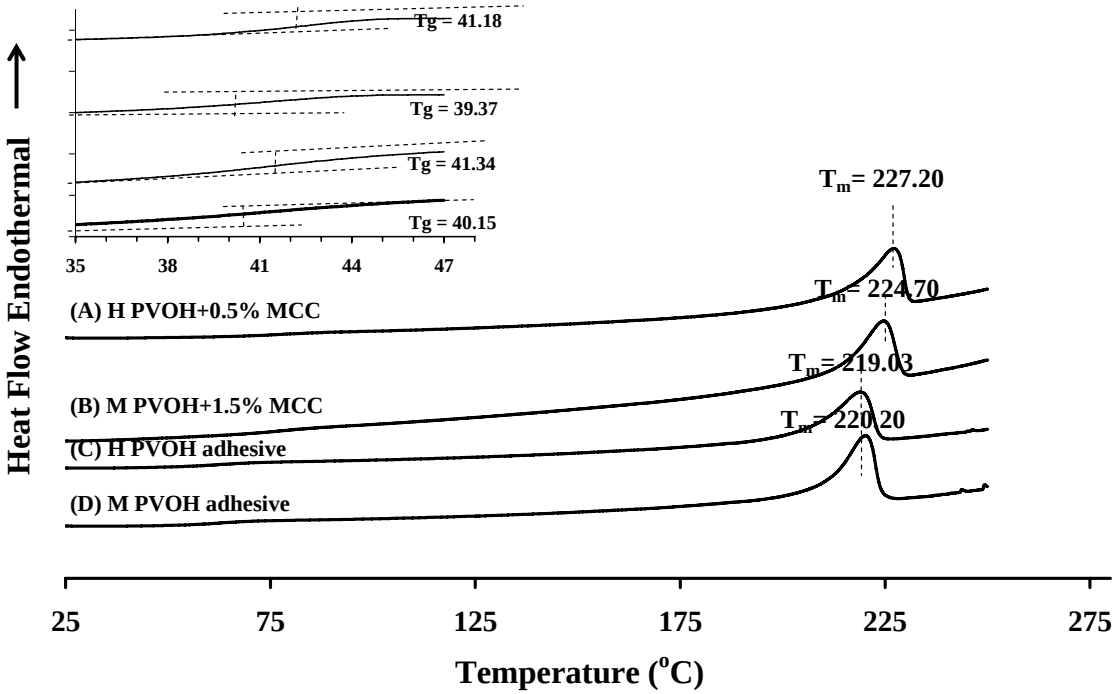

Figure 29. DSC thermograms of PVOH adhesives. H PVOH+0.5wt% MCC (A), M PVOH+1.5 wt% MCC (B), H PVOH (C) and M PVOH (D).

Table 17. Thermal properties of PVOH and PVOH composites adhesives.

Type of adhesive	T_g (°C)	ΔC_p (J/g)	T_m (°C)	ΔH_m (J/g)	X_c (%)
M PVOH	40.15	0.869	220.20	50.84	32.80
H PVOH	41.34	0.749	219.03	46.89	30.25
M PVOH+1.5% MCC	39.37	0.330	224.70	53.82	34.72
H PVOH+0.5% MCC	41.18	0.662	227.20	48.77	31.46

As shown in Figure 29, the thermograms of PVOH composite adhesives had two transitions: an initial endothermic transition peak which corresponds to T_g and endothermic peak that correspond to their melting temperature. It liked as the thermogram of PVOH adhesives. The first scan, it was observed the wide endothermic peaks around 60-130°C (data not shown), presumably associated with evaporation of free water and bound water that were absorbed in the adhesive samples (Limpan, 2009; Shi *et al*., 2008). The presence of T_g and T_m of PVOH adhesive reflected its partially crystalline structure. The T_g value of pure PVOH at concentration of 12 wt% of M and H PVOH were similarly around 40.15 and 41.34°C, respectively. It was lower than that reported in other works (Shi *et al*., 2008). This was because PVOH adhesives had already contained some water as plasticizer and thermogram showed broad T_g which might be because the commercial PVOH used consist of wide distribution of its molecular size (Limpan, 2009). The DSC curve of PVOH composite adhesives were compared with PVOH adhesives. It was observed that the addition of MCC showed no impact on T_g in both M and H PVOH adhesives at the same concentration of 12 wt%.

The peak at 219 to 220°C was assigned to the melting point-related peak of PVOH adhesives. When the MCC was added, the melting temperature increased and the height of the melting peak increased. Those containing the MCC consumed higher energy for material fusion, resulting in the increase of melting enthalpy (ΔH_m) and crystallinity percentage when MCC content was 0.5 and 1.5 wt% of M and H PVOH, respectively. This was in agreement with Luz *et al.* (2008), who found cellulignin addition that was nucleating agents and changed the crystallization

of the matrix around the fiber. Moreover, this might be because strong interactions between MCC and PVOH matrix. However, this strong interactions or cross-linking structure could be broken, resulting in a decrease in T_g (Wang *et al*., 2006). Because of the strong interaction between the PVOH molecules were little destroyed by addition of MCC, leading to an enhancement of the PVOH molecular mobility. However, the degree of crystallinity (X_c) of the material could be calculated from ΔH_m values (Roohani *et al*., 2008). The crystallinity of PVOH adhesive was determined by using the equation below:

$$X_c = \frac{\Delta H_m \times 100}{\Delta H^\circ_m \times W}$$

We calculated the enthalpy ΔH_m values through the numerical integration of areas covered by the melting peak and normalized by sample mass. Using the enthalpy of 155 J/g for a theoretical 100% crystalline PVOH (ΔH°_m) (Naebe *et al*., 2008; Probst *et al*., 2004) and W was given as the mass fraction of PVOH in the composite (Joseph *et al*., 2003; Luz *et al*., 2008). We estimated that pure PVOH exhibited a relatively crystallinity of ~32.80% and 30.25% for M and H PVOH, respectively. When compared with PVOH composite adhesive, the crystallinity slightly increased to 34.72 and 31.46% for M PVOH+1.5 wt% MCC and H PVOH+0.5 wt% MCC, respectively. The observed increase in the PVOH crystallinity indicated that MCC promoted crystallization of the PVOH in the MCC/PVOH composite adhesives.

7. Polyvinyl alcohol/Starch (PVOH/St) cross-linked adhesive

7.1 Viscosity, solid content and gel time of the PVOH/St cross-linked adhesive

The physical properties of adhesives did not only provide fundamental information for adhesive application, but also correlated results with those obtained from the adhesive composition. The viscosity of PVOH adhesives in this research depended on many factors such as the molecular weight, degree of cross-linking, starch ratio and gel time. Table 18 shows the viscosity, solid content and gel time of various adhesive formulations. The viscosity of H PVOH based adhesive was higher when compared to M PVOH adhesive ($p<0.05$). The viscosity and solid content had the relationships which tended to the same direction depending on the starch ratio in

adhesive composition. However, the adhesives with higher viscosity (>10000 cps) were hardly spread. They contributed the better adhesion, strong bonding and higher setting speed compared to the adhesive with lower viscosity. When the adhesive was spread on the wood test specimen, the lower viscous adhesive penetrated into the specimen rapidly (Kim, 2009). Therefore the optimal viscosity values of adhesives must not be over 10000 cps, depending on their ease of use.

Table 18. Viscosity, solid content and gel time of PVOH and PVOH/St cross-linked adhesive.

Type of adhesive	PVOH: Starch†	CA	Viscosity at 26°C*	Solid*	Gel time at 26°C*
	ratios	wt %	cps	%	h
M PVOH	1: 0	-	1468.00 ± 25.7^{a**}	11.05 ± 0.027^{a**}	-
	1: 0.5	-	2453.00 ± 34.9^{b}	20.42 ± 0.122^{b}	72.00
	1: 1	-	3980.00 ± 30.8^{c}	26.23 ± 0.162^{bcd}	72.00
	1: 1.8	-	7690.00 ± 40.9^{e}	29.61 ± 0.938^{d}	48.00
	1: 0.5	0.24	2453.00 ± 52.4^{b}	19.99 ± 0.044^{b}	1.80
	1: 1	0.24	5890.00 ± 19.7^{d}	23.14 ± 0.266^{bcd}	1.75
	1: 1.8	0.24	7890.00 ± 34.7^{f}	29.30 ± 0.196^{d}	1.42
H PVOH	1: 0	-	8570.00 ± 34.6^{g}	11.36 ± 0.159^{a}	-
	1: 0.5	-	9200.00 ± 45.9^{h}	20.73 ± 0.986^{b}	72.00
	1: 1	-	10009.00 ± 46.5^{i}	27.62 ± 1.601^{b}	48.00
	1: 1.8	-	13980.00 ± 87.6^{k}	29.42 ± 0.054^{d}	45.00
	1: 0.5	0.24	9340.00 ± 43.2^{h}	21.14 ± 1.567^{bc}	1.50
	1: 1	0.24	11329.00 ± 23.5^{j}	23.82 ± 0.689^{bcd}	1.50
	1: 1.8	0.24	14380.00 ± 65.0^{l}	28.82 ± 0.081^{cd}	0.92

* Mean ± SD from triplicate determinations.

† Based on dry basis weight.

** The different superscripts in the same column indicate the significant differences ($p<0.05$).

The gel time or pot life was important for an application of adhesive. It was the maximum time during which the adhesive system remained in a fluid state for use (Desai *et al*., 2003; Somani *et al*., 2003). Gelation was the incipient formation of a cross-linked network and it was the most distinguished characterization of a thermoset (Prime, 2010). In addition, gel time might be used to characterize the cure rate of adhesive (Gollob and Wellons, 2003). Therefore, a thermoset lost its ability to flow and was no longer processable above the gel point and gelation defined the upper

limit of the work life (Prime, 2010). The gel times of various adhesive formulations are shown in Table 18. The results indicated that PVOH/St cross-linked adhesive containing CA catalysts adduct gelled (initially cured) faster than PVOH/St cross-linked adhesive without CA at room temperature. It was due to the primary cross-linked in both of the cross-linked adhesive with and without CA. However, the interaction mechanism of PVOH and starch cross-linking was independent of CA catalyst, free of non-cross-linking side reactions, functionality, reactants, time and temperature. CA addition and high starch ratio in each formulation resulted to the gel time reduction. The CA catalyst and starch ratio had an effect on the gel time caused by the cross-linking reaction with HMMM cross-linker suitably. The higher ratio of starch contributed the more cross-linked bonding between PVOH, starch and HMMM which brought about the faster gel time compared to those with the lower starch ratio. Furthermore, the gel time of H PVOH/St cross-linked adhesive was slightly faster than that of M PVOH/St cross-linked adhesive. However, there was a limitation on the useable period time on application of the adhesive.

7.2 Mechanical properties: shear strength and mode of failure

Table 19 shows the potentiality of PVOH and PVOH/St cross-linked adhesive at different adhesive formulations. All of M and H PVOH/St cross-linked adhesives in both of with and without CA catalyst tended to increase in shear strength of adhesive ($p<0.05$). As the result, mode of wood failure and average wood failure related to the shear strength of adhesives. The higher shear strength of adhesive contributed the higher percentage of wood failure (S) because adhesive-bonded specimens failed primarily in the cohesive mode (Hagg *et al*., 2006). The shear strength of PVOH/St cross-linked adhesive with CA catalyst tend to increase when compared to PVOH/St cross-linked adhesive without CA at the same starch ratio ($p<0.05$). The wood failure caused by PVOH/St cross-linked adhesive was a fracture in the adherent and wood substrate, shown in Figure 30. It was due to the stronger interactions between the PVOH, starch and HMMM cross-linker which was confirmed by the cross-linking structure with the FT-IR results. Moreover, the starch ratio also affected to the adhesive shear strength. For M PVOH/St cross-linked adhesive, the shear strength value increased with increasing the starch ratio. The

maximum shear strength value was 26.5×10^5 N/m^2 which contributed the 100% wood failure at the starch ratio of 1.8. However, the results were reversed in the H PVOH cross-linked adhesive. The starch ratio increased from 0.5, 1 and 1.8 but the shear strength value of adhesive decreased to 30.3, 25.3 and 21.8×10^5 N/m^2, respectively ($p<0.05$), as shown in Table 19. These results might due to the high molecular weight of H PVOH, adding CA and especially, the viscosity of the cross-linked adhesive. As Table 18, the viscosity of H PVOH at the ratio of 1:1 and 1: 1.8 showed the viscosity values over 10000 cps. As mentioned above, the high viscosity had resulted to the flow behavior, the penetration into wood substrate and the bonding adhesion. Together with reasons of adding CA catalyst, CA could act as the catalyst, the cross-linker and the plasticizer in the starch/polyvinyl alcohol composites. Generally, the tensile or shear strength increased as the percentage of cross-linker increased. The results were opposite when the plasticizers increased (Shi *et al*., 2010). In addition, the high molecular weight of PVOH had a great influence on the reaction between starch and cross-linker and greatly indicated different properties of a polymer adhesive, like mechanical strength (Shi *et al*., 2010). Therefore, the optimal ratio between PVOH and starch composition in the cross-linked adhesives were the ratio of 1: 1.8 for M PVOH/Starch and the ratio of 1: 0.5 for H PVOH/Starch with using CA as a catalyst in the cross-linking reaction.

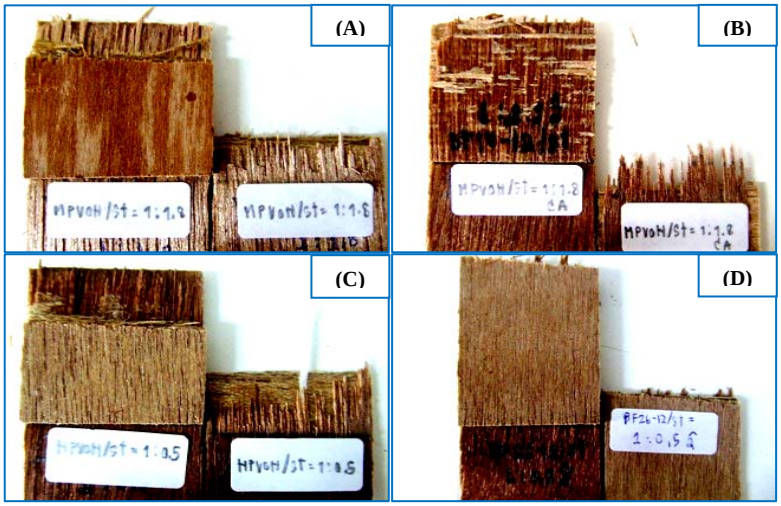

Figure 30. Photographs of the failure of PVOH/St cross-linked adhesive joints. M PVOH/St=1:1.8 (A), M PVOH/St=1:1.8 CA (B), H PVOH/St=1:0.5 (C) and H PVOH/St=1:0.5 CA (D), respectively.

Table 19. Shear strength, mode of failure and average wood failure of PVOH and PVOH/St cross-linked adhesive.

Type of adhesive	PVOH: Starch[†] ratios	CA wt %	Shear strength[*] $N/m^2 \times 10^5$	Mode of failure[**]	Average wood failure[*] %
Medium MW	1: 0	-	$15.45 \pm 0.68^{a***}$	C + S	80
	1: 0.5	-	21.10 ± 2.32^{cd}	S	100
	1: 1	-	18.08 ± 0.86^{a}	C + S	80
	1: 1.8	-	18.37 ± 1.19^{a}	S	100
	1: 0.5	0.24	23.37 ± 2.05^{cd}	C + S	80
	1: 1	0.24	23.02 ± 3.87^{cd}	C + S	80
	1: 1.8	0.24	26.48 ± 0.73^{d}	S	100
High MW	1: 0	-	17.94 ± 0.57^{a}	C + S	70
	1: 0.5	-	21.99 ± 1.88^{bc}	C + S	90
	1: 1	-	18.80 ± 1.12^{ab}	C + S	90
	1: 1.8	-	22.04 ± 1.68^{bc}	C + S	80
	1: 0.5	0.24	30.27 ± 4.35^{e}	S	100
	1: 1	0.24	25.29 ± 4.71^{cd}	S	100
	1: 1.8	0.24	21.80 ± 3.57^{bc}	C + S	90

[*] All values are reported as mean ($N \geq 10$)

[†] Based on dry basis weight.

[**] C-Cohesive failure of adhesive.
S-Failure of wood substrate.

[***] The different superscripts in the same column indicate the significant differences ($p<0.05$).

7.3 Effect of starch ratio on structural and thermal properties of the PVOH/St cross-linked adhesive

7.3.1 Fourier-transform infrared (FT-IR) spectroscopy

The effects of PVOH/Starch ratio on the structure of PVOH/St cross-linked adhesive were investigated and the results are shown in Figure 31. FT-IR analysis of the adhesives revealed the compositional changes in PVOH/St cross-linked adhesive compared to pure PVOH and starch adhesive. It could be seen clearly that the peak at 1023.2 cm^{-1} increased with increasing the starch ratio. This peak indicated the –C-O-C- stretching of the ether groups presented in the structure (Das *et al*., 2010). The increase of the peak height was excellent evidence for the degree of cross-linking reaction (Shi *et al*., 2008). Figure 31 (C) to (E) shows the effects of starch ratio on PVOH/St cross-linked adhesive at 0.5, 1 and 1.8, respectively. The

peak at 1023.2 cm^{-1} of PVOH/St cross-linked adhesive in the ratio of 1: 1.8 (Figure 31 (E)) was the highest. The peaks at 3434.8, 2855.4 and 2924.4 cm^{-1} depicted the O-H stretching vibration and C-H stretching vibration in the PVOH/Starch blending structure. They were decrease when starch ratio increased. This was one reason to confirm that the starch ratio had affect to the degree of cross-linking reaction of PVOH/St cross-linked adhesive using HMMM and CA as a cross-linker and catalyst, respectively.

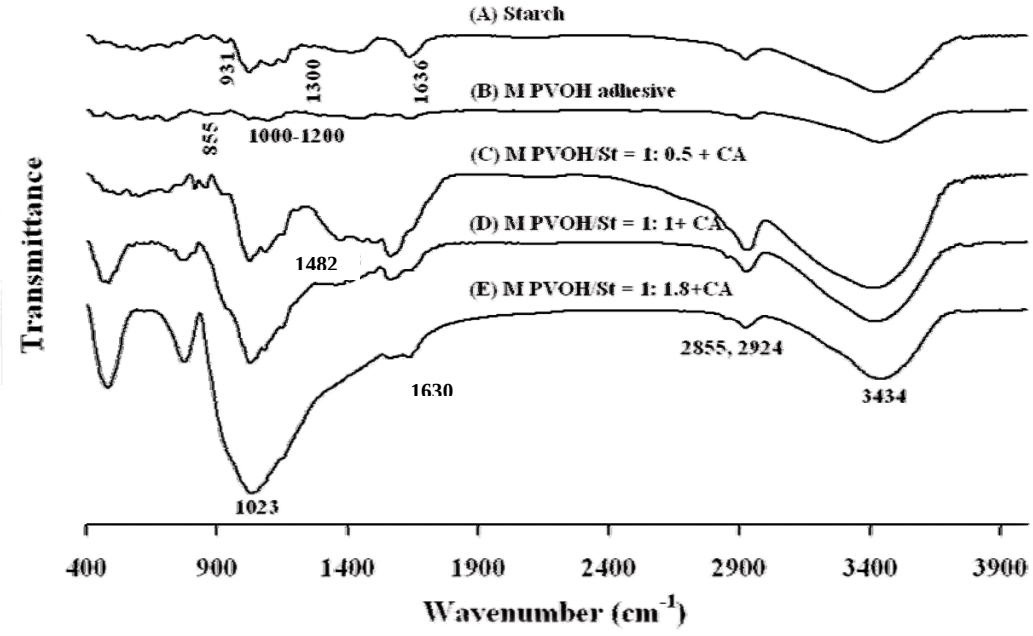

Figure 31. Effects of starch ratio on FT-IR spectra of PVOH/St cross-linked adhesive. Starch (A), M PVOH adhesive (B), M PVOH/St=1: 0.5+CA (C), M PVOH/St=1: 1+CA (D) and M PVOH/St=1: 1.8+CA (E).

The peak at 1482 cm^{-1} showed the free methoxy groups of HMMM which remained in PVOH/St cross-linked adhesive (Chen *et al*., 1997). This peak disappeared in the structure of PVOH/St cross-linked adhesive at the ratio of 1: 1.8 (Figure 31 (E)). It could be conclude that the methoxy groups of HMMM had participated completely in the cross-linking reaction at this ratio. Cross-linking occurred through a transetherification reaction between the methoxy groups of HMMM and hydroxyl groups of starch, PVOH, and wood (Figure 7). It produced an efficient network of inter- and intra cross-links between wood, starch, and PVOH, resulting in high bond strength (Imam *et al*., 2001; Limpan, 2009).

7.3.2 Differential scanning calorimetry (DSC)

The thermal properties of PVOH/St cross-linked adhesive were important in order to gauge their applicability. The DSC results obtained from PVOH adhesives and PVOH/St cross-linked adhesive at the different ratios are shown in Figure 32 and the data were summarized in Table 20.

Table 20. DSC data of PVOH and PVOH/St cross-linked adhesives.

Type of Adhesive	T_g (°C)	ΔC_p (J/g)	T_m (°C)	ΔH_m (J/g)
M PVOH adhesive	40.15	0.869	220.20	50.84
H PVOH adhesive	41.34	0.749	219.03	46.89
M PVOH/St = 1: 0.5	43.65	0.456	-	-
M PVOH/St = 1: 0.5 + CA	48.27	0.349	-	-
M PVOH/St = 1: 1.8	48.36	0.492	-	-
M PVOH/St = 1: 1.8 + CA	47.25	0.129	-	-
H PVOH/St = 1: 0.5	45.20	0.557	-	-
H PVOH/St = 1: 0.5 + CA	48.27	0.389	-	-
H PVOH/St = 1: 1.8	50.70	0.283	-	-
H PVOH/St = 1: 1.8 + CA	51.86	0.400	-	-

The changes of physical properties in PVOH/St cross-linked adhesive could be reflected by the glass-transition temperature (T_g) and melting point (T_m). The cross-linking would limit the movement of molecular segments, which resulted to increase the T_g value (Shi *et al*., 2008). The T_g values of PVOH/St cross-linked adhesive at the ratio of 1: 0.5 and 1: 1.8 shifted to higher temperature comparing to the T_g values of PVOH adhesive. The T_g values of M PVOH/St cross-linked adhesive at the ratio of 1: 0.5 and 1: 1.8 increased from 40.15°C for M PVOH adhesive to 48.27 and 47.25°C, respectively (Table 20). It meant that there was the good blend compatibility of these PVOH/St cross-linked adhesives. The T_g values increased significantly as the completely curing reaction due to the establishment of a cross-linked molecular structure, that agree with the FT-IR results. Eventually, as the degree of curing reaction of thermoset approaches 100% or completely cure, the T_g of the material will reach a limiting value, T_g (α) (Sichina, 2000). However, the presence of cross-linked network had affected the PVOH crystallization. T_m and ΔH_m hardly

changed upon cross-linking. The disappearance of the melting transition temperature in PVOH/St cross-linked adhesives indicated the thermoset property of the adhesives.

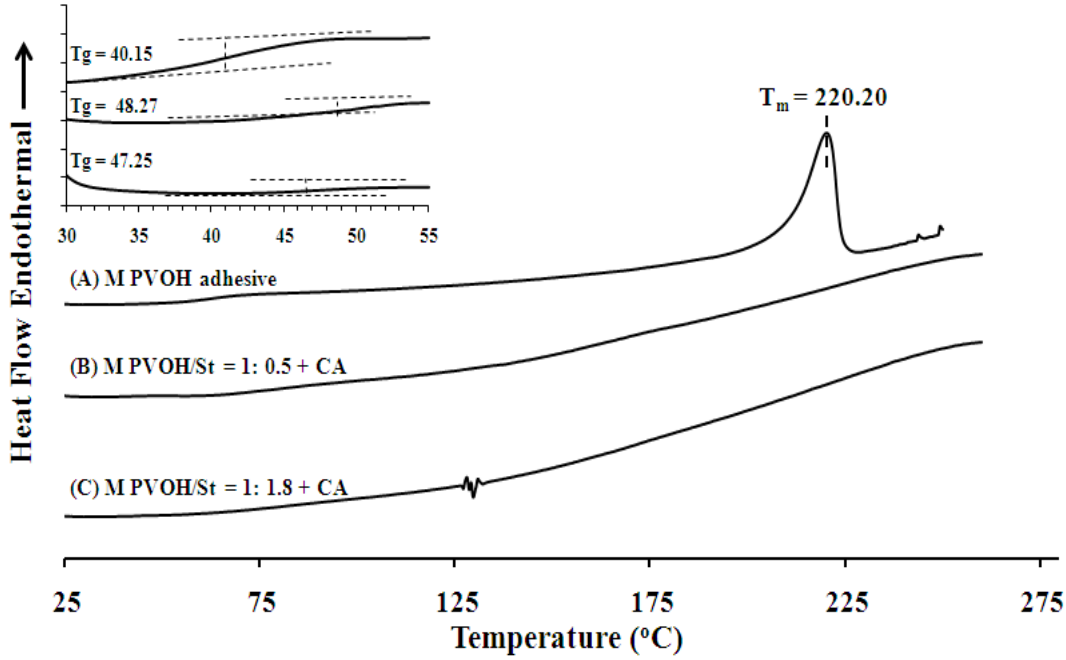

Figure 32. Effects of starch ratio on DSC curves of PVOH/St cross-linked adhesive. M PVOH adhesive (A), M PVOH/St=1:0.5+CA (B) and M PVOH/St=1:1.8+CA (C).

7.4 Effect of citric acid (CA) on the structural and thermal properties of the PVOH/St cross-linked adhesive

7.4.1 Fourier-transform infrared (FT-IR) spectroscopy

Infrared spectroscopy was used to evaluate the quality of PVOH and starch reaction with and without a CA catalyst by using HMMM as a cross-linker. Figure 33 shows the FT-IR spectra of starch (Figure 33 (A)), M and H PVOH (Figure 33 (B) and (C)), PVOH/St cross-linked adhesive without CA at PVOH/St ratio of 1: 1.8 (Figure 33 (D) and (E)) and PVOH/St cross-linked adhesive with CA at the PVOH/St ratio of 1: 1.8 (Figure 33 (F) and (G)). These Figure depicted the O-H stretching vibration (3434.8 cm^{-1}) and C-H stretching vibration (2855.4, 2924.4 cm^{-1}) in the structure of the PVOH and starch. The peaks at 1636.5, 1300.6 and 931.1 cm^{-1} in Figure 33 (A) were the intramolecular hydrogel which represented the -CH_2OH

stretching vibration and C-O-C ring vibration in the granular starch (Han *et al*., 2009).

For PVOH, the peak was observed at 1200-1000 cm^{-1} assigned as a dependent of the crystallinity in M and H PVOH and the peak at 855.55 cm^{-1} was due to C-H bending in the PVOH structure (Imam *et al*., 1999). Additionally, the ether group absorption peaks (1023.2 cm^{-1}) confirmed the cross-linking of HMMM with the hydroxyl group in the PVOH and starch chains.

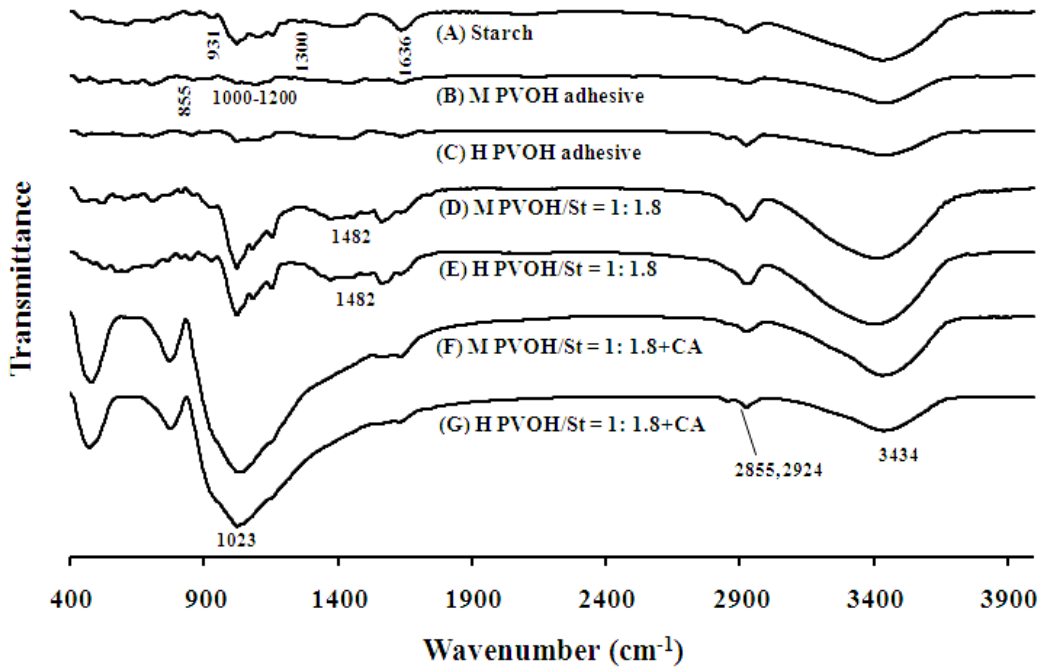

Figure 33. Effects of citric acid on FT-IR spectra of PVOH/St cross-linked adhesive at PVOH/St ratio of 1: 1.8. Starch (A), M PVOH adhesive (B), H PVOH adhesive (C), M PVOH/St=1:1.8 (D), H PVOH/St=1:1.8 (E), M PVOH/St=1:1.8+CA (F) and H PVOH/St=1:1.8+CA (G).

The sharp peak at 1023.2 cm^{-1} in Figure 33 (F) and (G) indicated the –C-O-C- stretching of the ether groups presented in the structure as described in item 7.1.1. However, the peaks in Figure 33 (D) and (E) were significantly lower than the peak in Figure 33 (F) and (G) due to the principal effect of the catalyst, CA. The peak at 1482 cm^{-1} in Figure 33 (D) and (E) indicated the free methyl groups of HMMM remained in PVOH/St cross-linked adhesive (Rahman *et al*., 2007). However, this peak disappeared in M and H PVOH/St cross-linked adhesive with CA (Figure 33 (F) and (G)). It implied that the methoxy groups in HMMM of PVOH/St cross-linked

adhesive without CA had not completely participated in the cross-linking reaction of the PVOH and starch. On the other hand, all the methoxy groups of HMMM in PVOH/St cross-linked adhesives with CA completely participated because these cross-linkers were oligomeric in nature with the main functionalities, methoxymethyl and imino. They reacted with PVOH and starch molecules according to general acid catalysis (CA) with a high tendency towards self-condensation reactions that improved the reaction speed but limit the flexibility of the treated material (Cytec, 2009).

7.4.2 Differential scanning calorimetry (DSC)

The changes of physical properties in blend and cross-linked polymer could be reflecting in glass-transition temperature (T_g) and melting point (T_m) (Hyder and Chen, 2009). In Figure 34, the T_g values of PVOH/St cross-linked adhesive with and without CA shifted to the higher temperature comparing to T_g value of PVOH adhesive. The T_g values of M and H PVOH cross-linked adhesive at the PVOH and starch ratio of 1: 1.8 increased from 40.15 and 41.34°C to 48.36 and 50.70°C for M and H PVOH/St cross-linked adhesive without CA and to 47.25 and 51.86°C for M and H PVOH/St cross-linked adhesive with CA at the same ratio, respectively (Figure 34 and Table 20). However, the PVOH hydroxyl groups contributed the hydrogen bonding to stiffen the linear polymer. By addition a cross-linking agent, the number of hydroxyl groups diminishes and hydrogen bonding interaction decreased which included the result of starch molecules obstruction (Krumova *et al*., 2000). The PVOH/St cross-linked adhesive produced the rigidity that affected to the T_g value increased but ΔC_p decreased due to the loss of linear polymer. The effect of CA on the T_g value of PVOH/St cross-linked adhesive also depended on the ratio of starch (Table 20). The T_g value of PVOH/St cross-linked adhesive with CA was trifling higher than the adhesive without CA at the highest ratio of PVOH/Starch (Table 20). These might cause by the blending had more effect on the thermal property than the cross-linking. However, this ratio help PVOH/St cross-linked adhesive to reach the complete cure which the T_g would reach with limited value, T_g (α) (Sichina, 2000), as

described. The result was due to the stronger interactions between PVOH, starch and HMMM cross-linker.

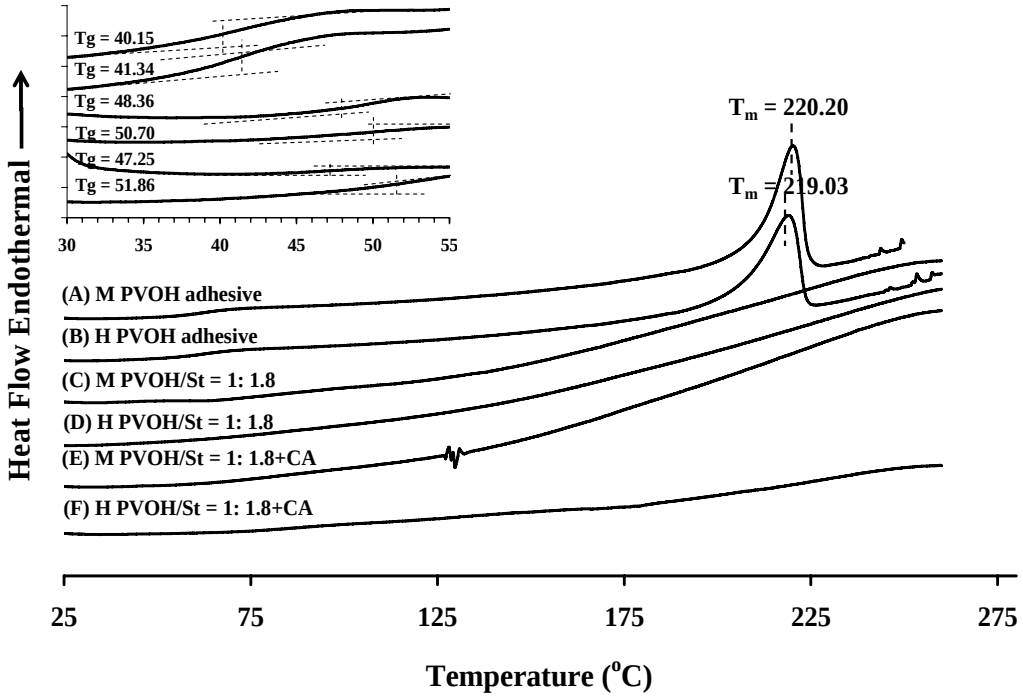

Figure 34. Effects of citric acid on DSC curves of PVOH/St cross-linked adhesive at PVOH/St ratio of 1: 1.8. M PVOH adhesive (A), H PVOH adhesive (B), M PVOH/St=1:1.8 (C), H PVOH/St=1:1.8 (D), M PVOH/St=1:1.8+CA (E) and H PVOH/St=1:1.8+CA (F).

7.5 Effect of type of polyvinyl alcohol (PVOH) on structure and thermal properties of PVOH/St cross-linked adhesive

7.5.1 Fourier-transform infrared (FT-IR) spectroscopy

The effects of PVOH type or molecular weight (MW) of PVOH on structural properties of PVOH/St cross-linked adhesive were evaluated by FT-IR spectroscopy. The FT-IR spectra of M and H PVOH adhesive are shown in Figure 35. The dominant peaks of starch and PVOH adhesives were the peaks at 3434, 2855.4 and 2924.4 cm^{-1}. They were representative of O-H stretching from the inter-molecular and intra-molecular hydrogen bonds (3434 cm^{-1}) and C-H stretching (2855.4 and 2924.4 cm^{-1}). The C-H bending peaks (855.5-859.8 cm^{-1}) were found due to the

PVOH structure. The peak of H PVOH at around 1141.2 cm^{-1} of Figure 35 (C) was due to the C-O stretching band that indicated crystalline portion of fully hydrolyzed PVOH (Imam *et al*., 1999). However, this peak disappeared in Figure 35 (B) (M PVOH). From the results of FT-IR spectra, the structure of PVOH/St cross-linked adhesives of M and H PVOH were similarly (Figure 35 (D), (E)). The sharp peak at 1023.2 cm^{-1} indicated that cross-linking structures (-C-O-C) were clearly in both of M and H PVOH adhesive with CA in Figure 35 (D), (E). In addition, the peaks at 1482 and 1141.2 cm^{-1}, which indicated the free methoxy groups of HMMM and crystalline portion of PVOH, disappeared in PVOH/St cross-linked adhesives. The FT-IR spectra showed that the cross-linked structure of PVOH/St cross-linked adhesive made from medium and high MW of the PVOH with the same composition of starch and PVOH ratio were not different. However, the cross-linking structure had loss the crystallinity of the PVOH after the cross-linked reaction due to the thermoset properties that occur (Prime, 2010).

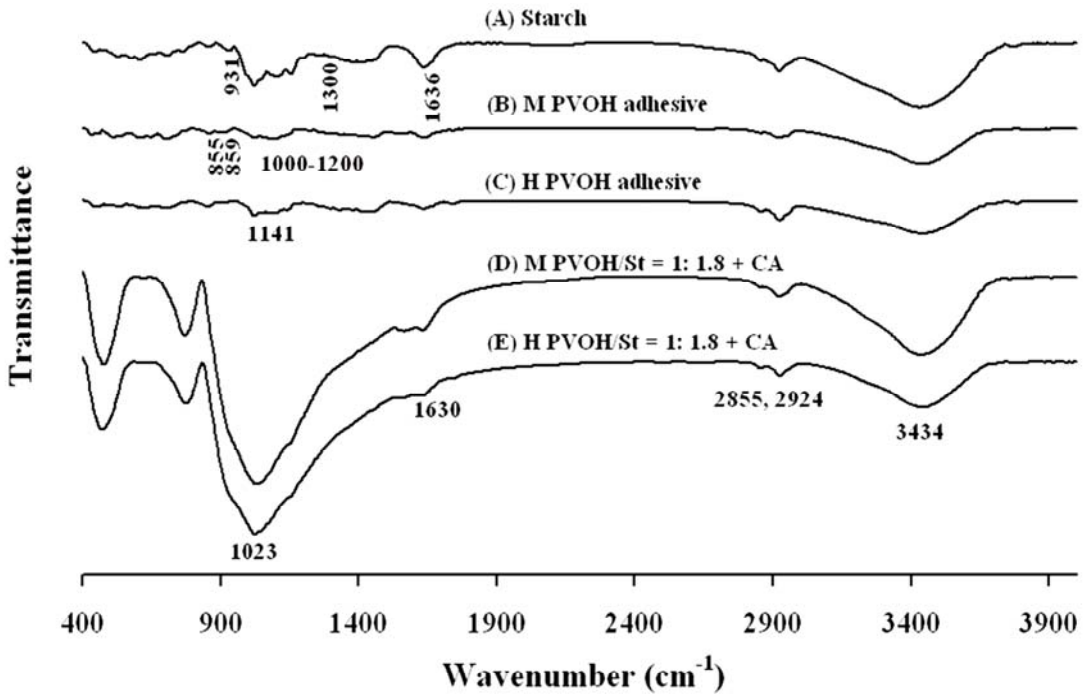

Figure 35. Effects of PVOH type on FT-IR spectra of PVOH/St cross-linked adhesive at PVOH/St ratio of 1: 1.8. Starch (A), M PVOH adhesive (B), H PVOH adhesive (C), M PVOH/St=1:1.8+CA (D) and H PVOH/St=1:1.8+CA (E).

7.5.2 Differential scanning calorimetry (DSC)

Figure 36 shows the DSC curve of M, H PVOH and PVOH/St cross-linked adhesive at the ratio of 1: 1.8. The T_g value of H PVOH adhesive was 41.34°C. They were higher than that of M PVOH which had the T_g of 40.15°C. It was known that the T_g increased with increasing in molecular weight. This was expressed by the Fox and Flory equation (2) (Sichina, 2000).

$$T_g = T_g(\alpha) - K_g/M \qquad (2)$$

Where $T_g(\alpha)$ is the limiting T_g at a very high molecular weight and K_g is a constant.

The effect of molecular weight of PVOH also resulted in a transition temperature of PVOH/St cross-linked adhesive. The T_g value of H PVOH/St cross-linked adhesive (51.86°C) was higher than M PVOH/St cross-linked adhesive (47.25°C). However, the increasing of T_g value of H PVOH/St cross-linked adhesive were obtained by the other factors such as starch ratio, degree of cure, molecular orientation and crystallinity.

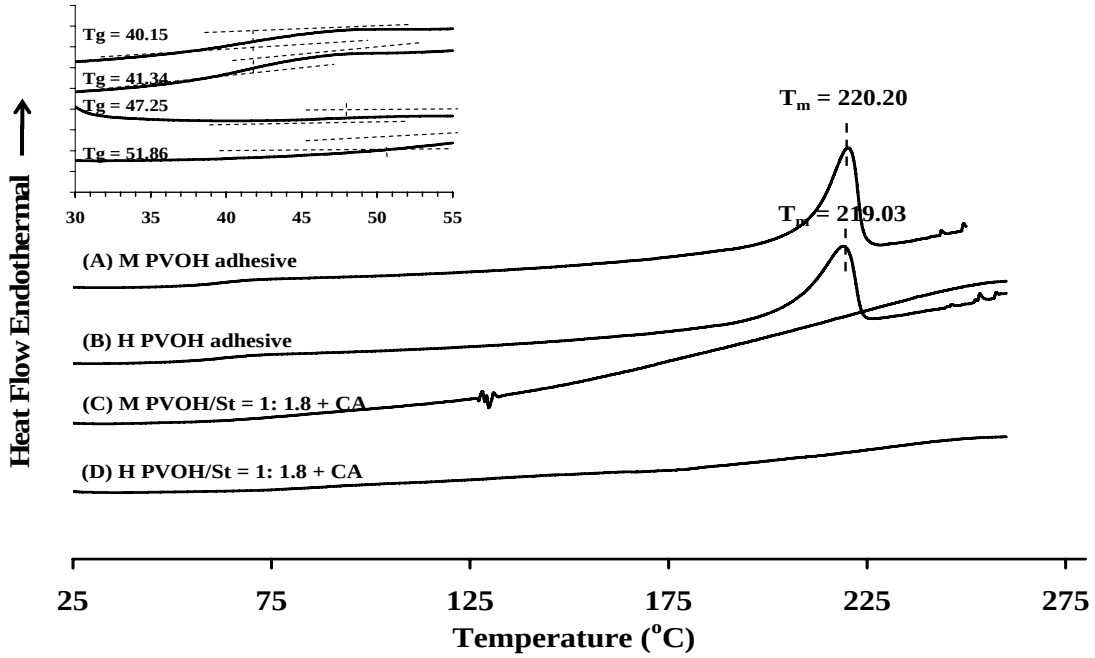

Figure 36. Effects of PVOH type on DSC curves of PVOH/St cross-linked adhesive at PVOH/St ratio of 1: 1.8. M PVOH adhesive (A), H PVOH adhesive (B), M PVOH/St=1:1.8+CA (C) and H PVOH/St=1:1.8+CA (D).

8. Effect of microcrystalline cellulose (MCC) addition on the properties of PVOH/St cross-linked adhesive

8.1 Solid content, viscosity and gel time

Physical properties of PVOH/St cross-linked composite adhesives (M PVOH/Starch ratio of 1: 1.8 and H PVOH/Starch ratio of 1: 0.5) containing various quantity of MCC were compared with those of M PVOH/St cross-linked adhesive ratio of 1: 1.8 and H PVOH/St cross-linked adhesive ratio of 1: 0.5 without MCC (Table 21). All M and H PVOH/St cross-linked adhesives had the viscosity of 7892-8670 cps and 9341-10988 cps, respectively. The viscosity values of the adhesive varied, depended on the type, ratio of PVOH/Starch and the amount of MCC. The viscosity values and solid content of PVOH/St cross-linked adhesive with MCC increased with the increase of MCC ($p<0.05$). The PVOH/St cross-linked composite adhesives added with 3.5 wt% MCC showed the higher viscosity value and solid content when compared with 0.5, 1.5 and 2.5 wt% MCC both of M PVOH and H PVOH type ($p<0.05$). However, the increase of the viscosity value was still in the range of optimal viscosity, not over 10000 cps. Therefore, it had not affected to the adhesive application. At the higher ratio of M PVOH/St cross-linked adhesive (1: 1.8) compared to H PVOH/St cross-linked adhesive (1: 0.5) showed the lower viscosity value due to molecular weight of PVOH had more impact on the viscosity property than the ratio of PVOH and starch.

When considering gel time of all PVOH/St cross-linked composite adhesives, those without MCC exhibited to use the longest time for adhesive gelling at 26°C. The PVOH/St cross-linked composite adhesives with MCC at 0.5, 1.5, 2.5 and 3.5 wt% were more quickly setting with increase of MCC content. The fastest gelling of the adhesive was 0.67 h at 3.5 wt% MCC in M PVOH/St cross-linked adhesive. These results were due to the MCC addition in the adhesive phase for deteriorating periods of application time. It indicated that when added MCC to PVOH/St cross-linked adhesive, the maximum time during the system remain in a fluid state for usage decreased (Gollob and Wellons, 2003). Generally, the formation of more cross-links effect on the curing lowers the gel time (Desai *et al*., 2003). However, these low gel times of PVOH/St cross-linked composite adhesive might

cause by MCC addition more than cross-linking reaction of adhesive that in accordance with FT-IR result in the next study.

The total solid content of all PVOH/St cross-linked adhesives were significantly increased when added MCC ($p<0.05$) (Table 21). The solid content only depended on the ratio of PVOH/Starch and amount of MCC. All M and H PVOH/St cross-linked adhesives had the total solid ranging from 29.30-30.74% and 21.14-22.69%, respectively. The MCC addition into PVOH/St cross-linked adhesive had a diminutive effect on total solid content of PVOH/St cross-linked adhesives. Furthermore, the solid content was more relationships together with the higher total solid, higher viscosity and speed of gel time of PVOH/St cross-linked adhesives.

Table 21. Effect of MCC addition on the viscosity, solid content and gel time of PVOH/St cross-linked adhesive with CA.

Type of adhesive	PVOH: Starch†	MCC†	Viscosity at 26°C*	Solid*	Gel time at 26°C*
	ratios	wt%	cps	%	h
M PVOH/St	1: 1.8	0	7892.00 ±7.2^{a**}	29.30±0.196^{c**}	1.42
	1: 1.8	0.5	8097.00 ±2.3^{b}	29.56±0.015^{cd}	1.00
	1: 1.8	1.5	8167.00 ±6.8^{c}	29.65±0.042^{cd}	1.00
	1: 1.8	2.5	8378.00 ±2.6^{d}	30.37±0.450^{cd}	0.75
	1: 1.8	3.5	8670.00 ±2.5^{e}	30.74±0.031^{d}	0.67
H PVOH/St	1: 0.5	0	9341.00 ±4.7^{f}	21.14±1.567^{a}	1.50
	1: 0.5	0.5	9456.00 ±5.3^{g}	21.36±0.025^{a}	1.25
	1: 0.5	1.5	9634.00 ±5.0^{h}	21.62±0.302^{ab}	0.75
	1: 0.5	2.5	10584.00 ±7.6^{i}	21.84±0.217^{ab}	1.00
	1: 0.5	3.5	10988.00 ±9.0^{j}	22.69±0.359^{b}	1.00

* Mean ± SD from triplicate determinations.

† Based on dry basis weight.

** The different superscripts in the same column indicate the significant differences ($p<0.05$).

8.2 Mechanical properties: shear strength and mode of failure

The shear strengths and mode of failure of all PVOH/St cross-linked composite adhesive systems were determined and the results are shown in Table 22. It was found that the amount of MCC at 1.5 wt% could improve the maximum shear strength from 26.50×10^5 to 32.93×10^5 N/m^2 for M PVOH/St cross-linked adhesive in

the ratio of 1:1.8 and from 30.30×10^5 to 31.73×10^5 N/m^2 for H PVOH/St cross-linked adhesive in the ratio of 1:0.5, respectively ($p<0.05$). Beyond 1.5 wt% MCC level (at 2.5 and 3.5 wt%) marked decrease in the shear strength ($p<0.05$). This could be attributing to heterogeneous dispersion of MCC in the cross-linked matrix. According to Wang and Sain (2006), the soybean nanofibers made them possible to improve the properties of material reinforced with a low level of filler. Since FT-IR results (Figure 39) indicated incomplete cross-linking reaction of the adhesive and also had free PVOH and starch molecules remained in the structure. There were occur strong interactions between hydroxyl groups at MCC surface which lead to the formation of a rigid network, resulting in the increase of shear strength of PVOH/St cross-linked composite adhesive. These were similarly to the improvement in mechanical properties of acacia cellulose whiskers reinforced acrylic films (Pu *et al*., 2007), cotton cellulose whiskers reinforced PVOH copolymer (Roohani *et al*., 2008), polylactic acid/cellulose whiskers modified by PVOH (Bondeson *et al*., 2007) and cellulose nano-reinforced composite that obtained from various sources such as flak bast fiber, hemp fibers, kraft pulp and rutabaga (Bhatnagar and Sain, 2005).

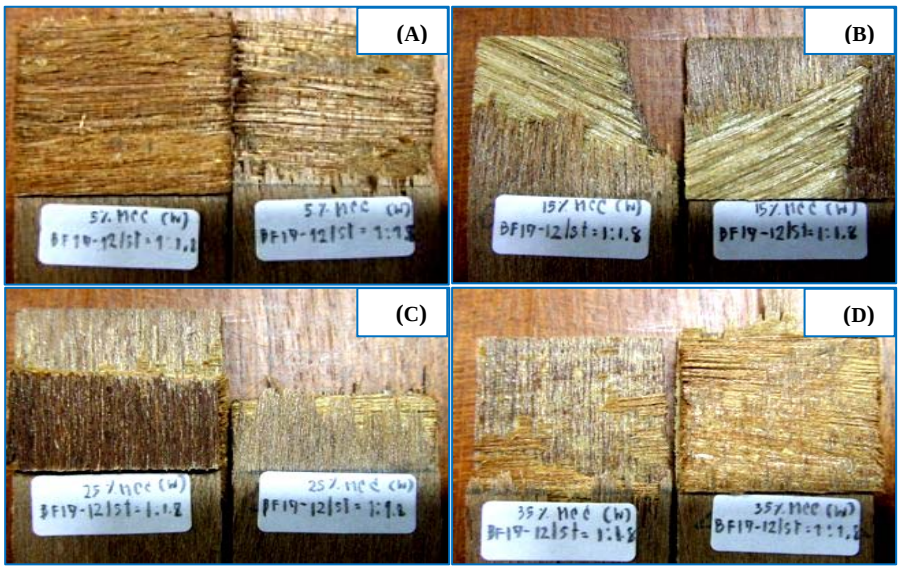

Figure 37. Photographs of the failure of the M PVOH/St cross-linked adhesive joint at various amount of MCC. 0.5 wt% (A), 1.5 wt% (B), 2.5 wt% (C) and 3.5 wt% (D), respectively.

Table 22. Effect of MCC addition on shear strength, mode of failure and average wood failure of PVOH/St cross-linked adhesive with CA.

Type of adhesive	PVOH: Starch† ratios	MCC† wt %	Shear strength* $N/m^2 \times 10^5$	Mode of failure**	Average wood failure* %
M PVOH/St	1: 1.8	0	$26.50 \pm 0.73^{c***}$	S	100
	1: 1.8	0.5	24.74 ± 1.37^{bc}	S	100
	1: 1.8	1.5	32.93 ± 1.10^{f}	C + S	90
	1: 1.8	2.5	29.03 ± 1.56^{d}	S	100
	1: 1.8	3.5	25.87 ± 0.62^{c}	C + S	90
H PVOH/St	1: 0.5	0	30.30 ± 0.43^{de}	S	100
	1: 0.5	0.5	30.47 ± 1.46^{de}	S	100
	1: 0.5	1.5	31.73 ± 1.14^{ef}	S	100
	1: 0.5	2.5	22.43 ± 1.19^{b}	S	100
	1: 0.5	3.5	18.57 ± 0.77^{a}	S	100

* All values are reported as mean ($N \geq 10$)

† Based on dry basis weight.

** C-Cohesive failure of adhesive.
S-Failure of wood substrate.

*** The different superscripts in the same column indicate the significant differences ($p<0.05$).

The observed failure modes of samples in this series lead to speculation about the cause of the differences in adhesive performance (Figure 37). The mode of failure found was mainly fracture in adherent at all of PVOH/St cross-linked composite adhesive. The fracture was interfacial when de-bonding occurred between adhesive and adherent. In most cases, the occurrences of interfacial fracture for a given adhesive to go along with smaller fracture toughness. The interfacial character of a fracture surface was usually to identify the precise location of the crack path in the interphase (Desai *et al*., 2003). This was probably because the MCC additions in the adhesive with various contents tend to fail adhesively between adhesive and adherent.

8.3 Morphology of PVOH/St cross-linked composite adhesive

The microstructure of PVOH/St cross-linked composites adhesive was characterized by SEM. The surface (at ×1000) and fracture surface (at ×4000) of PVOH/St cross-linked adhesive and PVOH/St cross-linked composite adhesive with

1.5 wt% MCC are shown in Figure 38. The micrographs of the surface of PVOH/St cross-linked and PVOH/St cross-linked composite adhesive were showed in the Figure 38 (A) and (C). They show the rough surface like an air bubble. There presented the starch granules were collapsed to a smaller size and embedded within the PVOH matrix. The PVOH and starch interfaces were highly diffused, indicated strong bonding through HMMM, cross-linker. The results were similarly with Das *et al*. (2010). They studied cross-linking between starch and PVOH with epichlorohydrin as a cross-linker. However, the surface of PVOH/St cross-linked adhesive without MCC had more smooth and uniform surface compare to the cross-linked composite adhesive. These caused by addition of reinforcement filler into the matrix. It was impossible to observe dispersion of MCC into the adhesive from surface characterization. Figure 38 (B) and (D) depicted the fractured surfaces of PVOH/St cross-linked adhesive without MCC and with MCC, respectively. As the figure, the MCC was embedded into the PVOH/St cross-linked matrix. Nevertheless, not discovered phase separation of the adhesive. Bondeson and Oksman (2007) found the miscibility between the polylactic acid (PLA), PVOH and cellulose whiskers and phase separation occurred with a continuous PLA phase. Their result indicated that there was poor interfacial adhesion between the PLA and PVOH. They believed that the cellulose whiskers were preferably located in the PVOH phase due to its greater affinity to PVOH than PLA. Moreover, Alemdar and Sain (2008a) investigated microstructure of the nanocomposites between cellulose and starch matrix which found the cellulose was well dispersed and covered by the matrix.

Therefore, as the results could explain that no fiber pull-out or de-bonding was observed because of the fine adhesion between MCC and polymer matrix. There was the fine interfacial adhesion between the MCC, PVOH, starch and PVOH cross-links starch matrix. Even if, MCC would obstruct the cross-linking reaction between PVOH and starch as the FT-IR result but the addition of MCC would result in an improvement in the mechanical properties of PVOH/St cross-linked composite adhesive at an optimal amount of MCC compared to PVOH/St cross-linked adhesive without MCC (Alemdar and Sain, 2008a).

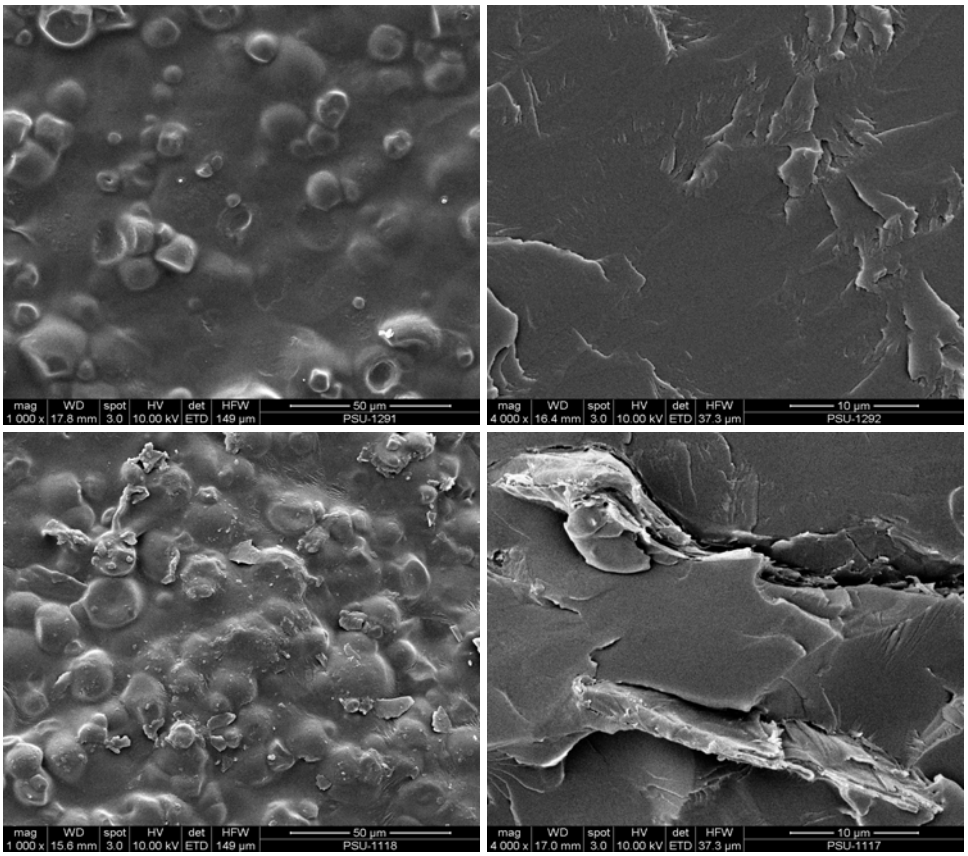

Figure 38. SEM micrographs of the surface (A) and cross-section (B) of M PVOH/St cross-linked adhesive at 1: 1.8 with CA and the surface (C) and cross-section (D) of PVOH/St cross-linked composite adhesive with 1.5 wt% MCC, respectively.

8.4 Fourier-transform infrared (FT-IR) spectroscopy

The FT-IR spectra of PVOH/St cross-linked composite adhesive, MCC and PVOH/St cross-linked adhesive prepared at M PVOH/Starch ratio of 1: 1.8 with CA are presented in Figure 39 (A), (B) and (C), respectively. Figure 39 shows the spectra of the samples in the range of 400-4000 cm^{-1}. The structure of PVOH/St cross-linked composite adhesive (Figure 39(A)) indicated the reduction in the area or the height of the ether groups (C-O-C stretching) that presented (Das *et al*., 2010) in with the peak at 1023 cm^{-1} compared to PVOH/St cross-linked adhesive (Figure 39 (C)). Addition, the peaks at 2922 and 3420 cm^{-1} of PVOH/St cross-linked composite adhesive which depicted the C-H and O-H stretching, respectively, were shift from 2924 and 3438 cm^{-1} of PVOH/St cross-linked adhesive. The area and the height in

both peaks of PVOH/St cross-linked composite adhesive had been higher than of PVOH/St cross-linked adhesive. Moreover, in the Figure 39 (A) appeared peak at 1497 cm^{-1} that meant the free methoxy groups of HMMM cross-linker remained in the structure (Rahman *et al*., 2007). However, this peak disappeared in the spectra of PVOH/St cross-linked adhesive without MCC in Figure 39 (C). The reduction, weakness, appearance and shift of the characteristic absorption bands might be result from the interaction of different C-O-C, C-H, O-H and methoxy groups of the PVOH, starch and PVOH/St cross-linked composite adhesive with MCC. Thus, it might be deduce from these results that the cross-linking reaction between PVOH and starch was incomplete when the MCC was added into the system. Li and Ding (2007) found the effect of cellulose nano-crystals (CNC) on cross-link reaction between of ternary blends of CNC/PEG1000/PEG600 (low molecular weight polyethylene glycol) that resulting on cross-linked structure changing. All these changes verified that the CNC was immobilized on the surface of matrixes. Therefore, MCC or cellulose could obstruct the network polymer based on cross-linking reaction of PVOH/Starch blending. However, PVOH/St cross-linked composite adhesive still had absorption bands related to C-H asymmetric of MCC, C-O stretching of primary and secondary alcohol on PVOH backbone and C-H stretching of monosubstituted vinyl group which was shift from PVOH spectra at 1372, 1080, 1153 and 1636, respectively (Ma *et al*., 2005; Das *et al*., 2010). The peaks were due to appearance of MCC and inactive PVOH chain in PVOH/St cross-linked composite adhesive. The appearance of the absorption spectrum also suggested the formation of intermolecular hydrogen bonding, similar to the results reported for cross-linked polyethylene glycol with CNC (Li and Ding, 2007).

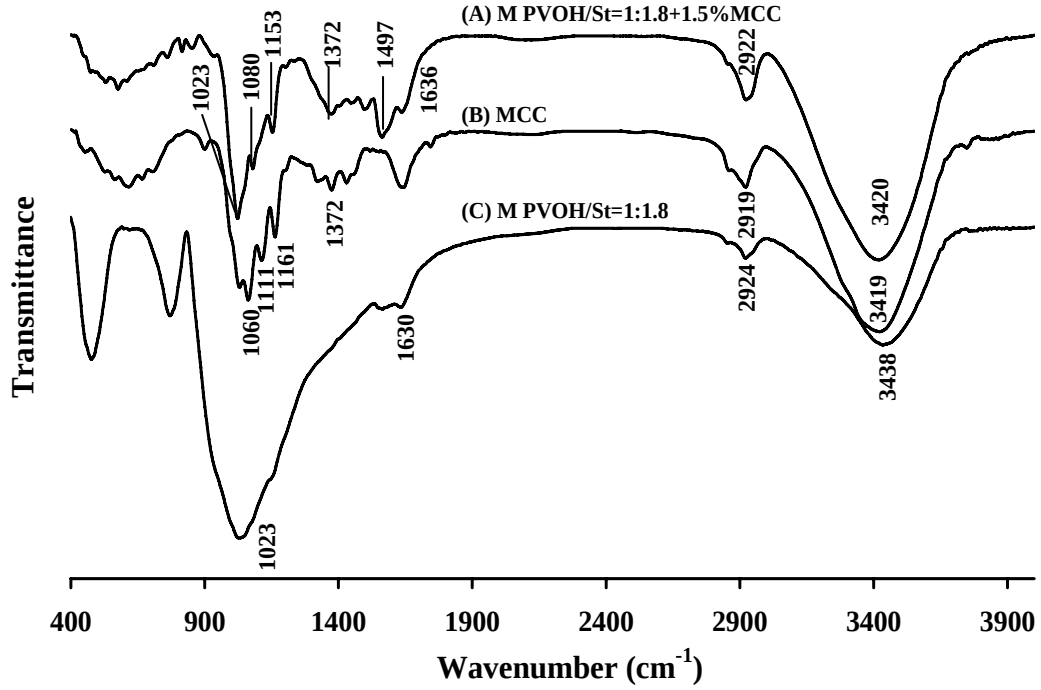

Figure 39. Effects of MCC addition on FT-IR spectra of M PVOH/St cross-linked adhesive at the ratio of 1: 1.8 with CA. The cross-linked adhesive+1.5% MCC (A), MCC (B) and the cross-linked adhesive without MCC (C).

8.5 Differential scanning calorimetry (DSC)

The thermal properties of PVOH/St cross-linked adhesives and PVOH/St cross-linked composite adhesives were analyzed by DSC. Their thermograms are shown in Figure 40. Figure 40 (A) and Figure 40 (B) were DSC thermogram of M PVOH/St cross-linked composite adhesive (M PVOH/Starch = 1:1.8+1.5% MCC) and M PVOH/St cross-linked adhesive (M PVOH/Starch = 1:1.8), respectively. The T_g value of PVOH/St cross-linked adhesive with MCC was 49.89°C. It shifted to higher temperature when compare to T_g value of PVOH/St cross-linked adhesive without MCC (47.25°C). Although, the FT-IR results showed the MCC had no effect to the cross-linking reaction in PVOH/St composite adhesives. The increase of T_g of PVOH/St cross-linked composite adhesive might cause by the much more interactions between free starch, PVOH and stiff crystallites. These interactions had effected to decrease the flexibility of macromolecular chain of starch and PVOH, according to Lu *et al*. (2005). Addition, the impact of their interactions had appeared an endothermic peak at 176.5°C which disappear in the thermogram of

completely cross-linking in the adhesives. Moreover, it found the exothermic peak at 158.83°C which similar to the DSC result of the starch composite adhesive. This peak was found when added MCC into the matrix due to the MCC was nucleating agents. They had influenced to mechanical property of adhesive (Luz *et al.*, 2008). This might be because of the strong interactions between MCC, PVOH, starch and cross-linked matrix (Joseph *et al.*, 2003). The result of this interaction was appearing of T_m of PVOH/St cross-linked composite adhesive. It indicated that PVOH/St cross-linked composite adhesive had the thermoplastic property and to be a semi-crystalline (Silverio *et al.*, 1996; Ge *et al.*, 2005; Kaewtatip and Tanrattanakul, 2008; Kumar and Singh, 2008).

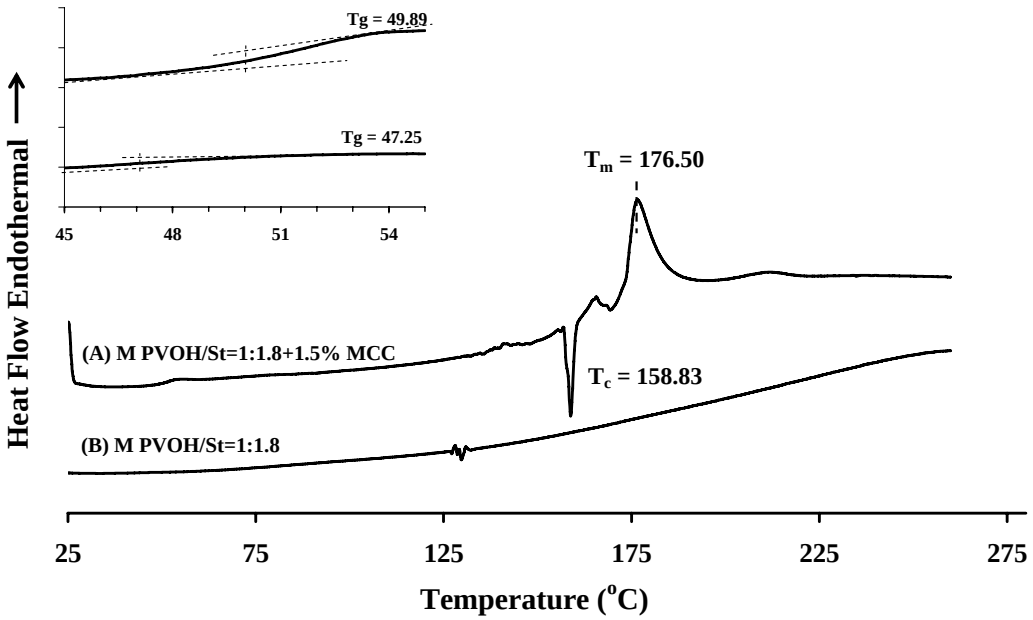

Figure 40. Effects of MCC addition on DSC of PVOH/St cross-linked adhesive at M PVOH/St ratio of 1: 1.8 with CA. The PVOH/St cross-linked adhesive+1.5%MCC (A) and PVOH/St cross-linked adhesive without MCC (B).

CHAPTER 4

CONCLUSION AND SUGGESTION

1. Microcrystalline cellulose (MCC) could be produced by acid hydrolysis of the sugarcane bagasse fiber (SBF). The optimal condition of acid hydrolysis was 15% (w/w) of nitric acid with the cooking temperature of 90°C for 30 min and followed by the bleaching process with 10% active chlorine of sodium hypochlorite. The chemical composition of MCC confirmed that this process could remove the most of hemicellulose, lignin, pectin and other non-cellulose from the SBF. The cellulose content and the crystallinity of MCC increased from 28% of cellulose and 30% of crystallinity to 80% of cellulose and 54.38% of crystallinity, respectively, after the acid treatment. The diameters and the lengths of MCC were reduced to the size of 5-10 μm and 100-300 μm, respectively.

2. The mechanical properties of PVOH adhesives depended on both of the type and concentration of PVOH used. Shear strength and viscosity of PVOH adhesive increased with increasing of molecular weight and concentration of PVOH. The optimal viscosity of PVOH to use as the adhesive could not over 10000 cps. The PVOH adhesives at the high concentration showed the higher shear strength and percentage of wood failure comparing to the commercial adhesive, phenol-formaldehyde (PF). L PVOH adhesive at the highest concentration (28 wt%) showed the best mechanical properties of adhesion.

3. Starch ratio of 0.5, 1 and 1.8 and citric acid (CA) of 0.24 wt% had affected on the physical, thermal and mechanical properties of PVOH/St cross-linked adhesive. The degree of cross-linking reaction increased with increasing of the starch ratio and the present of CA as a catalyst. However, the type of PVOH (high and medium molecular weight) had not affected to the cross-linking reaction but it had affected on the viscosity and gel time of PVOH/St cross-linked adhesive. In addition, the higher starch ratio and CA content had not only reduced the curing time of PVOH/St cross-linked adhesives but also increased the T_g value of them. All of PVOH/St cross-linked adhesives could improve the shear strength property of the adhesive comparing to the pure PVOH and starch adhesive. Then, the optimal ratio

between PVOH and starch in the cross-linked adhesives were the ratio of 1: 1.8 for M PVOH/Starch and the ratio of 1: 0.5 for H PVOH/Starch with using CA as a catalyst in the cross-linking reaction.

4. Microcrystalline cellulose (MCC) was able to use as reinforcement for both of bio-based adhesives such as starch, PVOH and PVOH/St cross-linked adhesives. The impacts of MCC content were more significant. The solid content, viscosity of the adhesives increased with increasing the MCC content while the gel time of the adhesives decreased. The MCC could disperse, covered and embedded, in all adhesive matrixes which were analyzed by SEM technique. The image showed that it had no aggregation of MCC in the matrix. The FT-IR and DSC results depicted the new and various interactions between MCC and adhesives matrix. The effect of MCC addition also act as the nucleating agents of thermoplastics, causing increase of T_g and change in crystallization and melting temperature of the final composite. MCC in the adhesive matrix could be used as the reinforcing filler because it could improve the mechanical properties. The optimal content of MCC for starch, PVOH and PVOH/St cross-linked composite adhesives were 0.5 to 1.5 wt%. However, the higher quantity of MCC had affected to the mixing process between MCC and adhesives matrix, especially at 3.5 wt% of MCC addition.

Suggestions

1. More researches on the cross-linking reaction of PVOH/St cross-linked adhesive, e.g. using other cross-linking agent and study the degree of cross-linking reaction to investigate the relationship between the mechanical properties and chemical structure of adhesives.

2. Further study, to retard the aggregation (or precipitation) of MCC in the PVOH composite adhesive.

3. To improve the yield of MCC by using other acid in the acid-hydrolysis process such as hydrochloric acid.

REFERENCES

Adel, A.M., Wahab, Z.H.A., Ibrahim, A. and Al-Shemy, M.T. 2010. Characterization of microcrystalline cellulose prepared from lignocellulosic materials. Part I. Acid catalyzed hydrolysis. Bioresource technol. 101: 4446-4455.

Alemdar, A. and Sain, M. 2008a. Biocomposites from wheat straw nanofibers: morphology, thermal and mechanical properties. Compos. Sci. Technol. 68: 557-565.

Alemdar, A. and Sain, M. 2008b. Isolation and characterization of nanofibers from agricultural residues-Wheat straw and soy hulls. Bio. Tech. 99: 1664-1671.

Angles, M.N. and Dufresne, A. 2000. Plasticized starch/tunicin whiskers nanocomposites. 1. Structural analysis. Macromolecules. 33 (22): 8344–8353.

Anon., 2009. Manual of CCP Polyvinyl alcohol. 3rd Ed. Chang Chun Petrochemicanm Ltd, Taiwan.

AOAC. 1999. Official Methods of Analysis. 16th Ed. The Association of Official Analytical Chemists, Washington, D.C, USA.

Arib, R.M.N., Sapuan, S.M., Ahmad, M.M.H.M., Paridah, M.T. and Zaman, H.M.D.K. 2006. Mechanical properties of pineapple leaf fibre reinforced polypropylene composites. Mater. Design. 27: 391-396.

Aryee, F.N.A., Oduro, I., Ellis, W.O. and Afuakwa, J.J. 2006. The physicochemical properties of flour samples from the roots of 31 varieties of cassava. Food Control. 17: 916-922.

Ashori, A. and Nourbakhsh, A. 2010. Performance properties of microcrystalline cellulose as a reinforcing agent in wood plastic composites. Compos. Part B.: In press.

ASTM. 1982. Standard test method for strength properties of adhesives in shear by tension loading (metal-to-metal): D1002-72 (Reapproved 1978). *In* ASTM Annual Book of American Standard Testing Methods, Vol. 13.06. p.260-264. Philadephia, PA.

Averous, L. and Boquillon, N. 2004. Biocomposites based on plasticized starch: thermal and mechanical behaviors. Carbohyd. Polym. 56 (2): 111–122.

Bangyekan, C., Aht-Ong, D. and Srikulkit, K. 2006. Preparation and properties evaluation of chitosan-coated cassava starch films. Carbohyd. Polym. 63: 61-71.

Bai, W. and Li, K. 2009. Partial replacement of silica with microcrystalline cellulose in rubber composites. Compos. Part A. 40: 1597-1605.

Baumann, M.G.D. and Conner, A.H. 2003. Carbohydrate polymers as adhesives. *In* Handbook of Adhesive Technology. 2nd Ed (Pizzi, A. and Mittal, K.L., eds.). p. 502-518. Marcel Dekker. New York.

Bhatnagar, A. and Sain, M. 2005. Processing of cellulose nanofiber-reinforced composites. J. Reinf. Plast. Compos. 00: 01-10.

Bhattacharya, D., Germinario, L.T. and Winter, W.T. 2008. Isolation, preparation and characterization of cellulose microfibers obtained from bagasse. Carbohydr. Polym. 73: 371-377.

Bikerman, J.J. 1961. The Science of Adhesive Joints. Academic Press. New York.

Bledzki, A.K. and Gassan, J. 1999. Composites reinforced with cellulose based fibres. Prog. Polym. Sci. 24: 221-274.

Bledzki, A.K., Zhang, W. and Chate, A. 2001. Natural-fibre-reinforced polyurethane microfoams. Compos. Sci. Technol. 61: 2405-2411.

Blomstrom, T.P. 1989. Vinyl acetal polymers. *In* Encyclopedia of Polymer Science and Engineering. vol. 17 (Mark, H.F., Bikales, N.M., Overberger, C.G. and Menges, G., eds.). p. 136-167. Wiley. New York.

Bondeson, D. and Oksman, K. 2007. Polylactic acid/cellulose whisker nanocomposites modified by polyvinyl alcohol. Compos. Part A. 38: 2486-2492.

Borredon, E., Bikiaris, D., Prinos, J. and Panayiotou, C. 1997. Properties of fatty-acid ester of starch and their blends with LDPE. J. Appl. Polym. Sci. 65: 705-721.

Bradbury, J.H. and Holloway, W.D. 1988. Introduction. *In* Chemistry of Tropical Root Crops: Significance for Nutrition and Agriculture in the Pacific. (Bradbury, J.H. and Holloway, W.D., eds.). p. 17-36. Ramsay Ware Printing. Melbourne.

Browning, B.L. 1967. Methods of Wood Chemistry. Vol. 2. John Wiley & Sons. USA.

Builders, P.F., Bonaventure, A.M., Tiwalade, A., Okpako, L.C. and Attama, A.A. 2010. Novel multifunctional pharmaceutical excipients derived from microcrystalline cellulose-starch microparticulate composites prepared by compatibilized reactive polymer blending. Int. J. Pharm. 388: 159-167.

Calandrelli, L., Immirzi, B., Malinconico, M., Volpe, M.G., Oliva, A. and Della Ragione, F. 2000. Preparation and characterisation of composites based on biodegradable polymers for “in vivo” application. Polymer. 41: 8027–8033.

Cazacu, G. and Popa, V.I. 2005. Blends and composites based on cellulose materials. *In* In: Polysaccharide: Structural Diversity and functional versatility. 2nd Ed. (Dumitriu, S., ed.). p. 1141-1177. Marcel Dekker. New York.

Charles, V.C. 1973. Handbook of adhesive bonding. p. 175. Mc-Graw Hill. New York.

Chebil, C. and Cartilier, L. 1998. Cross-linked cellulose as a tablet excipient: A binding: disintegrating agent. Int. J. Pharm. 171: 101-110.

Chen, L., Imam, S.H., Gordon, S.H. and Greene, R.V. 1997. Starch-polyvinyl alcohol crosslinked film-performance and biodegradation. J. Environ. Polym. Degrad. 5 (2): 111-117.

Chen, Y., Qian, Q., Liu, X., Xiao, L. and Chen, Q. 2010. LaOCl nanofibers derived from electrospun PVA/Lanthanum chloride composite fibers. Mater. Lett. 64: 6-8.

Chiou, B.S., Glenn, G.M., Imam, S.H., Inglesby, M.K., Wood, D.F. and Orts, W.J. 2005. Starch polymers: Chemistry, engineering, and novel products. *In* Natural Fibers, Biopolymers, and Biocomposites. 1st Ed. (Mohanty, A.K., Misra, M. and Drzal, L.T., eds.). p. 639-670. CRC Press. Taylor & Francis Group, LLC. USA.

Chung, K.M. and Seib, P.A. 1991. Thin-boiling and nongelling adhesive prepared from maize and wheat starches. Starch/Stärke. 43: 441-446.

Coffey, D.G., Bell, D.A. and Henderson, A. 2006. Cellulose and Cellulose Derivatives. *In* Food Polysaccharides and Their Application. 2nd Ed. (Stephen, A.M., Phillips, G.O. and Williams, P.A., eds.). p. 148-174. CRC Press. Taylor & Francis Group, LLC. New York.

Collado, L.S. and Corke, H. 2003. Starch properties and functionalities. *In* Characterization of Cereals and Flours. 1st Ed. (Kaletunc, G. and Breslauer, K.J., eds.). p. 473-506. Marcel Dekker. New York.

Colom, X. and Carrillo, F. 2002. Crystallinity changes in lyocell and viscose-type fibres by caustic treatment. Eur. Polym. J. 38: 2225-2230.

Cytec. 2009. Cymel-amino resin crosslinkers for the coating industry: product and application guide. Cytec. Inc. Europe, Middle East and Africa. USA.

Das, C.K., Rajasekar, R. and Reddy, C.S. 2009a. Vinyl polymer degradation. *In* Handbook of Vinyl Polymers: Radical Polymerization, Process, and Technology, 2nd Ed (Mishra, M. and Yagci, Y. eds.). p. 430-450. CRC Press. Taylor & Francis Group, LLC. New York.

Das, C.K., Mukherjee, M. and Das, T. 2009b. Fiber-Filled vinyl polymer composites. *In* Handbook of Vinyl Polymers: Radical Polymerization, Process, and Technology, 2nd Ed (Mishra, M. and Yagci, Y. eds.). p. 456-495. CRC Press. Taylor & Francis Group, LLC. New York.

Das, K., Ray, D., Bandyopadhyay, N.R., Gupta, A., Sengupta, S., Sahoo, S., Mohanty, A. and Misra, M. 2010. Preparation and characterization of cross-linked starch/poly(vinyl alcohol) green films with low moisture absorption. Ind. Eng. Chem. Res. 49: 2176-2185.

Davalos, J.F. and Qiao, P. 2003. Fracture Mechanics Methods for Interface Bond Evaluations of Fiber-Reinforced Plastic/Wood Hybrid Composites. *In* Handbook of Adhesive Technology. 2nd Ed (Pizzi, A. and Mittal, K.L., eds.). p. 357-384. Marcel Dekker. New York.

Dean, K. and Yu, L. 2005. Biodegradable protein-nanoparticle composites. *In* Biodegradable Polymers for Industrial Applications. 1st Ed (Smith, S., ed.). p. 289-307. CRC Press LLC. USA.

DeMerlis, C.C. and Schoneker, D.R. 2003. Review of the oral toxicity of polyvinyl alcohol (PVA). Food Chem. Toxicol. 41: 319-326.

Deryaguin, B.V. and Smilga, V.P. 1969. Adhesion: Fundamentals and Practice. Maclaren, Ministry of Technology, UK Ed. p. 152. London.

Deryaguin, B.V., Krotova, N.A. and Smilga, V.P. 1978. Adhesion of Soilds. Plenum Press. New York.

Desai, D. S., Patel, J. V. and Sinha, V. K. 2003. Polyurethane adhesive system from biomaterial-based polyol for bonding wood. J. Adhes. Adhes. 23: 393-399.

Dufresne, A. and Vignon, M.R. 1998. Improvement of starch film performances using cellulose microfibrils. Macromolecules. 31: 2693–2696.

Dunky, M. 2003. Adhesives in the wood industry. *In* Handbook of Adhesive Technology. 2nd Ed (Pizzi, A. and Mittal, K.L., eds.). p. 853-922. Marcel Dekker. New York.

Ebewele, R.O. 2000. Polymer Science and Technology. CRC Press LLC. USA.

Eliasson, A.C. and Gudmundsson, M. 2006. Starch: Physicochemical and functional aspects. *In* Carbohydrates in Food. 2nd Ed (Eliasson, A.C., ed.). p. 391-469. CRC Press Taylor & Francis Group, LLC. New York.

Emengo, F.N., Chukwu, S.R. and Mozie, J. 2002. Tack and bonding strength of carbohydrate-based adhesives from different botanical sources. J. Adhes. Adhes. 22: 93-100.

Fechner, P.M., Wartewig, S., Füting, M., Heilmann, A., Neubert, R.H.H. and Kleinebudde, Peter. 2003. Properties of Microcrystalline Cellulose and Powder Cellulose After Extru-sion/Spheronization as Studied by Fourier Transform Raman Spectroscopy and Environmental Scanning Electron Microscopy. AAPS. Pharm. Sci. 5 (4): 1-13.

Fink, H.P., Ganster. J. and Fraatz. J. 1994. Akzo-Nobel viskose chemistry seminar challenges in cellulosic man-made fibres. Stockholm. May 30–June 3.

Focher, B., Palma, M.T., Canetti, M., Torri, G., Cosentino, C. and Gastaldi, G. 2001. Structural differences between non-wood plant celluloses: evidence from solid

state NMR, vibrational spectroscopy and X-ray diffractometry. Ind. Crop. Prod. 2001: 193-208.

Follain, N., Joly, C., Dole, P. and Bliard, C. 2005. Properties of starch based blends. part 2. influence of polyvinyl alcohol addition and photocrosslinking on starch based materials mechanical properties. Carbohyd Polym. 60: 185-192.

Franz, G. and Blaschek, W. 1990. Cellulose. *In* Methods in Plants Biochemistry. Vol. 2 (Dey, P.M. and Harborne, J.B., eds.). p. 291-322. Carbohydrates. Academic Press.

Frihart, C.R. 2005. Wood adhesion and adhesives. *In* Handbook of Wood Chemistry and Wood Composites. (Rowell, R.M., ed.). p. 213-278. CRC Press. USA.

Garcia, F.C.P., Almeida, J.C.F., Osorio, R., Carvalho, R.M. and Toledano, M. 2009. Influence of set time and temperature on bond strength of contemporary adhesives to dentine. J. Dent. 37: 315-320.

Ge, X.C., Xu, Y., Meng, Y.Z. and Li, R.K.Y. 2005. Thermal and mechanical properties of biodegradable composites of poly(propylene carbonate) and starch-poly(methyl acrylate) graft copolymer. Compos. Sci. Technol. 65: 2219–2225.

Gollob, L. and Wellons, J.D. 2003. Wood adhesion. *In* Handbook of Adhesive Technology. 2nd Ed (Pizzi, A. and Mittal, K.L., eds.). p. 598-610. Marcel Dekker. New York.

Gu, S., He, G., Wu, X., Guo, Y., Liu, H., Peng, L. and Xiao, G. 2008. Preparation and characteristics of cross-linked sulfonated poly(phthalazinone ether sulfone ketone) with poly(vinyl alcohol) for proton exchange membrane. J. Membrane Sci. 312: 48-58.

Haag, A. P., Geesey, G. G. and Mittleman, M. W. 2006. Bacterially derived wood adhesive. J. Adhes. Adhes. 26: 177-183.

Hamarneh, A.I., Heeres, H.J., Broekhuis, A.A., Sjollema, K.A., Zhang, Y. and Picchioni, F. 2010. Use of soy proteins in polyketone-based wood adhesives. J. Adhes. Adhes.: In press.

Han, X., Chen, S. and Hu, X. 2009. Controlled-release fertilizer encapsulated by starch/polyvinyl alcohol coating. Desalination. 240: 21-26.

Hizukuri, S. Abe, J.I. and Hanashiro, I. 2006. *In* Carbohydrates in Food. 2nd Ed (Eliasson, A.C., ed.). p. 305-390. CRC Press Taylor & Francis Group, LLC. New York.

Hope, P.S. and Folkes, M.J. 1993. Introduction. *In* Polymer Blends and Alloys. 1st Ed. (Folkes, M.J. and Hope, P.S., eds.). p. 1-6. Blackie Academic & Professional. London.

Hyder, M.N. and Chen, P. 2009. Pervaporation dehydration of ethylene glycol with chitosan-poly(vinyl alcohol) blend membranes: Effect of CS-PVA blending ratios. J. Membrane. Sci. 340: 171-180

Imam, S.H., Gordon H.S., Mao L. and Chen L., 2001. Environmentally friendly wood adhesive from a renewable plant polymer: characteristics and optimization. Polym. Degrad. Stab. 73: 529–533.

Imam, S.H., Mao, L. and Greene, R.V. 1999. Wood adhesive from crosslinked poly(vinyl alcohol) and partially gelatinized starch: preparation and properties. Starch/Stärke. 51: 225-229.

Izydorczyk, M., Cui, S.W. and Wang, Q. 2005. Polysaccharide Gums: Structures, Functional Properties, and Applications. *In* Food Polysaccharides and Their Application. 2nd Ed. (Stephen, A.M., Phillips, G.O. and Williams, P.A., eds.). p. 181-216. CRC Press. Taylor & Francis Group, LLC. New York.

Jaffe, H.L. and Rosenblum, F.M. 1990. Poly(vinyl Alcohol) for adhesives. *In* Handbook of Adhesives. 3rd Ed. p. 401-407. Chapman and Hall. New York.

Jane, J.L. 2004. Starch: Structure and properties. *In* Chemical and Functional Properties of Food Saccharides; Series 5. (Tomasik, P., ed.). p. 81-102. CRC Press LLC. USA.

Jarowenko, W. 1977. Starch based adhesives. *In* Handbook of adhesives. (Skeist, I., ed.). p. 192–211. Van Nostrand Reinhold. New York.

Joseph, P.V., Joseph, K., Thomas, S., Pillai, C.K.S., Prasad, V.S., Groeninckx, G. and Sarkissova, M. 2003. The thermal and crystallization studies of short sisal fibre reinforced polypropylene composites. Compos. Part A-Appl. S. 34: 253-266.

Kaewtatip, K. and Tanrattanakul, V. 2008. Preparation of cassava starch grafted with polystyrene by suspension polymerization. Carbohyd Polym. 73: 647-655.

Kennedy, H.M. and Fischer, A.C. 1984. Starch and dextrins in prepared adhesives. *In* Starch: Chemistry and Technology. (Whistler, R.L., Bemiller, J.N. and Paschall, E.F., eds.). p. 593–609. Academic Press. USA.

Khan, M.A., Ashraf, S.M. and Malhotra, V.P. 2004. Development and characterization of a wood adhesive using bagasse lignin. J. Adhes. Adhes. 24: 485-493.

Kim, S. and Kim, H.J. 2005. Effect of addition of polyvinyl acetate to melamine-formaldehyde resin on the adhesion and formaldehyde emission in engineered flooring. J. Adhes. Adhes. 25: 456-461.

Kim, S. 2009. Environment-friendly adhesives for surface bonding of wood-based flooring using natural tannin to reduce formaldehyde and TVOC emission. Bioresource technol. 100: 744-748.

Knill, C.J. and Kennedy, J.F. 2005. Cellulosic Biomass-Derived Products. *In* Polysaccharides: Structural Diversity and Functional Versatility. 1st Ed (Dumitriu, S., ed.). p. 964-984. Marcel Dekker. New York.

Krumova, M., Lopez, D., Benavente, R., Mijangos, C. and Perena, J. M. 2000. Effect of crosslinking on the mechanical and thermal properties of poly(vinyl alcohol). Polym J. 41: 9265-9272.

Kumar, A.P. and Singh, R.P. 2008. Biocomposites of cellulose reinforced starch: Improvement of properties by photo-induced crosslinking. Bioresource technol. 99: 8803-8809.

Kumar, R., Choudhary, V., Mishra, S., Varma, I.K. and Mattiason, B. 2002. Adhesives and plastics based on soy protein products. Ind. Crops. Prod. 18: 155–172.

Kürschner, K. and Hoffer, A. 1967. The isolation and determination of cellulose. *In* Methods of Wood Chemistry. Vol. 2 (Browning, B.L. ed.). p. 406-407. Interscience Publishers, John Wiley & Sons. New York.

Laosinchai, W. 2002. Molecular and Biochemical Studies of Cellulose and Callose Synthase. Doctor of Philosophy. The University of Texas. Austin.

Leung, KCM., Chow, T.W., Woo, E.C.W. and Clark, R.K.F. 1999. Effect of adhesive set time on the bond strength of irreversible hydrocolloid to stainless steel. J. Prosthet. Dent. 81: 586-590.

Li, W.D. and Ding, E.Y. 2007. Preparation and characterization of poly(ethylene terephthalate) fabrics treated by blends of cellulose nanocrystals and polyethylene glycol. J. Appl. Polym. Sci. 105: 373-378.

Lima, M.M.S. and Borsali, R. 2004. Rodlike cellulose microcrystals: Structure, properties, and applications. Macromol. Rapid. Commun. 25: 771-787.

Limpan, N. 2009. Properties of biodegradable film based on fish myofibrillar protein and polyvinyl alcohol blend. Master of Science in Packaging Technology. Prince of Songkla University. Thailand.

Lin, H. and Gunasekaran, S. 2010. Cow blood adhesive: Characterization of physicochemical and adhesion properties. J. Adhes. Adhes. 30: 139-144.

Lin, Z., Renneckar, S. and Hindman, D.P. 2008. Nanocomposite-based lignocellulosic fibers 1. Thermal stability of modified fibers with clay-polyelectrolyte multilayers. Cellulose. 15: 333-346.

Liu, Y. and Li, K. 2007. Development and characterization of adhesives from soy protein for bonding wood. J. Adhes. Adhes. 27: 59-67.

Lu, J., Wang, T. and Drzal, L.T. 2008. Preparation and properties of microfibrillated cellulose polyvinyl alcohol composite materials. Compos. Part A. 39: 738–746.

Lu, Y., Weng, L. and Cao, X. 2005. Biocomposites of plasticized starch reinforced with cellulose crystallites from cottonseed linter. Macromol. Biosci. 5: 1101-1107.

Lu, Y., Weng, L. and Cao, X. 2006. Morphological, thermal and mechanical properties of ramie crystallites-reinforced plasticized starch biocomposites. Carbohydr. Polym. 63: 198-204.

Luz, S.M., Tio, J.D., Rocha, G.J.M., Goncalves, A.R. and Del'Arco, J.A.P. 2008. Cellulose and cellulignin from sugarcane bagasse reinforced polypropylene composites: effect of acetylation on mechanical and thermal properties. Compos. Part A-Appl. S. 39: 1362-1369.

Ma, Z., Kotaki, M. and Ramarkrishna, S. 2005. Electrospun cellulose nanofiber as affinity membrane. J. Membrane. Sci. 265: 115-123.

Mano, J.F., Koniarova, D. and Reis, R.L. 2003. Thermal properties of thermoplastic starch/synthetic polymer blends with potential biomedical applicability. J. Mater Sci-Mater M. 14: 127–135.

Mark, R.E. 1981. Adhesion in cellulosic and wood-based composites. *In* Molecular and Cell Wall Structure of Wood. (Oliver, J.F., ed.). p.7–51.Plenum Press. New York.

Mathew, A.P. and Dufresne, A. 2002. Morphological investigation of nanocomposites from sorbitol plasticized starch and tunicin whiskers. Biomacromolecules 3: 609–617.

Matsui, K.N., Larotonda, F.D.S., Paes, S.S., Luiz, D.B., Pires, A.T.N. and Laurindo, J.B. 2004. Cassava bagasse-Kraft paper composites: analysis of influence of impregnation with starch acetate on tensile strength and water absorption properties. Carbohydr. Polym. 55: 237-243.

McCann, M., Weels, B. and Roberts, K. 1990. Direct visualization of cross-links in the primary cell walls. J. Cell. Sci. 96: 323–334.

Mequanint, K. and Sanderson, R. 2003. Nano-structure phosphorus-containing polyurethane dispersions: synthesis and crosslinking with melamine formaldehyde resin. Polym J. 44: 2631-2639.

Moorthy, S.N. 2004. Tropical sources of starch. *In* Starch in Food: Structure, Function and Applications. (Eliasson, A.C. ed.). p. 327-366. CRC Press LLC. New York.

Müller, C.M.O., Laurindo, J.B. and Yamashita, F. 2009. Effect of cellulose fibers on the crystallinity and mechanical properties of starch-based films at different relative humidity values. Carbohydr. Polym. 77: 293-299.

Naebe, M., Lin, T., Staiger, M.P., Dai, L. and Wang, X. 2008. Electrospun single-walled carbon nanotube/polyvinyl alcohol composite nanofibers: structure–property relationships. Nanotechnology. 19: 1-9.

Nordqvist, P., Khabbaz, F. and Malmström, E. 2010. Comparing bond strength and water resistance of alkali-modified soy protein isolate and wheat gluten adhesives. J. Adhes. Adhes. 30: 72-79.

Oh, S.Y., Yoo, D.I., Shin, Y., Kim, H.C., Kim, H.Y., Chung, Y.S., Park, W.H. and Youk, J.H. 2005. Crystalline structure analysis of cellulose treated with sodium hydroxide and carbon dioxide by means of X-ray diffraction and FT-IR spectroscopy. Carbohyd. Res. 340: 2376-2391.

Ott, E., Spurlin, H.M. and Grafflin, M.W. 1954. Cellulose and Cellulose Derivatives. 2nd Ed. Interscience Publishers. London.

Pérez, S. and Mazeau, K. 2005. Conformations, Structures, and Morphologies of Celluloses. *In* Polysaccharides: Structural Diversity and Functional Versatility. 1st Ed (Dumitriu, S., ed.). p. 41-69. Marcel Dekker. New York.

Peshkova, S and Li, K. 2003. Investigation of chitosan-phenolics systems as wood adhesives. J. Biotechnol. 102: 199-207.

Pollution Control Department. 2001. Chemical data bank. Bangkok (Online). Available. http://www.Thaiclinic.com/medbible/bonetumor.html/ (16 July 2010).

Prime, R. B. 2010. An introduction to thermosets (Online). Available. http://www.primethermosets.com (27 February 2010).

Probst, O., Moore, E.M., Resasco, D.E. and Grady, B.P. 2004. Nucleation of polyvinyl alcohol crystallization by single-walled carbon nanotubes. Polym. J. 45: 4437-4443.

Proniewicz, L.M., Paluszkiewicz, C., Birczynska, A.W., Majcherczyk, H., Baranski, A. and Konieczna, A. 2001. FT-IR and FT-Raman study of hydrothermally degradated cellulose. J. Mol. Struct. 596: 163–169.

Pu, Y., Zhang, J., Elder, T., Deng, Y., Gatenholm, P. and Ragauskas, A.J. 2007. Investigation into nanocellulosics versus acacia reinforced acrylic films. Compos. Part B. 38: 360-366.

Ramaraj, B. 2007. Crosslinked poly(vinyl alcohol) and starch composite films. II. Physicomechanical, thermal properties and swelling studies. J. Appl. Polym. Sci. 103 (2): 909-916.

Rahman, M. M., Kim, E. Y., Kwon, J. Y., Yoo, H. J., and Kim, H. D. 2007. Cross-linking reaction of waterborne polyurethane adhesives containing different amount of ionic groups with hexamethoxymethyl melamine. J. Adhes. Adhes. 28: 47-54.

Roohani, M., Habibi, Y., Belgacem, N.M., Ebrahim, G., Karimi, N. and Dufresne, A. 2008. Cellulose whiskers reinforced polyvinyl alcohol copolymers nanocomposites. Eur. Polym. 44: 2489-2498.

Rosa, M.F., Medeiros, E.S., Malmonge, J.A., Gregorski, K.S., Wood, D.F., Mattoso, L.H.C., Glenn, G., Orts, W.J. and Imam, S.H. 2010. Cellulose nanowhiskers from coconut husk fibers: effect of preparation conditions on their thermal and morphological behavior. Carbohydr. Polym. 81: 83-92.

Saxena, S.K. 2004. Polyvinyl alcohol (PVA), Chemical and technical assessment. In Meeting of the 31st of the Joint FAO/WHO Expert Committee on Food Additives 2003 (JECFA). Rome. June 10-19.

Schultz, J. and Nardin, M. 2003. Theories and mechanisms of adhesion. *In* Handbook of Adhesive Technology. 2nd Ed (Pizzi, A. and Mittal, K.L., eds.). p. 52-67. Marcel Dekker. New York.

Sekine, M. 1996. Measurement of dynamic viscoelastic behavior of starch during gelatinization in a xanthan-gum solution. Nippon Shokuhin Kagaku Kogaku Kaishi 43: 683–688.

Shao, C., Kim, H.Y., Gong, J., Ding, B., Lee, D.R. and Park, S.J. 2003. Fiber mats of poly(vinyl alcohol)/silica composite via electrospinning. Mater. Lett. 57: 1579-1584.

Sherman, C.P. 1997. Infrared spectroscopy. *In* Handbook of Instrumental Techniques for Analytical Chemistry. Har/Cdr Ed. (Settle, F.A.. ed.). p. 247–283. Prentice Hall. United Kingdom.

Shi, R., Bi, J., Zhang, Z., Zhu, A., Chen, D., Zhou, X., Zhang, L. and Tian, W. 2008. The effect of citric acid on the structural properties and cytotoxicity of the polyvinyl alcohol/starch films when molding at high temperature. Carbohyd Polym. 74: 763-770.

Sichina, W. J. 2000. Measurement of Tg by DSC. PerkinElmer Instruments, Inc. USA.

Siddaramaiah, S., Raj, B., and Somashekar, R. 2004. Structure-property relation in polyvinyl alcohol/starch composites. J. Appl. Polym. Sci. 91: 630-635.

Silverio, J., Svensson, E., Eliasson, A.C. and Olofsson, G. 1996. Isothermal microcalorimetric studies on starch retrogradation. J. Therm. Anal. 47 (5): 1179–1200.

Skeist, I. 1990. Handbook of Adhesives. 3rd Ed. Chapman & Hall. New York.

Socrates, G. 2010. Infrared and raman characteristic group frequencies. p. 366. John Wiley & Sons. New York.

Somani, K. P., Kansara, S. S., Patel, N. K. and Rakshit, A. K. 2003. Castor oil based polyurethane adhesives for wood-to-wood bonding. J. Adhes. Adhes. 23: 269-275.

Spoljaric, S., Genovese, A. and Shanks, R.A. 2009. Polypropylene–microcrystalline cellulose composites with enhanced compatibility and properties. Compos. Part A. 40: 791-799.

Sridach, W. 2010. Pulping and paper properties of Palmyra palm fruit fibers. Songklanakarin. J. Sci. Tecnol. 32(2): 201-205.

Steel, R.G.D. and Torrie, J.H. 1980. Principles and Procedure of Statistic: a Biometrical Approach. 2nd Ed. McGraw-Hill. New York.

TIS. 2523. Standard for synthetic resin adhesives (phenolic and aminoplastic) for wood: TIS.360-2523. *In* Thai industrial standards institute ministry of industry. Bangkok, Thailand.

TIS. 2530. Standard for polyvinyl acetate emulsion adhesives: TIS.181-2530. *In* Thai industrial standards institute ministry of industry. Bangkok, Thailand.

Tudorachi, N., Cascaval, C.N., Rusu, M. and Pruteanu, M. 2000. Testing of polyvinyl alcohol and starch mixtures as biodegradable polymeric materials. Polym. Test. 19: 785-799.

Uesu, N.Y., Pineda, E.A.G. and Hechenleitner, A.A.W. 2000. Microcrystalline cellulose from soybean husk: effects of solvent treatments on its properties as acetylsalicylic acid carrier. Int. J. Pharm. 206: 85-96.

Van Soest, P.J. and Wine, R.H. 1968. Determination of lignin and cellulose in acid-detergent fiber with permanganate. J. Assoc. Off. Anal. Chem. 51: 780-785.

Wang, B. and Sain, M. 2006. Dispersion of soybean stock-based nanofiber in a plastic matrix. Polym. Int. 56: 538-546.

Wang, D., Shang, S.H., Song, Z-q. and Lee, M.K. 2010. Evaluation of microcrystalline cellulose prepared from kenaf fibers. J. Ind. Eng. Chem. 16: 152-156.

Wang, Y., Cao, X. and Zhang, L. 2006. Effect of cellulose whiskers on properties of soy protein thermoplastics. Macromol. Biosci. 6: 524-531.

Wyman, C.E., Decker, S.R., Himmel, M.E., Brady, J.W., Skopec, C.E. and Viikari, L. 2005. Hydrolysis of cellulose and hemicellulose. *In* Polysaccharides: Structural Diversity and Functional Versatility. 1st Ed (Dumitriu, S., ed.). p. 1023-1062. Marcel Dekker. New York.

Xiao, B., Sun, X.F. and Sun, R.C. 2001. Chemical, structural, and thermal characterizations of alkali-soluble lignins and hemicelluloses, and cellulose from maize stems, rye straw, and rice straw. Polym. Degrad. Stab. 74: 307–319.

Xie, K., Yu, Y. and Shi, Y. 2009. Synthesis and characterization of cellulose/silica hybrid materials with chemical crosslinking. Carbohydr. Polym. 78: 799-805.

Yu, J.P., Wang, N. and Ma, X.F. 2005. The effects of citric acid on the properties of thermoplastic starch plasticized by glycol. Starch/Stärke. 57: 494-504.

Yuan, Y., Zhang, L., Dai, Y. and Yu, J. 2007. Physicochemical properties of starch obtained from *Dioscorea nipponica* Makino comparison with other tuber starches. J. Food. Eng. 82: 436-442.

Zaidul, I.S.M., Norulaini, N.A.N., Omar, A.K.M., Yamauchi, H. and Noda, T. 2007. RVA analysis of mixtures of wheat flour and potato, sweet potato, yam, and cassava starches. Carbohydr. Polym. 69: 784-791.

Zanin, G.M., Santana, C.C., Bon, E.P.S., Giordano, R.C.L., Moraes, F.F. and Andrietta, S.R. 2000. Brazilian bioethanol program. Appl. Biochem. Biotech. 84-86(1-9): 1147-1161.

Zhao, H., Kwak, J.H., Zhang, Z.C., Brown, H.M., Arey, B.W. and Holladay, J.E. 2007. Studying cellulose fiber structure by SEM, XRD, NMR and acid hydrolysis. Carbohydr. Polym. 68: 235-241.

APPENDIX

ANALYTICAL METHODS

1. Moisture content (AOAC, 1999)

Method

1. Dry the empty dish and lid in the oven at 105°C for 30 min and transfer to desiccator to cool (30 min). Weigh the empty dish and lid.
2. Weigh about 5 g of sample to the dish. Spread the sample with spatula.
3. Place the dish with sample in the oven. Dry for 16 h or overnight at 105°C.
4. After drying, transfer the dish with partially covered lid to the desiccator to cool. Reweigh the dish and its dried content.

Calculation

$$\% \text{ Moisture} = \frac{(W_1 - W_2)}{W_1} \times 100$$

Where W_1 = weight (g) of sample before drying

W_2 = weight (g) of sample after drying

2. Ash (AOAC, 1999)

Method

1. The crucible and lid is firstly placed in the furnace at 550°C overnight to ensure that impurities on the surface of crucible is burned off. The crucible is then cool in the desiccator (30 min).
2. Weigh the crucible and lid to 3 decimal places.
3. Weigh about 5 g sample into the crucible. Heat over low Bunsen flame with lid haft covered. When fumes are no longer produced, place crucible and lid in furnace.
4. Heat at 550°C overnight. During heating, do not cover the lid. Place the lid after complete heating to prevent loss of fluffy ash. Cool down in the desiccator.
5. Weigh the ash with crucible and lid when the sample turns to gray. If not, return the crucible and lid to the furnace for the further ashing.

Calculation

$$\% \text{ Ash content} = \frac{\text{Weight of ash}}{\text{Weight of sample}} \times 100$$

3. Cellulose and lignin (AOAC, 1999)

Reagents

- Acetone
- 72% H_2SO_4 solution
- Decahydronapthalene
- Acid detergent solution: Add 20 g of CTAB (Cetyl Trimethyl Ammonium Bromide) to 1 L 1.0 N H_2SO_4

Method

1. Weigh 1 g sample (S) ground to pass 1 mm screen, into beaker (600 ml). Add 100 ml acid detergent solution.
2. Heat to boiling in 5-10 min, reduce heat to avoid foaming as boiling begins. Reflux 60 min from onset of boiling, adjusting boiling to slow, even level.
3. Remove container, swirl, and filter thru weighed (W_1) fritted glass crucible, using min suction. Break up filtered mat with rod and fill crucible 2/3 full with hot (90-100°C) water. Stir and let soak 15-30 sec. Dry with vacuum and repeat water washing, rising sides of crucible. Wash twice similarly with acetone and remove residual acetone with vacuum.
4. Dry 3 h or overnight in 100°C oven and weigh (W_2).
5. Cover contents of crucible with cooled (15°C) 72% H_2SO_4 and stir with glass rod to smooth paste. Fill crucible about half-way with acid and stir, refill with 72% H_2SO_4 and stir hourly as acid drains.
6. After 3 h, filter as completely as possible with vacuum, and wash with hot water until acid-free to pH paper.
7. Dry crucible in 100°C oven, cool in desiccator and weigh (W_3).
8. Ignite crucible in 500°C furnace 2 h or until C-free. Transfer to desiccator, cool, and weigh (W_4).

Calculation

$$ADF = \frac{(W_2 - W_1) \times 100}{S}$$

$$L = \frac{(W_3 - W_4) \times 100}{S}$$

$$C = ADF - L$$

Where:

ADF = Acid detergent content (%)

L = Lignin content (%)

C = Cellulose content (%)

W_1 = weight (g) of crucible

W_2 = weight (g) of crucible and sample after passed acid detergent

W_3 = weight (g) of crucible and sample after passed 72% H_2SO_4

W_4 = weight (g) of crucible and sample after ignited

S = weight (g) of sample

4. Cellulose (Nitric acid method; Kurschner and Hoffer, 1967)

Reagents

- Alcohol nitric acid solution: 65% nitric acid in 96% ethanol of the ratio of 1:4.

Method

1. Weigh 5 g of fiber sample ground to pass 1 mm screen, into beaker. Add 125 ml of alcohol nitric acid solution.
2. The sample is refluxed for 1 h with alcohol nitric acid solution.
3. The residue is filtered off and digested with hot water, then extracted 3 times with alcohol nitric acid solution again until they were 4 cycles (1 cycle, 1 h).
4. The residue is washed with water, dried at 105°C and weigh.

VITAE

Name Miss Sunan Jonjankiat

Student ID 5111020029

Educational Attainment

Degree	Name of Institution	Year of Graduation
Bachelor of Science (Polymer Science, Second Class Honors)	Prince of Songkla University	2006

Scholarship Awards during Enrolment

The University–Industry Research Collaboration Program (U-IRC) Scholarship from National Science and Technology Development Agency and Thai Government, Thailand.

List of Publication and Proceedings

Jonjankiat, S., Wittaya, T. and Sridach, W. 2010. Effects of citric acid and tapioca starch on the properties of the cross-linked poly(vinyl alcohol)/starch adhesives. *In* Proceedings of the 10th International Conference on Applied Science, Engineering and Technology 2010. Singapore. August 25-27.

Jonjankiat, S., Wittaya, T. and Sridach, W. 2010. Impact of important factors on the properties of cross-linked poly(vinyl alcohol)/starch adhesives. J. Appl. Polym. Sci. (Submitted).

Saithai, P., **Jonjankiat, S**., Chinpa, W. and Tanrattanakul, V. 2007. Preparation of epoxidized soybean oil. KMUTT Research and Development Journal 30th. 4 (select volume): 583-589.